UNIVERSITY OF CALIFORNIA
RIVERSIDE

The Role of Astrocyte Specific Regulation of Ephrin-B1 in Refining Hippocampal Circuits During Memory Formation

A Dissertation submitted in partial satisfaction
of the requirements for the degree of

Doctor of Philosophy

in

Cell, Molecular, and Developmental Biology

by

Jordan Adam Koeppen

December 2018

Dissertation Committee:
Dr. Iryna M. Ethell, Chairperson
Dr. Monica J. Carson
Dr. Seema K. Tiwari-Woodruff

The Dissertation of Jordan Adam Koeppen is approved:

Committee Chairperson

University of California Riverside

Acknowledgements

Dr. Angeliki M. Nikolakopoulou, whose previous work on astrocytic ephrin-B1 mediated synapse regulation in the hippocampus during traumatic brain injury provided the basis for this research. Dr. Khaleel Abdulrazak for allowing me the use of his fear conditioning chamber. The Journal of Neuroscience, for the publication of much of the data presented here.

Dedication

I would like to thank my advisor Dr. Iryna Ethell for all her guidance and encouragement. I had no experience with neuroscience research before entering her lab and the direction and drive she gave me allowed me to learn a wide range of techniques and instilled a lasting interest in astrocyte biology. I would also like to thank all the lab members in the Ethell and Abdulrazak labs for all their support in the completion of my dissertation research project. I would like to thank my dissertation committee members; Dr. Monica Carson and Dr. Seema Tiwari-Woodruff for taking time to advice me and provide me with feedback on my project.

I could not have completed my dissertation without the help of my family and friends. To my parents, thank you for all your support and always encouraging me in my academic pursuits. To my grandpa Ralph and grandma Elizabeth, your care and support has helped me through some of the most trying times of my dissertation research. Thank you also to my wife, Hashini Batugedara, whom I would never have been able to complete my graduate studies without.

ABSTRACT OF THE DISSERTATION

The Role of Astrocyte Specific Regulation of Ephrin-B1 in Refining Hippocampal Circuits During Memory Formation

by

Jordan Adam Koeppen

Doctor of Philosophy, Graduate Program in
Cell, Molecular, and Development Biology
University of California, Riverside, December 2018
Dr. Iryna M. Ethell, Chairperson

The hippocampus is a region of the brain required for associative memory formation, and hippocampal neurons retain a high level of synaptic plasticity in the adult that is thought to contribute to life-long learning in adults. Astrocytes play a critical role in synaptic plasticity and maintenance in the adult hippocampus and astrocyte dysfunctions are implicated in neurodevelopmental disorders associated with impaired learning and memory. In addition, many astrocyte-secreted factors are found to promote synaptogenesis and synaptic maturation, the close proximity of astrocytic processes to synapses suggests contact mediated factors contribute to synapse dynamics. This research investigates the role of astrocytic ephrin-B1 regulation in CA1 hippocampal synapses during memory formation. EphB receptors are expressed in both presynaptic CA1 and postsynaptic CA1 neurons, and trans-synaptic Eph/ephrin interactions have been shown to promote synaptic maturation by the clustering and recruitment of synaptic NMDA and AMPA receptors. These studies indicate that astrocytic ephrin-B1 mediates the elimination of immature hippocampal synapses possibly through competitive binding with neuronal EphB receptors triggering the trans-phagocytosis of synapses inhibiting

memory formation. Ablation of astrocytic ephrin-B1 increased the number of immature glutamatergic synapses in the SR of the CA1 hippocampus. In contrast, overexpression of ephrin-B1 decreased synapse number and remaining synapses were more mature than tdTomato expressing WT mice. Excess immature synapses in KO mice contributed to enhanced contextual recall by activity dependent maturation. KO mice had a significant increase in vGlut1/PSD95 co-localization after fear conditioning and deficits in synaptic AMPAR found in naïve mice were no longer seen after fear conditioning. In addition, OE mice had deficits in contextual recall. Diminished recall may be attributed to a reduction in synaptic connection after fear conditioning, as OE of astrocytic ephrin-B1 also inhibited activity dependent dendritic spine formation. Activity dependent AMPAR recruitment is also not observed in OE mice possibly due to a lack of immature synapses available for maturation prior to fear conditioning. *In vitro* studies suggest astrocytes eliminate synapses by trans-phagocytosis induced by neuronal EphB stimulated activation of ephrin-B1 reverse signaling.

Table of Contents

List of Figures

Abbreviations

AAV: adeno-associated virus

ACM: Astrocyte conditioned media

AMPA α-amino-3-hydroxy-5-methyl-4-isoxazolepropionic acid

AMPAR: AMPA receptors

CA1: *Cornu Ammonis 1* region of the hippocampus

CA3: *Cornu Ammonis 3* region of the hippocampus

CNS: Central nervous system

DG: Dentate gyrus

DIV: Days *in vitro*

EC: entorhinal cortex

Eph: erythropoietin-producing human hepatocellular

F-actin: filamentous actin

FAK: focal adhesion kinase

FMRP: Fragile X mental retardation protein

GABA: γ-Aminobutryic acid

GAD65: glutamic acid decarboxylase 65

GAPDH: Glyceraldehyde 3-phosphate dehydrogenase

GFP: green fluorescence protein

GluA1: Glutamate receptor 1

GluA 2/3: Glutamate receptor 2/3

GPI: glycophosphatidylinositol

KO: knock out

LTP: long term potentiation

MeCP2: methyl-CpG–binding protein 2

MEGF10: multiple EGF like domains 10

MERTK: Proto-oncogene tyrosine-protein kinase MER

NMDA: N-methyl-D-aspartate receptors

NMDAR: NMDA receptors

OE: over expressing

P72-80: postnatal day 72-80

PSD: postsynaptic density

PSD95: (postsynaptic density protein 95)

PV: Parvalbumin

RGCs: Retinal ganglion cells

SPARC: Secreted Protein Acidic And Cysteine Rich

Src: proto-oncogene c-Src

TNFα: Tumor necrosis factor-α

TSP1: Thrombospondin-1

vGlut1: Vesicular glutamate transporter 1

WT: wild type

Chapter 1 – Introduction

Investigation of astrocytes role in the formation, maturation, and elimination of synapses has become a growing area of research in recent decades. Despite increased interest, research into astrocyte-synapse interactions is still in its infancy and many synaptic regulatory mechanisms by astrocytes are still unclear. I propose a new role for astrocytic ephrin-B1 in regulating CA1 hippocampal neurons during memory formation.

Astrocytes

Astrocytes are the most abundant cell type in the central nervous system and are highly heterogeneous. They are highly branched structures that form fine processes which may contact blood vessels, neighboring astrocytes, or surround the synaptic cleft (Oberheim *et al.*, 2009). Protoplasmic astrocytes in the rat CA1 hippocampus occupy discrete regions and contact each other through processes at distinct boundaries (Bushong *et al.*, 2002). Within these regions a single astrocyte may contact thousands of synapses. Astrocytes in the mouse cortex are estimated to contact around 100,000 synapses (Bushong *et al.*, 2002) and as much as 2,000,000 in humans (Oberheim *et al.*, 2009; Allen and Eroglu, 2017). The close interactions between astrocytic processes and synapses allow astrocytes to have significant influence on synaptic development and maintenance.

Recently, astrocyte dysfunction has been implicated in synapse pathologies associated with intellectual disabilities and learning impairments (Lioy *et al.*, 2011; Ballas *et al.*, 2009; Higashimori *et al.*, 2016) . Deletion of methyl-CpG–binding protein 2

(MeCP2) from neural stem/ progenitor cells has been used as a model for Retts syndrome (RTT) in the mouse. Interestingly wild type (WT) neurons treated with astrocyte conditioned media (ACM) from $MeCP2^{-/-}$ astrocytes had an increase in the number of neurons with short dendrites compare to WT ACM treated neurons (Ballas *et al.*, 2009). Restoring expression of MeCP2 in astrocytes also recovered behavioral deficits seen in KO mice (Lioy *et al.*, 2011). In addition, deletion of Fragile X mental retardation protein (FMRP) from astrocytes co-cultured with WT neurons lead to morphological difference in neurons and an increase in pre and post-synaptic protein co-localization. However, by 21 days *in vitro* (DIV) astrocyte specific FMRP KO co-cultures showed no differences in morphology or protein co-localization compared to WT cultures. (Jacobs, Nathwani and Doering, 2010). Astrocyte specific deletion of FMRP in P4 mice had a decrease in Glt1 expression levels leading to a decrease in glutamate uptake. This decrease corresponded to an increase in dendritic spine density in the cortex (Higashimori *et al.*, 2016). The evidence for astrocytes contributing to synapse pathologies is not surprising given recent evidence for astrocytes contributions to synapse dynamics.

Astrocytes are shown to regulate synaptic function through the release and uptake of neurotransmitters ATP, D-Serine, and glutamate at the synapse (Bezzi *et al.*, 1998; Zhang *et al.*, 2003; Stellwagen and Malenka, 2006; Henneberger *et al.*, 2010). In addition to modulating synaptic neurotransmitter levels, astrocytes influence the formation and maturation of synapses. Early work on astrocytes role in synaptogenesis found isolated retinal ganglion cells (RGCs) cultured with astrocytes had a greater

number of pre- and postsynaptic sites compared to neurons in the absence of astrocytes (Ullian *et al.*, 2001).

It was later found that astrocyte secreted factors play a role in promoting synaptogenesis. Retinal ganglion cells (RGCs) cultured in the absence of astrocytes but treated with astrocyte conditioned media (ACM) had an increase in synaptic number (Christopherson *et al.*, 2005). Isolated Thrombospondin-1 (TSP-1) from ACM was found to promote synaptogenesis in RGCs by binding to neuronal Gabapentin receptor α2δ-1 (Christopherson *et al.*, 2005; Eroglu *et al.*, 2009). In addition to synaptogenic effects, astrocyte derived secreted factors can promote synaptic maturation. Astrocytes increased synaptic receptivity in embryonic RGCs by disrupting neuronal neurexin1β localization (Barker *et al.*, 2008) and astrocyte derived Glypican 4 increased mEPSCs in cultured RGCs by increasing the localization of the AMPAR subunit GluA1 to the synaptic membrane (Allen *et al.*, 2012). TNFα was also found to increase recruitment of AMPAR to the synaptic surface (Beattie, 2002). Astrocytic factors may also have opposing biological functions. Astrocyte derived Hevin increases synaptogenesis in cultured RGCs, but astrocyte secreted SPARC antagonizes Hevin function (Kucukdereli *et al.*, 2011). Loss of SPARC also increased synaptic AMPAR and SPARC KO mice showd deficits in synaptic placticity (Jones *et al.*, 2011).

Although astrocyte secreted factors clearly have a role in the formation of mature synapses, the proximity of astrocytic processes with presynaptic boutons and dendritic spines suggest contact mediated factor influence synaptogenesis and synaptic maturation (Araque et al., 1999). Interestingly, RGCs treated with ACM had fewer

synapses than neurons in direct contact with astrocytes (Christopherson *et al.*, 2005). Contact mediated signaling through integrins was found to increase the number of synapses on cultured hippocampal neurons (Hama *et al.*, 2004) and γ-Protocadherins increased synaptic number through a contact dependent signal (Garrett and Weiner, 2009). In addition to synaptogenesis there is increasing evidence that astrocytes are involved in synapse elimination.

Astrocytes are implicated in pruning and clearing unwanted axons and synapses during synapse development (J. Lauterbach and Klein, 2006; Eroglu and Barres, 2010; Caberoy *et al.*, 2012; Chung *et al.*, 2013; Schafer, Lehrman and Stevens, 2013), allowing for increased efficiency of neuronal transmission and refinement of functional circuits (Luo and O'Leary, 2005; Cowan *et al.,* 1984). Electron microscopy studies revealed possible trans-endocytosis between hippocampal neurons and astrocytes (Spacek, 2004). Astrocytes have also been shown to use multiple EGF like domains 10 (MEGF10) and proto-oncogene tyrosine-protein kinase MER (MERTK) signaling pathways to prune synapses in adult CNS through phagocytosis (Chung *et al.*, 2013). Despite evidence for synaptic pruning, an "eat me" signal from neurons that initiates synapse elimination by astrocytes is unknown. Our research investigates astrocytic ephrin-B1 and neuronal EphB receptors as a possible contact mediated "eat me" signal for synapse elimination by trans-endocytosis.

Eph/ephrins

Eph Receptors are the largest family of receptor tyrosine kinases, and can be subdivided into A and B-type Eph receptors (Egea and Klein, 2007). In mammals, nine EphA receptors (EphA1-8, EphA10) and five EphB receptors (EphB1-4, EphB6) have been found (Egea and Klein, 2007). While EphA and EphB receptors are structurally very similar, their binding affinities differ. EphA receptors bind to membrane bound ephrin-A ligands (ephrinA1-5) characterized by a glycosylphosphatidylinositol (GPI) anchor and lack of cytosolic domain. EphB receptors bind to ephrin-B's (ephrin-B1-3) which have a trans-membrane and cytosolic region (Egea and Klein, 2007).

Eph/ephrins are activated in a contact mediated manner leading to auto-phosphorylation of EphB receptors and ephrinB ligands initiating EphB "forward" signaling and "reverse" signaling in ephrin expressing cells (Pasquale, 1997; Bush and Soriano, 2009; Sloniowski and Ethell, 2012a; Xu and Henkemeyer, 2012). Eph receptors associate with the ephrin binding domain with a high affinity forming a heterodimer, as well as also bind to a second ligand with lower affinity leading to a clustering of receptors into tetramers forming a ring structure (Himanen *et al.*, 2001). Eph and ephrin clustering is promiscuous within each subclass, however A and B type cross binding is more restricted. While EphA4 receptors can also bind to ephrin-B2 and ephrin-B3 and EphB2 may bind with ephrin-A5, affinity between these proteins is reduced compared to EphA/ephrinA and EphB/ephrinB interactions (Pasquale, 2004; Martínez and Soriano, 2005). In addition to differences in binding affinities, A and B-type ephrin signaling pathways differ due to their carboxy-terminal regions (Pasquale, 2005; Dalva,

McClelland and Kayser, 2007; Egea and Klein, 2007a). EphrinAs can signal through association with other signaling proteins that contain a transmembrane domain while ephrinBs can signal through a cytosolic PDZ domain on its c-terminus (Pasquale, 2008; Klein, 2009). Despite these differences in signaling domain both A and B type receptors are associated with the activation of Src family Kinases and Ras/Rho family GTPases leading to reorganization of actin (Pasquale, 2008; Klein, 2009; Gaitanos, Koerner and Klein, 2016).

Eph/ephrin mediated modulation of the cytoskeleton play an important role in axon guidance and synaptogenesis (Klein, 2004; Martínez and Soriano, 2005; Filosa *et al.*, 2009; Sloniowski and Ethell, 2012) and the heterogeneity of receptor complexes suggest Eph/ephrins may have varying roles at different points in CNS development and maturation depending on which combination of receptors are present in the cell. Eph receptors have been heavily studied with regard to their role in axon guidance, synaptogenesis, and synaptic maturation (Klein, 2004; Martínez and Soriano, 2005; Sloniowski and Ethell, 2012) and are highly expressed in the developing CNS (Egea and Klein, 2007). Ablation of EphB1 and EphB2 in (RGC) or ephrinB1 and ephrinB2 from radial glial cells during development leads to a reduction in ipsilateral innervation (Chenaux and Henkemeyer, 2011). Interestingly, cell repulsion can be mediated by the removal of Eph/ephrin complexes through endocytosis, causing vesicles to contain fragments of the other cell (Pasquale, 2008). In general, the expression of Eph/ephrins is reduced after development periods however there are specific regions that maintain increased Eph/ephrin levels, and many of the regions that retain high levels of Eph/ephrin

mRNA including the hippocampus are characterized by their retention of high synaptic plasticity in the adult brain (Liebl *et al.*, 2002; Yamaguchi and Pasquale, 2004).

Dendritic Spines

Synapses are small junctions between two neurons that consist of a pre-synaptic site that release neurotransmitters, which cross the synaptic cleft, and bind to receptors on the postsynaptic site. First described by Santiago Ramon y Cajal on the surface of Purkinje cell dendrites after staining with a silver impregnation method more than a 100 years ago, dendritic spines are small protrusions on neuronal dendrites that constitute an excitatory synapse's postsynaptic site (Ramon y Cajal, 1888,1899). Spine structure can vary widely and spines of different morphologies can reside next to each other on the same dendrite (Harris' and Stevens, 1989). Based on morphology spines can be classified into 4 groups that reflect synapse maturation: filipodia and thin spines have long necks with a very small or absent heads and are considered immature, mature mushroom and stubby spines are characterized by a short neck and large bulbous head (Ethell and Pasquale, 2005).

These small protrusions provide a biochemical compartmentalization and prevent the dissipation of localized signals (Harris' and Stevens, 1989; Ethell and Pasquale, 2005). Electron microscopy (EM) imaging of dendritic spines found an electron dense region called the postsynaptic density (PSD) adjacent to the synaptic active zone (Scannevin and Huganir, 2000; Li and Sheng, 2003), structured around an actin cytoskeleton (Wyszynski *et al.,*1997; Bernhardt Ani Matus, 1984; Cohen, Chung and Pfaff, 1985; Kaech *et al.*, 1997). Measurements found PSD size (Harris, Jensen and Tsao,

1992; Yuste and Bonhoeffer, 2004; Tashiro and Yuste, 2003) and presynaptic vesicle number (Harris and Stevens, 1989) are increased in spines with a greater head volume.

In addition to structural differences, postsynaptic receptor profiles differ between mature and immature spines. Large head volume corresponded with increased α-amino-3-hydroxy-5-methyl-4-isoxazolepropionic acid receptors (AMPARs) but not N-methyl-D-aspartate receptors (NMDARs) in sections using immunogold labeled (Takumi *et al.,* 1999). Increased synaptic AMPARs leads to higher glutamate sensitivity in mushroom spine compared to filipodia (Matsuzaki *et al.*, 2001). Due to the low or absent AMPAR levels in filipodia, they are considered functionally "silent" and are regarded as immature. Dendritic spines are plastic structures that have been observed to change morphology in two photon studies (Yuste and Bonhoeffer, 2004). These synaptic connections can undergo changes based on fluctuations in neuronal activity and the environment in the adult brain (Yasumatsu *et al.*, 2008). Although individual spines are highly motile and morphologically dynamic (Dunaevsky *et al.*, 1999; Bonhoeffer and Yuste, 2002), synaptic plasticity diminishes in much of the brain after critical periods of development (Yuste and Bonhoeffer, 2004). However, the hippocampus, a structure essential for memory formation, maintains a relatively high level of synaptic plasticity in the adult (Harris, 1999).

The Hippocampus and Memory Formation

The hippocampus is divided into regions starting with the entorhinal cortex, which receives the majority of cortical inputs to the hippocampal formation. The entorhinal cortex (EC) receives nearly two-thirds of its inputs from the perirhinal and

parahippocampal cortex (Squire and Zola, 1996). The hippocampus is innervated in a unidirectional excitatory pathway beginning with the entorhinal cortex. Neuronal projections from EC layers II along the perforant pathway to the dentate gyrus (DG), in addition to a subset that innervates CA1 pyramidal cells from EC layer III neurons (Amaral and Witter, 1989; Squire and Zola, 1996; Neves, Cooke and Bliss, 2008). DG granular cells signal through mossy fibers to CA3 pyramidal neurons which innervate CA1 pyramidal neurons through Schaffer collaterals and sub-sequentially signal to the subiculum and EC layer V (Squire and Zola, 1996; Neves, Cooke and Bliss, 2008).

The hippocampus has been associated with memory formation since the 1950's. Early psychological studies on patients that received bilateral medial temporal lobe resections revealed that patients experienced amnesia (Scoville *et al.,* 1954; Scoville and Milner, 1957). Interestingly, patients that received the most extensive removal of the hippocampus had the largest deficits in memory, with some presenting with complete anterograde amnesia (Scoville *et al.,* 1954; Scoville and Milner, 1957). Amnesic patients, however, did not show deficits in all types of memory formation, as they had an equivalent ability in learning to read mirror text compared to non-amnesic individuals (Cohen and Squire, 1980; Cohen, Chung and Pfaff, 1985). Patients appeared to have deficits in declarative memory (the acquisition of memories about facts or recalling events), but retained non declarative memory, or the acquisition of skilled behavior or response to stimuli (Milner, Squire and Kandel, 1998). It also became clear that lesions confined to specific regions of the hippocampus results in amnesia. Anterograde amnesia due to lesions confined to the CA1 hippocampus was first reported in patient R.B. (Zola-

Morgan *et al.,* 1986) and later in three other patients: D.G., L.M, and W.H. (Rempel-Clower *et al.*, 1996). In order to further understand how the hippocampus is involved in memory formation, researchers began studying animal models, A reversible ischemia in monkeys caused bilateral cell loss in the CA1 hippocampus and a loss of somatostatin positive cells in the DG, along with a 12.7% deficit in a delayed to nonmatching sample task (Squire and Zola, 1996). More recent investigations with mouse models have shown activation in CA1 pyramidal cells measured by c-fos and JunB staining after contextual memory retrieval (Strekalova *et al.*, 2003).

Hippocampal synapses

Hippocampus dependent declarative memory deficits in resection patients (Milner, Squire and Kandel, 1998), activation of hippocampal excitatory neurons during contextual recall (Strekalova *et al.*, 2003), and maintained synaptic plasticity in the adult hippocampus (Neves, Cooke and Bliss, 2008) suggest hippocampal synapses are a crucial component to life-long learning and memory. Early experiments stimulating perforant pathways recorded long-term potentiation (LTP) in granular neurons of the DG (Bliss and Lømo, 1973), demonstrating that hippocampal synapses follow Hebb's first postulate "When an axon of cell A is near enough to excite a cell B and repeatedly and persistently takes part in firing it, some growth process or metabolic change takes place in one or both cells such that A's efficiency, as one of the cells firing B, is increased" (Attneave, B. and Hebb, 1950; Brown and Milner, 2003). This experiment demonstrated how hippocampal synapses might function as a computational unit for associative memory formation. Neuronal activation leads the recruitment of signaling proteins focal adhesion kinase

(FAK), Src, and paxillin (Moeller *et al.*, 2006) increasing synaptic AMPARs levels, spine volume, and PSD size after LTP (Harris, 1999) demonstrating a molecular basis for a Hebb's synapse.

NMDARs at the synapse require a partial depolarization of the postsynaptic site to release Mg^{2+} and a release of presynaptic glutamate to activate (Neves, Cooke and Bliss, 2008). Interestingly, activation of glutamate channels in immature filipodia leads to synaptic AMPAR recruitment and enlarged dendritic spines (Matsuzaki *et al.*, 2001) and LTP induced increases synaptic area (Desmond and Levy, 1988). Enhanced synaptic transmission through biochemical modification of synaptic structures following depolarization of the postsynaptic cell provide a molecular basis for modeling associative learning in the hippocampus (McNaughton and Morris, 1987).

Although synaptic plasticity is found throughout the hippocampus in adult mice, differences in spine maturation can be observed in specific synaptic connections. CA1 dendritic spines had fewer synaptic AMPAR and greater NMDAR compared to Mossy fibers (Takumi *et al.,* 1999), with as much as 17% of dendritic spines immune-negative for AMPAR receptor on Schaffer collaterals to CA1 pyramidal neuron synapses (Nusser *et al.*, 1998). An increased prevalence of immature synapses in the CA1 may provide a substrate for new memory formation during hippocampal dependent learning. In fact, deletion of NMDAR1 in CA1 pyramidal neurons inhibited LTP, impaired learning in a Morris water maze (Tsien and Huerta, 1996), and inhibited recruitment of AMPAR to mushroom spines 24h after fear-conditioning (Matsuo, Reijmers and Mayford, 2008).

EphB/ephrinBs and synapses

EphB/ephrinB interactions have multiple functions in the formation and maturation of synapses. EphB2 was found to cluster NMDAR after activation with ephrin-B1 independent of EphB2's intracellular domain, but it was noted that removal of EphB2 kinase domains did lead to disruption of synapse development (Dalva *et al.*, 2000). Curiously, activation of EphB2 by ephrinB1-Fc increased surface AMPAR levels which can be disrupted by mutating EphB2 PDZ domain in primary cortical neurons (Kayser *et al.*, 2006). The activation of EphB2 increases signaling pathways associated with synaptic plasticity (Grunwald *et al.*, 2001) including ERK/MAPK and Src family kinases (Impey, Obrietan and Storm, 1999; Takasu *et al.*, 2002) that can phosphorylate NMDA subunits and increase channel gating (Ali and Salter, 2001). Hippocampal recordings in EphB2$^{-/-}$ mice showed deficits in LTP that were seen after attenuation of EphB2 kinase domain (Henderson *et al.*, 2001). In addition to recruitment and modulation of synaptic receptors, EphB/ephrinB also influence postsynaptic structure.

Neuronal EphB receptors promote the formation of large postsynaptic dendritic spines. EphB1/2/3 KO neurons show deficits in spine morphology resulting in filipodia-like structures rather than mushroom spines compared to WT neurons *in vitro* (Henkemeyer *et al.*, 2003). In addition, transfection of primary cortical neurons with shEphB2 results in reduced filipodia motility and reductions in dendritic spine formation (Kayser, Nolt and Dalva, 2008). Further, *in vivo* triple EphB KO mice had deficits in spine structure predominantly in CA1 spines receiving inputs from the CA3 (Henkemeyer *et al.*, 2003) which express EphB2 (Grunwald *et al.*, 2001). Postsynaptic

ephrin-B2 was also shown to be necessary for LTP in the CA1 hippocampus (Grunwald *et al.*, 2004). Interestingly, this effect is specific to excitatory synapses as GABAergic synapses on dendritic shafts saw no differences in EphB1,2,3 KO mice compared to WT (Henkemeyer *et al.*, 2003).

Although these studies indicate EphB/ephrinB interactions are involved in maturation and stabilization of the synapse during LTP they focus on trans-synaptic interactions. Little is known about how neuronal EphB and astrocytic ephrinB interactions alter synapses. Microglia and astrocytes have been shown to increase ephrin-B1 and ephrin-B2 expression after injury (Wang *et al.*, 2005; Goldshmit, McLenachan and Turnley, 2006; Du *et al.*, 2007; Nikolakopoulou *et al.*, 2016). Increased astrocytic ephrin-B1 after a controlled cortical impact (CCI) was correlated with a decrease in glutamatergic puncta in the CA1 hippocampus. Further deletion of astrocyte specific ephrin-B1 resulted in a faster recovery in vGlut1 positive synapses in the CA1 after CCI (Nikolakopoulou *et al.*, 2016). This suggests astrocytic ephrin-B1 may have a negative effect on synaptogenesis in contrast to trans-synaptic interactions. Interestingly ephrin-B-expressing astrocytes can engulf neuronal EphB2 in mixed neuron/astrocyte co-cultures (Jenny Lauterbach and Klein, 2006), which raises the possibility that astrocytic ephrin-B1 neuronal EphB interactions may be an "eat me" signal for synapse elimination.

Eph/ephrins in learning and memory

The retention of Eph receptors and ephrins in adult hippocampal neurons (Gerlai *et al.*, 1999; Liebl *et al.*, 2002; Grunwald *et al.*, 2004) and EphB mediated activation of pathways involved in synaptic plasticity (Impey, Obrietan and Storm, 1999; Grunwald *et*

al., 2001) suggest Eph and ephrins are key to synaptic plasticity during learning and memory (Dines and Lamprecht, 2016). Despite extensive evidence of EphB facilitated synaptic maturation most research into Ephs and memory formation has focused on A-type receptors. Within the small group of receptors studied to date, a wide range of behavioral changes occur dependent on which Eph receptor is activated (Dines and Lamprecht, 2016). Hippocampal injections of the EphA5 antagonist (EphA5-IgG) induced deficits in contextual recall and T-maze alternation rate. Conversely injections of EphA5 agonist (ephrinA5-IgG) showed enhanced recall (Gerlai *et al.*, 1999). Transgenic mice expressing dominate negative EphA5 that inhibits kinase activity also increased latency for platform location in a water maze (Halladay *et al.*, 2004) demonstrating that EphA5 kinase activity contributes to memory formation. Initial studies showed no changes in contextual recall in EphA4 KO mice (Willi *et al.*, 2012), but later research has shown that EphA4$^{-/-}$ mice had deficits in recall but EphA4 forward signaling is not required (Dines *et al.*, 2015). The differences observed in EphA4$^{-/-}$ mice may be attributed to neuron specific deletion of EphA4 in the Dines study. Contextual recall was also impaired in EphA6 (Savelieva *et al.*, 2008) and ephrin-A3 (Carmona *et al.*, 2009) KO mice. Interestingly, deletion of EphB2 impaired short (1h after training) and long-term (24h after training) contextual recall but only long-term recall required EphB2 forward signaling (Dines *et al.*, 2015).

This research presents a new role for astrocyte specific ephrin-B1 as a possible signal for immature synapse elimination by trans-phagocytosis in the adult hippocampus during memory formation.

References:

Ali, D. W. and Salter, M. W. (2001) 'NMDA receptor regulation by Src kinase signalling in excitatory synaptic transmission and plasticity', *Current Opinion in Neurobiology*, 11(3), pp. 336–342. doi: 10.1016/S0959-4388(00)00216-6.

Allen, N. J. *et al.* (2012) 'Astrocyte glypicans 4 and 6 promote formation of excitatory synapses via GluA1 AMPA receptors', *Nature*. Nature Publishing Group, 486(7403), pp. 410–414. doi: 10.1038/nature11059.

Allen, N. J. and Eroglu, C. (2017) 'Cell Biology of Astrocyte-Synapse Interactions', *Neuron*. doi: 10.1016/j.neuron.2017.09.056.

Amaral, D. G. and Witter$, M. P. (1989) *THE THREE-DIMENSIONAL ORGANIZATION OF THE HIPPOCAMPAL FORMATION: A REVIEW OF ANATOMICAL DATA*.

Attneave, F., B., M. and Hebb, D. O. (1950) 'The Organization of Behavior; A Neuropsychological Theory', *The American Journal of Psychology*. doi: 10.2307/1418888.

Ballas, N. *et al.* (2009) 'Non-cell autonomous influence of MeCP2-deficient glia on neuronal dendritic morphology', *Nature Neuroscience*, 12(3), pp. 311–317. doi: 10.1038/nn.2275.

Barker, A. J. *et al.* (2008) 'Developmental Control of Synaptic Receptivity', *Journal of Neuroscience*, 28(33), pp. 8150–8160. doi: 10.1523/JNEUROSCI.1744-08.2008.

Beattie, E. C. (2002) 'Control of Synaptic Strength by Glial TNFalpha', *Science*, 295(5563), pp. 2282–2285. doi: 10.1126/science.1067859.

Bernhardt Ani Matus, R. A. (1984) *Light and Electron Microscopic Studies of the Distribution of Microtubule-Associated Protein 2 in Rat Brain: A Difference Between Dendritic and Axonal Cytoskeletons*, *THE JOURNAL OF COMPARATIVE NEUROLOGY*.

Bezzi, P. *et al.* (1998) 'Prostaglandins stimulate calcium-dependent glutamate release in astrocytes', *Nature*, 391(6664), pp. 281–285. doi: 10.1038/34651.

Bliss, T. V. P. and L0mo, T. (1973) *LONG-LASTING POTENTIATION OF SYNAPTIC TRANSMISSION IN THE DENTATE AREA OF THE ANAESTHETIZED RABBIT FOLLOWING STIMULATION OF THE PERFORANT PATH*, *J. Physiol*.

Bonhoeffer, T. and Yuste, R. (2002) *Review Spine Motility: Phenomenology, Mechanisms, and Function Purkinje cells' dendrites were covered with small thorns ('espinas') (Ramó n y Cajal he put spines in the spotlight of the nervous system by proposing that*, *Neuron*. Available at: http://www.pnas.org/cgi/content/full/96/23/13438/.

Brown, R. E. and Milner, P. M. (2003) 'The legacy of Donald O. Hebb: More than the Hebb Synapse', *Nature Reviews Neuroscience*. doi: 10.1038/nrn1257.

Bush, J. O. and Soriano, P. (2009) 'Ephrin-B1 regulates axon guidance by reverse signaling through a PDZ-dependent mechanism', *Genes and Development*, 23(13), pp. 1586–1599. doi: 10.1101/gad.1807209.

Bushong, E. A. *et al.* (2002) 'Protoplasmic Astrocytes in CA1 Stratum Radiatum Occupy Separate Anatomical Domains', 22(1), pp. 183–192.

Caberoy, N. B. *et al.* (2012) 'Galectin-3 is a new MerTK-specific eat-me signal', *Journal of Cellular Physiology*, 227(2), pp. 401–407. doi: 10.1002/jcp.22955.

Carmona, M. A. *et al.* (2009) 'Glial ephrin-A3 regulates hippocampal dendritic spine morphology and glutamate transport.', *Proceedings of the National Academy of Sciences of the United States of America*, 106(30), pp. 12524–9. doi: 10.1073/pnas.0903328106.

Chenaux, G. and Henkemeyer, M. (2011) 'Forward signaling by EphB1/EphB2 interacting with ephrin-B ligands at the optic chiasm is required to form the ipsilateral projection', *European Journal of Neuroscience*. doi: 10.1111/j.1460-9568.2011.07845.x.

Christopherson, K. S. *et al.* (2005) 'Thrombospondins are astrocyte-secreted proteins that promote CNS synaptogenesis', *Cell*, 120(3), pp. 421–433. doi: 10.1016/j.cell.2004.12.020.

Chung, W. S. *et al.* (2013) 'Astrocytes mediate synapse elimination through MEGF10 and MERTK pathways', *Nature*. Nature Publishing Group, 504(7480), pp. 394–400. doi: 10.1038/nature12776.

Cohen, R. S., Chung, S. K. and Pfaff, D. W. (1985) *Immunocytochemical Localization of Actin in Dendritic Spines of the Cerebral Cortex Using Colloidal Gold as a Probe*, *Cellular and Molecular Neurobiology*.

Dalva, M. B. *et al.* (2000) 'EphB receptors inetreact with NMDA receptors and regulate excitatory synapse formation', *Cell*, 103, pp. 945–956.

Dalva, M. B., McClelland, A. C. and Kayser, M. S. (2007) 'Cell adhesion molecules: Signalling functions at the synapse', *Nature Reviews Neuroscience*. doi:

10.1038/nrn2075.

Desmond, N. L. and Levy, W. B. (1988) *Synaptic interface surface area increases with long-term potentiation in the hippocampal dentate gyrus*.

Dines, M. *et al.* (2015) 'The roles of Eph receptors in contextual fear conditioning memory formation', *Neurobiology of Learning and Memory*. Elsevier Inc., 124, pp. 62–70. doi: 10.1016/j.nlm.2015.07.003.

Dines, M. and Lamprecht, R. (2016) 'The Role of Ephs and Ephrins in Memory Formation', *International Journal of Neuropsychopharmacology*. doi: 10.1093/ijnp/pyv106.

Du, J. *et al.* (2007) 'Upregulation of EphB2 and ephrin-B2 at the optic nerve head of DBA/2J glaucomatous mice coincides with axon loss', *Investigative Ophthalmology and Visual Science*, 48(12), pp. 5567–5581. doi: 10.1167/iovs.07-0442.

Dunaevsky, A. *et al.* (1999) *Developmental regulation of spine motility in the mammalian central nervous system*. Available at: www.pnas.org.

Egea, J. and Klein, R. (2007) 'Bidirectional Eph-ephrin signaling during axon guidance', *Trends in Cell Biology*, 17(5), pp. 230–238. doi: 10.1016/j.tcb.2007.03.004.

Eroglu, Ç. *et al.* (2009) 'Gabapentin Receptor α2δ-1 Is a Neuronal Thrombospondin Receptor Responsible for Excitatory CNS Synaptogenesis', *Cell*, 139(2), pp. 380–392. doi: 10.1016/j.cell.2009.09.025.

Eroglu, C. and Barres, B. A. (2010) 'Regulation of synaptic connectivity by glia', *Nature*, 468(7321), pp. 223–231. doi: 10.1038/nature09612.

Ethell, I. M. and Pasquale, E. B. (2005) 'Molecular mechanisms of dendritic spine development and remodeling', *Progress in Neurobiology*. doi: 10.1016/j.pneurobio.2005.02.003.

Filosa, A. *et al.* (2009) 'Neuron-glia communication via EphA4/ephrin-A3 modulates LTP through glial glutamate transport', *Nature Neuroscience*. Nature Publishing Group, 12(10), pp. 1285–1292. doi: 10.1038/nn.2394.

Gaitanos, T. N., Koerner, J. and Klein, R. (2016) 'Correction: Tiam-Rac signaling mediates trans-endocytosis of ephrin receptor EphB2 and is important for cell repulsion [(2016), Vol. 214, No. 6, September 12, Pages 735-752.]', *Journal of Cell Biology*, 215(3), pp. 431–431. doi: 10.1083/jcb.20151201010212016c.

Garrett, A. M. and Weiner, J. A. (2009) 'Control of CNS Synapse Development by -Protocadherin-Mediated Astrocyte-Neuron Contact', *Journal of Neuroscience*, 29(38), pp. 11723–11731. doi: 10.1523/JNEUROSCI.2818-09.2009.

Gerlai, R. *et al.* (1999) 'Regulation of learning by EphA receptors: a protein targeting study.', *The Journal of neuroscience : the official journal of the Society for Neuroscience*, 19(21), pp. 9538–49. Available at: http://www.ncbi.nlm.nih.gov/pubmed/10531456.

Goldshmit, Y., McLenachan, S. and Turnley, A. (2006) 'Roles of Eph receptors and ephrins in the normal and damaged adult CNS', *Brain Research Reviews*. doi: 10.1016/j.brainresrev.2006.04.006.

Grunwald, I. C. *et al.* (2001) *Kinase-Independent Requirement of EphB2 Receptors in Hippocampal Synaptic Plasticity (E-LTP) require protein synthesis (reviewed in Impey et al duces a reduction in synaptic efficacy in the CA1 region*, *Neuron*. Available at: http://www.neuron.org/cgi/content/full/.

Grunwald, I. C. *et al.* (2004) 'Hippocampal plasticity requires postsynaptic ephrinBs', *Nature Neuroscience*. doi: 10.1038/nn1164.

Halladay, A. K. *et al.* (2004) 'Neurochemical and behavioral deficits consequent to expression of a dominant negative EphA5 receptor', *Molecular Brain Research*. doi: 10.1016/j.molbrainres.2004.01.005.

Hama, H. *et al.* (2004) 'PKC Signaling Mediates Global Enhancement of Excitatory Synaptogenesis in Neurons Triggered by Local Contact with Astrocytes', *Neuron*. doi: 10.1016/S0896-6273(04)00007-8.

Harris', K. M. and Stevens, J. K. (1989) *Dendritic Spines of CA1 Pyramidal Cells in the Rat Hippocampus: Serial Electron Microscopy with Reference to Their Biophysical Characteristics*, *The Journal of Neuroscience*.

Harris, K. M. (1999) 'Structure, development, and plasticity of dendritic spines', *Current Opinion in Neurobiology*, 9(3), pp. 343–348. doi: 10.1016/S0959-4388(99)80050-6.

Harris, K. M., Jensen, F. E. and Tsao, B. (1992) 'Three-dimensional structure of dendritic spines and synapses in rat hippocampus (CA1) at postnatal day 15 and adult ages: implications for the maturation of synaptic physiology and long-term potentiation.', *The Journal of neuroscience : the official journal of the Society for Neuroscience*, 12(7), pp. 2685–2705. doi: 10.1016/j.tcb.2009.06.001.

Henderson, J. T. *et al.* (2001) 'The receptor tyrosine kinase EphB2 regulates NMDA-dependent synaptic function', *Neuron*, 32(6), pp. 1041–1056. doi: 10.1016/S0896-

6273(01)00553-0.
Henkemeyer, M. *et al.* (2003) 'Multiple EphB receptor tyrosine kinases shape dendritic spines in the hippocampus', *Journal of Cell Biology*, 163(6), pp. 1313–1326. doi: 10.1083/jcb.200306033.

Henneberger, C. *et al.* (2010) 'Long-term potentiation depends on release of d-serine from astrocytes', *Nature*, 463(7278), pp. 232–236. doi: 10.1038/nature08673.

Higashimori, H. *et al.* (2016) 'Selective Deletion of Astroglial FMRP Dysregulates Glutamate Transporter GLT1 and Contributes to Fragile X Syndrome Phenotypes In Vivo', *Journal of Neuroscience*, 36(27), pp. 7079–7094. doi: 10.1523/JNEUROSCI.1069-16.2016.

Himanen, J.-P. *et al.* (2001) 'Crystal structure of an Eph receptor- ephrin complex', *Nature*, 414(1998), pp. 933–8.
Impey, S., Obrietan, K. and Storm, D. R. (1999) 'Making New Connections : Role of ERK / MAP Kinase Signaling in Neuronal Plasticity', *Neuron*, 23(1), pp. 11–14. doi: 10.1016/S0896-6273(00)80747-3.

Jacobs, S., Nathwani, M. and Doering, L. C. (2010) 'Fragile X astrocytes induce developmental delays in dendrite maturation and synaptic protein expression', *BMC Neuroscience*, 11, pp. 1–11. doi: 10.1186/1471-2202-11-132.

Jones, E. V. *et al.* (2011) 'Astrocytes Control Glutamate Receptor Levels at Developing Synapses through SPARC- -Integrin Interactions', *Journal of Neuroscience*. doi: 10.1523/JNEUROSCI.4757-10.2011.
Kaech, S. *et al.* (1997) *Isoform Specificity in the Relationship of Actin to Dendritic Spines*.

Kayser, M. S. *et al.* (2006) 'Intracellular and Trans-Synaptic Regulation of Glutamatergic Synaptogenesis by EphB Receptors', *Journal of Neuroscience*, 26(47), pp. 12152–12164. doi: 10.1523/JNEUROSCI.3072-06.2006.

Kayser, M. S., Nolt, M. J. and Dalva, M. B. (2008) 'EphB Receptors Couple Dendritic Filopodia Motility to Synapse Formation', *Neuron*, 59(1), pp. 56–69. doi: 10.1016/j.neuron.2008.05.007.

Klein, R. (2004) 'Eph/ephrin signaling in morphogenesis, neural development and plasticity', *Current Opinion in Cell Biology*, 16(5), pp. 580–589. doi: 10.1016/j.ceb.2004.07.002.

Klein, R. (2009) 'Bidirectional modulation of synaptic functions by Eph/ephrin signaling', *Nature Neuroscience*, 12(1), pp. 15–20. doi: 10.1038/nn.2231.
Kucukdereli, H. *et al.* (2011) 'Control of excitatory CNS synaptogenesis by astrocyte-

secreted proteins Hevin and SPARC.', *Proceedings of the National Academy of Sciences of the United States of America*, 108(32), pp. E440-9. doi: 10.1073/pnas.1104977108.
Lauterbach, J. and Klein, R. (2006) 'Release of full-length EphB2 receptors from hippocampal neurons to cocultured glial cells.', *The Journal of neuroscience : the official journal of the Society for Neuroscience*, 26(45), pp. 11575–11581. doi: 10.1523/JNEUROSCI.2697-06.2006.

Lauterbach, J. and Klein, R. (2006) 'Release of Full-Length EphB2 Receptors from Hippocampal Neurons to Cocultured Glial Cells', *Journal of Neuroscience*. doi: 10.1523/JNEUROSCI.2697-06.2006.

Li, Z. and Sheng, M. (2003) 'Some assembly required: The development of neuronal synapses', *Nature Reviews Molecular Cell Biology*. doi: 10.1038/nrm1242.

Liebl, D. J. *et al.* (2002) *mRNA Expression of Ephrins and Eph Receptor Tyrosine Kinases in the Neonatal and Adult Mouse Central Nervous System*.

Lioy, D. T. *et al.* (2011) 'A role for glia in the progression of Rett-syndrome', *Nature*. Nature Publishing Group, 475(7357), pp. 497–500. doi: 10.1038/nature10214.

Luo, L. and O'Leary, D. D. M. (2005) 'Axon Retraction and Degeneration in Development and Disease', *Annual Review of Neuroscience*, 28(1), pp. 127–156. doi: 10.1146/annurev.neuro.28.061604.135632.

Martínez, A. and Soriano, E. (2005) 'Functions of ephrin/Eph interactions in the development of the nervous system: Emphasis on the hippocampal system', *Brain Research Reviews*, 49(2), pp. 211–226. doi: 10.1016/j.brainresrev.2005.02.001.

Matsuo, N., Reijmers, L. and Mayford, M. (2008) 'Spine-Type – Specific Recruitment of Newly Synthesized AMPA Receptors with Learning', *Science*, (February), pp. 1104–1108.

Matsuzaki, M. *et al.* (2001) 'Dendritic spine geometry is critical for AMPA receptor expression in hippocampal CA1 pyramidal neurons', *Nature Neuroscience*. doi: 10.1038/nn736.

McNaughton, B. L. and Morris, R. G. M. (1987) 'Hippocampal synaptic enhancement and information storage within a distributed memory system', *Trends in Neurosciences*. doi: 10.1016/0166-2236(87)90011-7.

Milner, B., Squire, L. and Kandel, E. (1998) 'Cognitive Neuroscience and the Study of Memory', *Neuron*, 20, pp. 445–468. doi: 10.1016/S0896-6273(00)80987-3.

Moeller, M. L. *et al.* (2006) 'EphB receptors regulate dendritic spine morphogenesis through the recruitment/phosphorylation of focal adhesion kinase and RhoA activation', *Journal of Biological Chemistry*. doi: 10.1074/jbc.M511756200.

Neves, G., Cooke, S. F. and Bliss, T. V. P. (2008) 'Synaptic plasticity, memory and the hippocampus - a neural network aproach to causality', *Nature Reviews Neuroscience*, 9(January 2008), pp. 65–75. doi: nrn2303 [pii] 10.1038/nrn2303.

Nikolakopoulou, A. M. *et al.* (2016) 'Astrocytic Ephrin-B1 Regulates Synapse Remodeling Following Traumatic Brain Injury', *ASN Neuro*. doi: 10.1177/1759091416630220.

Nusser, Z. *et al.* (1998) 'Cell type and pathway dependence of synaptic AMPA receptor number and variability in the hippocampus', *Neuron*. doi: 10.1016/S0896-6273(00)80565-6.

Oberheim, N. A. *et al.* (2009) 'Uniquely Hominid Features of Adult Human Astrocytes', *Journal of Neuroscience*, 29(10), pp. 3276–3287. doi: 10.1523/JNEUROSCI.4707-08.2009.

Pasquale, E. B. (1997) 'The Eph family of receptors', *Current Opinion in Cell Biology*, 9(5), pp. 608–615. doi: 10.1016/S0955-0674(97)80113-5.

Pasquale, E. B. (2004) 'Eph-ephrin promiscuity is now crystal clear', *Nature Neuroscience*, 7(5), pp. 417–418. doi: 10.1038/nn0504-417.

Pasquale, E. B. (2005) 'Eph receptor signalling casts a wide net on cell behaviour', *Nature Reviews Molecular Cell Biology*. doi: 10.1038/nrm1662.

Pasquale, E. B. (2008) 'Eph-Ephrin Bidirectional Signaling in Physiology and Disease', *Cell*, 133(1), pp. 38–52. doi: 10.1016/j.cell.2008.03.011.

Rempel-Clower, N. L. *et al.* (1996) *Three Cases of Enduring Memory Impairment after Bilateral Damage Limited to the Hippocampal Formation*.

Savelieva, K. V. *et al.* (2008) 'Learning and memory impairment in Eph receptor A6 knockout mice', *Neuroscience Letters*, 438(2), pp. 205–209. doi: 10.1016/j.neulet.2008.04.013.

Scannevin, R. H. and Huganir, R. L. (2000) 'Postsynaptic organization and regulation of excitatory synapses.', *Nature reviews. Neuroscience*, 1(2), pp. 133–141. doi: 10.1038/35039075.

Schafer, D. P., Lehrman, E. K. and Stevens, B. (2013) 'The "quad-partite" synapse: Microglia-synapse interactions in the developing and mature CNS', *Glia*, 61(1), pp. 24–36. doi: 10.1002/glia.22389.

Scoville, W. B. and Milner, B. (1957) 'LOSS OF RECENT MEMORY AFTER BILATERAL HIPPOCAMPAL LESIONS', *Journal of Neurology, Neurosurgery & Psychiatry*. doi: 10.1136/jnnp.20.1.11.

Sloniowski, S. and Ethell, I. M. (2012) 'Looking forward to EphB signaling in synapses', *Seminars in Cell and Developmental Biology*. Elsevier Ltd, 23(1), pp. 75–82. doi: 10.1016/j.semcdb.2011.10.020.

Spacek, J. (2004) 'Trans-Endocytosis via Spinules in Adult Rat Hippocampus', *Journal of Neuroscience*. doi: 10.1523/JNEUROSCI.0287-04.2004.
Squire, L. R. and Zola, S. M. (1996) *Memory: Recording Experience in Cells and Circuits*.

Stellwagen, D. and Malenka, R. C. (2006) 'Synaptic scaling mediated by glial TNF-??', *Nature*, 440(7087), pp. 1054–1059. doi: 10.1038/nature04671.

Strekalova, T. *et al.* (2003) 'Memory retrieval after contextual fear conditioning induces c-Fos and JunB expression in CA1 hippocampus', *Genes, Brain and Behavior*. doi: 10.1034/j.1601-183X.2003.00001.x.

Takasu, M. A. *et al.* (2002) 'Modulation of NMDA receptor-dependent calcium influx and gene expression through EphB receptors.', *Science*, 295(5554), pp. 491–495. doi: 10.1126/science.1065983.

Takumi, Y., Ramírez-León, V., Laake, P., Rinvik, E., & Ottersen, O. P. (1999). Different modes of expression of AMPA and NMDA receptors in hippocampal synapses. *Nature neuroscience*, *2*(7), 618.

Tsien, J. Z. and Huerta, P. T. (1996) *The Essential Role of Hippocampal CA1 NMDA Receptorâ€"Dependent Synaptic Plasticity in Spatial Memory*, *CELL*. doi: 10.1016/S0092-8674(00)81827-9.

Ullian, E. M. *et al.* (2001) 'Control of synapse number by glia', *Science*. doi: 10.1126/science.291.5504.657.

Wang, Y. *et al.* (2005) 'Induction of ephrin-B1 and EphB receptors during denervation-induced plasticity in the adult mouse hippocampus', *European Journal of Neuroscience*, 21(9), pp. 2336–2346. doi: 10.1111/j.1460-9568.2005.04093.x.

Willi, R. *et al.* (2012) 'Loss of EphA4 impairs short-term spatial recognition memory performance and locomotor habituation', *Genes, Brain and Behavior*. doi: 10.1111/j.1601-183X.2012.00842.x.

Xu, N. J. and Henkemeyer, M. (2012) 'Ephrin reverse signaling in axon guidance and synaptogenesis', *Seminars in Cell and Developmental Biology*. Elsevier Ltd, 23(1), pp. 58–64. doi: 10.1016/j.semcdb.2011.10.024.

Yamaguchi, Y. and Pasquale, E. B. (2004) 'Eph receptors in the adult brain', *Current Opinion in Neurobiology*. doi: 10.1016/j.conb.2004.04.003.

Yasumatsu, N. *et al.* (2008) 'Principles of Long-Term Dynamics of Dendritic Spines', *Journal of Neuroscience*, 28(50), pp. 13592–13608. doi: 10.1523/JNEUROSCI.0603-08.2008.

Yuste, R. and Bonhoeffer, T. (2004) 'Genesis of dendritic spines: Insights from ultrastructural and imaging studies', *Nature Reviews Neuroscience*. doi: 10.1038/nrn1300.

Zhang, J. M. *et al.* (2003) 'ATP Released by Astrocytes Mediates Glutamatergic Activity-Dependent Heterosynaptic Suppression', *Neuron*, 40(5), pp. 971–982. doi: 10.1016/S0896-6273(03)00717-7.

Chapter 2: Astrocytic ephrin-B1 controls synapse maintenance in the adult hippocampus

Abstract

Abnormal astrocyte-neuron interactions are implicated in neurodevelopmental disorders and neurodegenerative diseases associated with impaired learning and memory. Only recently, however, has the role of astrocytes in synaptic dynamics been investigated. Astrocyte derived secreted and contact mediated factors are been shown to promote synapse formation, maturation, and synaptic pruning. Here, I propose astrocytic ephrin-B1 as a negative regulator of synaptogenesis in adult hippocampus. I found astrocyte-specific ablation of ephrin-B1 in male mice triggers an increase in the density of dendritic spines and excitatory synaptic sites in the adult CA1 hippocampus. Interestingly, reduced dendritic spine volume and deficits in synaptic AMPAR levels suggest excess synapses are immature AMPAR silent synapses. In contrast, overexpression of astrocytic ephrin-B1 in the adult CA1 hippocampus leads to the loss of immature dendritic spines, shifting the population of dendritic spines to have larger spine heads and increased synaptic AMPAR.

Introduction

Recent studies have demonstrated the need to understand how astrocytes influence synapses, particularly because astrocyte dysfunctions are implicated in synapse pathologies associated with intellectual disabilities and learning impairments (Ballas et al. 2009; Higashimori et al. 2016; Jacobs, Nathwani, and Doering 2010; Lioy et al. 2011). Given the large number of synapses a single astrocyte may contact (Allen and Eroglu 2017; Bushong et al. 2002; Oberheim et al. 2009), it is not suprising astrocytes are involved in the development and maintenance of synapses (Allen and Eroglu 2017; Clarke and Barres 2013). Several astrocyte-secreted factors such as TSP-1, glypicans, and hevin, are known to affect both synapse structure and function by regulating synapse formation, recruiting AMPARs, and modulating synaptic functions during development (Allen et al. 2012; Christopherson et al. 2005; Ç. Eroglu et al. 2009; Kucukdereli et al. 2011; Ullian et al. 2001). Astrocytic processes are also found in direct contact with synapses, suggesting contact-mediated glial-neuronal interactions may also play a role in synapse regulation (Araque et al., 1999). Indeed, neurons directly contacting astrocytes show robust synaptogenesis, whereas neurons treated with ACM form fewer synapses (Ullian et al. 2001).

In addition to promoting synapse formation through contact-mediated mechanisms (Barker et al. 2008; Garrett and Weiner 2009; Hama et al. 2004), astrocytes may also regulate synapse elimination by phagocytosis. Astrocytes have been linked to pruning and clearing unwanted axons and synapses during synapse development (Chung et al. 2013; C. Eroglu and Barres 2010; Lauterbach and Klein 2006), allowing for

increased efficiency of neuronal transmission and refinement of functional circuits (Luo and O'Leary 2005; Cowan et al., 1984). The hippocampus which maintains a high level of synaptic plasticity in the adult brain can undergo synapse growth or elimination based on the fluctuations in neuronal activity (Yasumatsu et al. 2008). Astrocytic pruning of hippocampal synapses may contribute to persistent synaptic plasticity seen in the adult hippocampus and refinement of neural circuits during memory formation. Indeed, early electron microscopy (EM) studies revealed neuronal debris in adult hippocampal astrocytes (Spacek 2004).

Here I present new evidence suggesting a role of astrocytic ephrin-B1 in regulating hippocampal circuits, which express EphB/ephrinB (Grunwald et al. 2004; Liebl et al. 2002) in the adult mouse brain. Ephrin-B1 is a membrane-bound protein that acts as a ligand for the EphB receptors. EphB/ephrin-B interactions activate bidirectional signaling in both cells expressing EphB receptor and ephrin-B (Bush and Soriano 2009; Sloniowski and Ethell 2012; Xu and Henkemeyer 2012), and trans-synaptic ephrin-B/EphB interactions between neurons are shown to promote synapse formation and maturation in the mouse brain (Ethell et al. 2001; Grunwald et al. 2004; Henderson et al. 2001; Henkemeyer et al. 2003; Takasu et al. 2002). Although EphB/ephrinBs up-regulation is observed in glial cells after injury (Du et al. 2007; Goldshmit, McLenachan, and Turnley 2006; Nikolakopoulou et al. 2016; Wang et al. 2005), little is known regarding how astrocytic ephrinB neuronal EphB interactions effect synapse dynamics.

Our *in vivo* studies show astrocyte-specific ephrin-B1 deletion in the adult hippocampus of ERT2-Cre^{GFAP}*ephrin-B1*$^{\text{flox/y}}$ (KO) mice triggers an increase in the

number of synaptic sites and dendritic spines on CA1 hippocampal neurons. However, despite increased synapse numbers, I observed smaller dendritic spines with decreased synaptic AMPAR levels. In contrast, overexpression of ephrin-B1 in the adult astrocytes using an AAV viral transfection approach leads to reduced vGlut-positive synapses and reduced numbers of immature spines on CA1 pyramidal neurons. In addition, remaining dendritic spines in overexpressing (OE) mice had increased synaptic AMPAR subunit GluA1. These results provide evidence that astrocytic ephrin-B1 may compete with neuronal ephrin-B1 and trigger astrocyte-mediated elimination of EphB receptor-containing hippocampal synapses.

Materials and Methods

Ethics statement

All animal care protocols and procedures were approved by the UC Riverside Animal Care & Use Program, which is accredited by AAALAC International, and animal welfare assurance number A3439-01 is on file with the Office of Laboratory Animal Welfare (OLAW).

Mice

B6.Cg-Tg(*GFAP*-cre/ERT2)505Fmv/J (ERT2-Cre^{GFAP}, RRID: IMSR_JAX:012849) male mice were crossed with 129S-*Efnb1*^{tm1Sor}/J female mice (*ephrin-B1*$^{flox/+}$, RRID: IMSR_JAX:007664) to obtain ERT2-Cre^{GFAP}*ephrin-B1*$^{flox/y}$ (KO), or ERT2-Cre^{GFAP} (WT) male mice (Fig. 2.1 A). Adult WT and KO littermates received tamoxifen intraperitoneally (IP; 1 mg in 5 mg/ml of 1:9 ethanol/sunflower seed oil solution) once a day for 7 consecutive days (Fig. 2.1B). We did not detect any changes in ephrin-B1 levels in astrocytes or neurons in ERT2-Cre^{GFAP}*ephrin-B1*$^{flox/y}$ non-injected or injected with sunflower seed oil without tamoxifen as previously reported (Nikolakopoulou et al., 2016). Ephrin-B1 immunoreactivity was analyzed in ERT2-Cre^{GFAP}*ephrin-B1*$^{flox/y}$ (KO) and ERT2-Cre^{GFAP} (WT) mice (Fig. 2.2 B-F). Astrocyte-specific Cre expression was confirmed in tamoxifen-treated ERT2-Cre^{GFAP} using Rosa-CAG-LSL-tdTomato reporter mice (CAG-tdTomato, RRID:IMSR_JAX:007909; Fig. 2.2 A). Ephrin-B1 immunoreactivity was observed in cell bodies and dendrites of CA1 neurons but not hippocampal astrocytes of tamoxifen-treated KO mice (Fig. 2.2B-C). There were no changes in ephrin-B1 levels in astrocytes and neurons of untreated and tamoxifen-treated

WT animals. Genotypes were confirmed by PCR analysis of genomic DNA isolated from mouse-tails. Mice were maintained in an AAALAC accredited facility under 12-h light/dark cycle and fed standard mouse chow. All mouse studies were done according to NIH and Institutional Animal Care and Use Committee guidelines.

Stereotaxic micronjections

To induce expression of ephrin-B1 and tdTomato in hippocampal astrocytes we used adeno-associated viruses (AAV7) containing *AAV7.GfaABC1D.ephrin-B1.SV40* or *AAV7.GfaABC1D.tdTomato.SV40*, respectively (both obtained from UPenn Vector Core, http://www.med.upenn.edu/gtp/vectorcore). Viral titers were 7.56 X 10^{12} viral particles (VP)/ml for AAV7.GfaABC1D.ephrin-B1.SV40 (AAV-ephrin-B1) and 4.46 X 10^{12} VP/ml for AAV7.GfaABC1D.tdTomato.SV40 (AAV-tdTomato). VP were further concentrated with Amicon ultra-0.5 centrifugal filter (UFC505024, Sigma-Aldrich) pretreated with 0.1% Pluronic F-68 non-ionic surfactant (24040032, Thermofisher). VP were stereotaxically injected into the dorsal hippocampus of adult postnatal day (P) 70-90 C57BL/6 or Thy1-EGFP mice as follows. Mice were anesthetized by intraperitoneal injections (IP) of ketamine/xylazine mix (80 mg/kg ketamine and 10 mg/kg xylazine). Adequate anesthesia was assessed by paw pad pinch test, respiratory rhythm, righting reflex, and/or loss of corneal reflex. Animals received craniotomies (1 mm in diameter) and stereotaxic injections were performed at 2.5 mm posterior to bregma, 1.0 mm lateral to midline, and 1.2 mm from the pial surface (Fig. 2.6A,B). Control mice were bilateral injected with 2 µl of 1.16 X 10^{13} VP/ml AAV7.GfaABC1D.tdTomato.SV40 and

experimental animals received 1 μl of 3.78 X 10^{13} VP/ml AAV7,GfaABC1D.ephrin-B1.SV40 + 1 μl of 2.32 X 10^{13} VP/ml AAV7.GfaABC1D.tdTomato.SV40. Post-surgery mice received 0.3 ml of buprenorphine by subcutaneous injection every 8 h for 48 h as needed for pain and animals were alowed to recover for 14 days prior to fear conditioning tests and/or immunohistochemistry (Fig. 2.6B).

Immunohistochemistry

Animals were anesthetized with isoflurane and transcardially perfused first with 0.9% NaCl followed by fixation with 4% paraformaldehyde in 0.1 M phosphate-buffered saline (PBS), pH 7.4. Brains were post-fixed overnight with 4% paraformaldehyde in 0.1 M PBS and 100 μm coronal brain sections were cut with a vibratome. Excitatory presynaptic boutons were labeled by immunostaining against vesicular glutamate transporter 1 (vGlut1) using rabbit anti-vGlut1 antibody (0.25 mg/ml, Invitrogen Cat# 482400, RRID: AB_2533843), postsynaptic sites were identified with mouse anti-postsynaptic density-95 (PSD95) antibody (1.65 μg/ml, Invitrogen Cat# MA1-045, RRID: AB_325399). Inhibitory sites were detected with mouse anti-glutamic acid decarboxylase 65 (GAD65) antibody (10 μg/ml, BD Pharmingen Cat# 559931, RRID: AB_397380). Astrocytes were identified by immunolabeling against glial fibrillary acidic protein (GFAP) using mouse anti-GFAP antibody (1:500, Sigma-Aldrich Cat# G3893, RRID: AB_477010), and ephrin-B1 levels were detected by immunostaining with goat anti-ephrin-B1 antibody (20 μg/ml, R&D Systems Cat# AF473, RRID: AB_2293419). Secondary antibodies used were Alexa Fluor 594-conjugated donkey anti-mouse IgG (4

mg/ml, Molecular Probes Cat# A-21203, RRID: AB_141633), Alexa Fluor 647-conjugated donkey anti-rabbit IgG (4 mg/ml, Molecular Probes Cat# A-31573, RRID: AB_2536183), Alexa Fluor 647-conjugated donkey anti-goat IgG (4 mg/ml, Molecular Probes Cat# A-21447, RRID: AB_141844), or Alexa Fluor 488-conjugated donkey anti-goat IgG (4 mg/ml, Molecular Probes Cat# A-11055, RRID: AB_2534102). Sections were mounted on slides with Vectashield mounting medium containing DAPI (Vector Laboratories Inc. Cat# H-1200, RRID: AB_2336790).

Confocal Imaging and Analysis

Confocal images of the stratum radiatum (SR) and stratum lacunosum-moleculare (SLM) layers of CA1 hippocampus were taken with a Leica SP2 confocal laser-scanning microscope. A series of high-resolution optical sections (1,024 x 1,024-pixel format) were captured with a 20x or 63x water-immersion objective (1.2 numerical aperture) and 1x zoom at 1-μm step intervals (z-stack of 10 optical sections). All images were acquired under identical conditions. Each z-stack was collapsed into a single image by projection, converted to a tiff file, encoded for blind analysis, and analyzed using Image J Software. Three adjacent projections from SR were analyzed per each hippocampus from at least three animals/group. Cell area, integrated fluorescent intensity, and cell perimeter were determined for each GFAP-positive and ephrinB1-positive cell (100–300 astrocytes, z-stacks at least 10 optical images, 5–11 brain slices, 3–4 mice per group). For the analysis of vGlut1, GAD65, and PSD95 immunolabeling, at least six sequential images were captured for selected area at 1-μm step intervals, each image in the series was threshold-

adjusted to identical levels (0-160 intensity) and puncta (0.5-10 μm^2) were measured using ImageJ software (RRID: nif-0000-30467). Cell body and dendritic labeling were excluded from the analysis. Three adjacent areas from SR and SLM were imaged and analyzed per each hippocampus from at least three animals/group. Statistical analysis was performed with one-way ANOVA followed by Tukey post-hoc analysis using GraphPad Prism 6 software (RRID: SCR_002798), data represent mean ± standard error of the mean (SEM).

Dendritic spine analysis

Animals were anesthetized with isoflurane and transcardially perfused with 4% paraformaldehyde in 0.1 M PBS, pH 7.4. Brains were post-fixed for 2 h in 4% paraformaldehyde in 0.1 M PBS and 100 μm coronal sections were cut with a vibratome. Dendritic spines were labeled using a DiOlistic approach (Henkemeyer et al., 2003). Tungsten particles coated with fluorescent lipophilic dye 1,1'-dioctadecyl-3,3,3',3'-tetramethyl-indocarbocyanine perchlorate (DiI, D282, Molecular Probes) were delivered by helium-powered ejection (Bio-Rad Helios Gene Gun System) into hippocampal slices. Labeled neurons were imaged using a LSM 510 Carl Zeiss confocal microscope. 10-15 DiI-labeled neurons were randomly selected per group and dendrites were imaged using a 63x objective (1.2 NA), 1x zoom. Three-dimensional fluorescent images were created by the projection of each z stack containing 50-100 high-resolution optical serial sections (1,024 x 1,024-pixel format) taken at 0.5 μm intervals in the X-Y plane. Quantifications of the spine density (spines per 10 μm dendrite), lengths (μm), and volumes (μm^3) were

carried out using Neurolucida 360 software (MicroBrightField RRID: SCR_001775). Statistical analysis was performed with one-way ANOVA followed by Tukey post-hoc analysis using GraphPad Prism 6 software (Graphpad Prism, RRID: SCR_002798), data represent mean ± SEM.

Synaptosome Purification

Synaptosome purification was performed as previously described (Hollingsworth et al., 1985). Hippocampal tissues from adult WT or EphB1,2,3 KO mice were homogenized in 1 ml synaptosome buffer (124 mM NaCl, 3.2 mM KCl, 1.06 mM KH_2PO_4, 26 mM $NaHCO_3$, 1.3 mM $MgCl_2$, 2.5 mM $CaCl_2$, 10 mM Glucose, 20 mM HEPES). Homogenates were filtered through a 100 μm nylon net filter (NY1H02500, Millipore) and 5 μm nylon syringe filter (SF15156, Tisch International). Homogenate flow through was collected and synaptosomes were spun down at 10,000 g, 4^{o}C, for 30 min. Synaptosomes were resuspended in 800 μl synaptosome buffer. To confirm synaptosome enrichment, levels of synapsin-1, PSD95, and histone deacetylase (HDAC I) were analyzed in tissue homogenates and synaptosome fractions with western blot analysis. Synaptosomes for engulfment assays were also stained with 5% (w/v) DiI (D282, Molecular Probes) in DMSO for 10 min.

Western Blot Analysis

Tissue homogenate or purified synaptosome samples were centrifuged at 10,000 g, 4^{o}C, for 30 min, pellets were re-suspended in lysis buffer (50 mM Tris, 100 mM NaCl, 2%

TritonX-100, 10 mM EDTA,) containing 2% protease inhibitor cocktail (P8340, Sigma-Aldrich) and incubated for 2 h at 4^{o}C. Samples were added to 2X Laemmli Buffer (S3401, Sigma-Aldrich) and run on an 8-16% Tris-Glycine Gel (EC6045BOX, Invitrogen). Protein samples were transferred onto a nitrocellulose blotting membrane (10600007, GE Healthcare). Blots were blocked with 5% milk in TBS (10 mM Tris, 150 mM NaCl, pH 8.0) followed by immunostaining with mouse anti-PSD95 (1.65 µg/ml, Invitrogen Cat# MA1-045, RRID: AB_325399), rabbit anti-GluA1 (1:100, Millipore Cat# AB1504, RRID: AB_2113602), rabbit anti-GluA2/3 (0.1 µg/ml, Millipore Cat# AB1506, RRID: AB_90710), rabbit anti-HDAC I (0.40 µg/ml, Santa Cruz Biotechnologies Cat# sc-7872, RRID: AB_2279709), rabbit anti-synapsin-1 (0.2 µg/ml, Millipore Cat# AB1543P, RRID: AB_90757), or mouse anti-GAPDH (0.2 µg/ml, Thermo Fisher Scientific Cat# 39-8600, RRID:AB_2533438) antibodies in 0.1% tween 20/TBS at 4^{o}C for 16 h. Secondary antibodies used were HRP conjugated donkey anti-mouse IgG (Jackson ImmunoResearch Cat#715-035-150, RRID: AB_2340770) or HRP conjugated goat anti-rabbit IgG (Jackson ImmunoResearch Cat# 111-035-003, RRID: AB_2313567). Blots were incubated in ECL 2 Western Blotting Substrate (Pierce Cat# 80196) and a signal was collected with CL-XPosure film (34090, Pierce). Band density was analyzed by measuring band and background intensity using Adobe Photoshop CS5.1 software (RRID: SCR_014199). Statistical analysis was performed with a one-way ANOVA followed by Tukey post-hoc analysis using GraphPad Prism 6 software (RRID: SCR_002798), data represent mean ± SEM.

Results

Targeted ablation of ephrin-B1 in adult astrocytes triggers an increase in excitatory synapses on CA1 hippocampal neurons

To determine the role of astrocytic ephrin-B1 in the maintenance of hippocampal circuits we first examined whether the loss of ephrin-B1 from adult astrocyte would affect synapse numbers in CA1 hippocampus. Analysis of pre- and post-synaptic sites was performed in the adult hippocampus following tamoxifen-induced deletion of ephrin-B1 from astrocytes in ERT2-Cre^{GFAP}*ephrin-B1*$^{flox/y}$ mice. Adult ERT2-Cre^{GFAP} (WT) and ERT2-Cre^{GFAP}*ephrin-B1*$^{flox/y}$ (KO) male littermates received tamoxifen intraperitoneally (IP; 1 mg in 5mg/ml of 1:9 ethanol/sunflower seed oil) once a day for 7 days and analyzed 2 weeks after the first tamoxifen injection (Fig. 2.1B). Ephrin-B1 immunoreactivity was selectively disrupted in hippocampal astrocytes (Fig. 2.2F), but not neurons, of tamoxifen-treated KO (KO+TAM) as compared to tamoxifen-treated WT (WT+TAM) mice (Fig. 2.2B-E). Astrocyte-specific Cre expression was confirmed in tamoxifen-treated ERT2-Cre^{GFAP} mice using Rosa-CAG-LSL-tdTomato reporter (Fig. 2.2A). A significant 30% increase of dendritic spine density was observed in the SR area of CA1 hippocampus of KO+TAM mice as compared to untreated WT or WT+TAM adult mice (Fig. 2.3B, WT: 8.91 ± 0.93 WT+TAM: 8.65 ± 0.51 vs KO+TAM: 11.77 ± 0.46; $F_{(2,98)}$ =9.199, p=0.0002, ANOVA). In addition, KO mice had a greater proportion of spines with smaller heads (0-0.5 um^3 group) than WT animals (Fig. 2.3D, $F_{(14,45)}$ =36.19, p<0.0001, ANOVA). The increase in the density of dendritic spines was also accompanied by a significant increase in the number of excitatory pre-synaptic boutons,

which were immunolabeled against vGlut1 (Fig. 2.4A-C). We observed a 25% increase in vGlut1-positive puncta in the SR but not the SLM area of CA1 hippocampus of KO mice as compared to WT mice (Fig. 2.4G; WT+TAM: 2.09 ± 0.11 vs KO+TAM: 2.61 ± 0.14, t(64) =2.89, p=0.0053, t-test). In addition, we observed an increase in the co-localization of pre-synaptic vGlut1 and post-synaptic PSD95 puncta on CA1 hippocampal neurons of KO mice as compared to WT mice (Fig. 2.4I; WT+TAM: 0.800 ± 0.031 vs KO+TAM: 1.666 ± 0.232, $t_{(14)}$= 4.198, p=0.0009, t-test). The effects of astrocyte-specific ephrin-B1 deletion appear specific to excitatory synapses, as we did not detect significant differences in the number of inhibitory GAD65-positive puncta on CA1 hippocampal neurons between the groups (Fig. 2.4H; WT+TAM: 1.68 ± 0.18 vs KO+TAM: 1.97 ± 0.13, $t_{(64)}$ =1.124, p=0.2654, t-test).

Our results suggest that astrocytic ephrin-B1 is a negative regulator of new glutamatergic synapse formation specifically in the SR area of adult CA1 hippocampus.

Astrocyte-specific deletion of ephrin-B1 in the adult hippocampus triggers formation of synapses with reduced levels of AMPA receptors

Increased numbers of excitatory synapses may suggest an overall increase in excitatory drive on CA1 hippocampal neurons. Although greater in numbers, dendritic spines were structurally less mature in KO+TAM mice as compared to untreated WT or WT+TAM mice showing a 1.5-2-fold increase in the proportion of dendritic spines with smaller heads (Fig. 2.3F). To assess synapse maturation, I determined the levels of synaptic AMPAR subunits GluA1 and GluA2/3 in the adult hippocampus of WT and KO

mice. Crude synaptosomes were isolated from P90-P120 hippocampi of WT and KO mice following tamoxifen treatment and analyzed with immunoblotting (Fig. 2.5A). To normalize crude synaptosomes for increased number of synapses observed in our vGlut1/PSD95 and dendritic spines GluA1 and GluA2/3 levels were normalized to PSD95. We found a significant decrease in synaptic levels of AMPAR subunits GluA1 (Fig. 2.5C; WT+TAM: 1.04 ± 0.13 vs KO+TAM: 0.65 ± 0.079, $t_{(8)}$ =2.564, p= 0.0335, *t*-test) and GluA2/3 (Fig. 2.5D; WT+TAM: 1.01 ± 0.15 vs KO+TAM: 0.54 ± 0.09, $t_{(8)}$ =2.687, p=0.0276). This is consistent with the increase spines with an immature spine morphology (Fig. 2.3F) observed in KO mice as compared to WT mice. PSD95 levels were also normalized to GAPDH levels and an increase in PSD95 levels was observed in KO compared to WT group (Fig. 2.5B; WT+TAM: 1.252 ± 0.204 vs KO+TAM: 5.058 ± 1.895, $t_{(8)}$ = 2.505, p=0.0366). The data suggest an increase in synapse numbers, which is consistent with the observed increase in dendritic spine density (Fig. 2.3D).

Despite the increase in dendritic spine density and synaptic PSD95 levels following astrocyte-specific ephrin-B1 deletion in the adult hippocampus, it appears that the synapses are immature with reduced levels of synaptic AMPARs.

Overexpression of astrocytic ephrin-B1 inhibits immature synapse formation.

If astrocytic ephrin-B1 acts as a negative regulator of new synapse formation then we expect that overexpression of ephrin-B1 in adult hippocampal astrocytes would affect new synapse formation. To induce expression of ephrin-B1 and/or tdTomato in astrocytes, mouse hippocampi were bilaterally injected with AAV virus containing

GfaABC1D.ephrin-B1.SV40 and/or *GfaABC1D.tdTomato.SV40* (Fig. 2.6A,B). Viral microinjections targeted dorsal CA1 hippocampus of P60-70 mice allowing for expression of tdTomato or tdTomato + ephrin-B1 in CA1 hippocampal astrocytes 2 weeks later (Fig 2.6C). Transfected astrocytes were identified by tdTomato fluorescence and ephrin-B1 overexpression was confirmed by immunostaining (Fig. 2.7A,B). Astrocytic ephrin-B1 levels were significantly increased in animals injected with AAV-ephrinB1 +AAV-tdTomato as compared to AAV-tdTomato only injected mice (Fig. 2.7C; ephrin-B1 OE: 42.930 ±5.663 vs Control: 9.678 ± 1.729; $t_{(4)}$= 5.616; p=0.0049; n=3 animals, 10 astrocytes per animal).). Overexpression of ephrin-B1 also lead to a 34% decrease in dendritic spine density (Fig. 2.8C; control 6.675 ± 0.192 vs ephrin-B1 OE 4.444 ± 0.187, $t_{(183)}$= 8.305, p> 0.0001), and a 28% increase in spine volume (Fig. 2.8D; control 0.664 ± 0.024 vs ephrin-B1 OE 0.851 ± 0.04, t(171)= 3.866, p= 0.0002) without the changes in spine length (Fig. 2.8C; control: 2.007 ± 0.021 vs ephrin-B1 OE 2.080 ± 0.033, t(185)= 1.785, p= 0.0758), supporting our assumption that astrocytic ephrin-B1 promotes removal of immature spines. In addition, OE mice had a 25% decrease in the number of vGlut1-positive puncta, but not GAD65 puncta, in SR area of CA1 hippocampus compared to control group (Fig. 2.9G; control 4.30 ± 0.446 vs ephrin-B1 OE 3.22 ± 0.297, $t_{(58)}$ = 2.016, p=0.0484, *t*-test) and an increase in synaptic AMPAR subunit GluA1 levels (Fig 2.10C; GluA1; control: 0.999 ± 0.013 vs ephrin-B1 OE 1.563 ± 0.238, $t_{(6)}$= 2.068, p= 0.042. *t*-test). However only slight increases in synaptic GluA2/3 levels were observed (Fig. 2.10D; GluA2/3; control: 0.915 ± 0.116 vs ephrin-B1 OE 1.491 ± 0.412, $t_{(6)}$= 1.188, p= 0.14). In addition, a slight decrease in PSD95/GAPDH

levels are seen in OE (0.76 ± 0.131) compare to WT (Fig. 2.10 B; 1.01 ± 0.049; $t_{(6)}$= 1.24, p= 0.13; *t*-test) synaptosomes.

Increased synaptic AMPAR in OE mice suggest astrocytes are preferentially eliminating immature AMPA silent synapses, consistent with the observed increase in dendritic spine volume.

Discussion

The studies presented here demonstrate the potential role of astrocytes in maintaining hippocampal circuits in the adult mouse brain via astrocytic ephrin-B1, acting as a regulator of synaptic homeostasis in the adult hippocampus. It is thought that the plastic nature of hippocampal circuits underlies life-long learning and memory formation and as such, ongoing synapse pruning and restructuring play an important role in maintaining synaptic homeostasis in the adult hippocampus (Maletic-Savatic et al. 1999; Paolicelli et al. 2011; Spacek 2004; Stevens et al. 2007). Synapse numbers can be maintained by regulating new synapse formation or by removing weak, potentially silent, synaptic connections creating an opportunity for new connections to form. Our findings are consistent with the role of astrocytic ephrin-B1 as a negative regulator of synapse formation in the adult hippocampus, as astrocyte-specific ablation of ephrin-B1 in adult mice triggers an increase in the density of glutamatergic synapses and dendritic spines and OE decreases glutamatergic synapses. Although these effects appear to be specific to excitatory synapses, as no change were observed in the number of inhibitory GAD65-positive sites on CA1 hippocampal neurons following astrocyte-specific deletion of ephrin-B1, an in-depth investigation into the effects of excitatory inputs onto inhibitory circuits may yield interesting results. This increase in excitatory synapses was observed in SR but not SLM area of CA1 hippocampus. The layer-specific changes are noteworthy considering the role of postsynaptic ephrin-B in CA3-CA1 excitatory connections (Grunwald et al. 2004), where EphB1 and EphB2 receptors are expressed on pre-synaptic CA3 fibers that contact CA1 dendrites expressing ephrin-B ligands (Liebl et al. 2002).

Therefore, astrocytic ephrin-B1 may restrict the formation of new CA3-CA1 connections by interfering with the interactions between pre-synaptic EphB receptors and dendritic ephrin-B, whereas reduced expression of ephrin-B1 in astrocytes may promote new synapse formation. It is possible that pre-synaptic input received from entorhinal cortex by CA1 neurons in SLM area is not sensitive to the changes in ephrin-B1 expression in hippocampal astrocytes due to low expression of EphB1 and EphB2 receptors (Chenaux and Henkemeyer 2011; Liebl et al. 2002).

Aside from its pre-synaptic role in CA3-CA1 synapses, EphB2 receptor is also expressed post-synaptically on the dendrites of CA1 neurons, and is implicated in synapse development both *in vitro* and *in vivo* (Ethell et al. 2001; Henderson et al. 2001; Henkemeyer et al. 2003; Liebl et al. 2002; Takasu et al. 2002). Post-synaptic EphB receptors are implicated in both clustering and recruitment of NMDARs and AMPARs to the postsynaptic sites (Dalva et al. 2000; Kayser et al. 2006; Nolt et al. 2011; Takasu et al. 2002). Therefore, it is possible that astrocytic ephrin-B1 may also influence post-synaptic functions by disrupting post-synaptic EphB signaling and I would expect an increase in synaptic strength in the adult hippocampus following the deletion of ephrin-B1 from astrocytes. To our surprise, despite an increase in synapse numbers, I observed reduced synaptic maturation.

Synapse formation does not always correlate with an increase in synaptic strength, as newly formed synapses are often associated with silent post-synaptic spines that are usually smaller and are characterized by the presence of NMDA but absence of AMPA receptors (Durand et al., 1996; Isaac et al., 1995). Indeed, deletion of astrocytic ephrin-

B1 resulted in a nearly two-fold increase in the number of immature dendritic spines with small heads, overall reduction in the proportion of mature spines and a two-fold decrease in the synaptic levels of AMPARs. Our results suggest that the loss of ephrin-B1 may lead to impaired ability of ephrin-B1 KO astrocytes to prevent an excessive formation of immature synapses in the adult hippocampus that may also compete for synaptic proteins with existing synapses. OE of astrocytic ephrin-B1 also lead to a decrease in dendritic spine density and an increase in average spine volume as well as an increase in synaptic GluA1 levels most likely due to excessive elimination of immature synapses. Despite no changes to GAD65 puncta levels, this does not rule out changes to inhibitory circuitry within the CA1 hippocampus following astrocytic ephrin-B1 deletion, there may an increased drive of perisomatic inhibition of CA1 pyramidal neurons (Miles et al. 1996).

In contrast to ephrin-B1 that signals through its intracellular domain, astrocyte expression of GPI-linked ephrin-A3 was previously suggested to regulate glutamate transport in the hippocampus (Carmona et al. 2009; Filosa et al. 2009). Ephrin-A3 null mice exhibited increased levels of GLT1 and GLAST, which play an important role in glutamate homeostasis and the modulation of hippocampal circuits (Carmona et al. 2009). Astrocytic ephrin-A3 can also regulate synaptic functions through its interaction with synaptic EphA4 (Carmona et al. 2009; Filosa et al. 2009; Murai et al. 2003), whereas ephrin-B1 preferentially interacts with B type Eph receptors. Indeed, the increased formation of new synapses following astrocyte-specific deletion of ephrin-B1 was not observed in ephrin-A3 KO mice (Carmona et al. 2009) indicating a different role for ephrin-B1 in astrocytes.

In summary, our studies demonstrate that astrocyte specific ephrin-B1 is involved in the maintenance of excitatory glutamatergic synapses in the adult hippocampus by acting as a negative regulator of synaptogenesis (Fig. 2.11A). Therefore, the regulation of ephrin-B1 expression in astrocytes can be targeted to manipulate new synapse formation and potentially prevent synapse loss in neurodegenerative diseases. Further understanding the role of astrocytic ephrin-B1 in synaptogenesis may also provide insights into astrocyte-specific mechanisms underlying abnormal synapse development in neurodevelopmental disorders.

References

Allen, Nicola J. et al. (2012). "Astrocyte Glypicans 4 and 6 Promote Formation of Excitatory Synapses via GluA1 AMPA Receptors." *Nature* 486(7403): 410–14. http://dx.doi.org/10.1038/nature11059.

Allen, Nicola J., and Cagla Eroglu. (2017). "Cell Biology of Astrocyte-Synapse Interactions." *Neuron*.

Araque, A., Parpura, V., Sanzgiri, R. P., & Haydon, P. G. (1999). Tripartite synapses: glia, the unacknowledged partner. *Trends in neurosciences*, *22*(5), 208-215.

Ballas, Nurit, Daniel T. Lioy, Christopher Grunseich, and Gail Mandel. (2009). "Non-Cell Autonomous Influence of MeCP2-Deficient Glia on Neuronal Dendritic Morphology." *Nature Neuroscience* 12(3): 311–17.

Barker, A. J. et al. (2008). "Developmental Control of Synaptic Receptivity." *Journal of Neuroscience* 28(33): 8150–60. http://www.jneurosci.org/cgi/doi/10.1523/JNEUROSCI.1744-08.2008.

Bush, Jeffrey O., and Philippe Soriano. (2009). "Ephrin-B1 Regulates Axon Guidance by Reverse Signaling through a PDZ-Dependent Mechanism." *Genes and Development* 23(13): 1586–99.

Bushong, Eric A, Maryann E Martone, Ying Z Jones, and Mark H Ellisman. (2002). "Protoplasmic Astrocytes in CA1 Stratum Radiatum Occupy Separate Anatomical Domains." 22(1): 183–92.

Carmona, Maria A et al. (2009). "Glial Ephrin-A3 Regulates Hippocampal Dendritic Spine Morphology and Glutamate Transport." *Proceedings of the National Academy of Sciences of the United States of America* 106(30): 12524–29. http://www.pubmedcentral.nih.gov/articlerender.fcgi?artid=2718351&tool=pmcentrez&rendertype=abstract.

Chenaux, George, and Mark Henkemeyer. (2011). "Forward Signaling by EphB1/EphB2 Interacting with Ephrin-B Ligands at the Optic Chiasm Is Required to Form the Ipsilateral Projection." *European Journal of Neuroscience*.

Cowan, W. M., Fawcett, J. W., O'Leary, D. D., & Stanfield, B. B. (1984). Regressive events in neurogenesis. *Science*, *225*(4668), 1258-1265.

Christopherson, Karen S. et al. (2005). "Thrombospondins Are Astrocyte-Secreted Proteins That Promote CNS Synaptogenesis." *Cell* 120(3): 421–33.

Chung, Won Suk et al. (2013). "Astrocytes Mediate Synapse Elimination through MEGF10 and MERTK Pathways." *Nature*.

Clarke, Laura E., and Ben A. Barres. (2013). "Emerging Roles of Astrocytes in Neural Circuit Development." *Nature Reviews Neuroscience*.

Dalva, M B et al. (2000). "EphB Receptors Inetreact with NMDA Receptors and Regulate Excitatory Synapse Formation." *Cell* 103: 945–56.

Du, Juan, Tony Tran, Christine Fu, and David W. Sretavan. (2007). "Upregulation of EphB2 and Ephrin-B2 at the Optic Nerve Head of DBA/2J Glaucomatous Mice Coincides with Axon Loss." *Investigative Ophthalmology and Visual Science* 48(12): 5567–81.

Durand, G. M., Kovalchuk, Y., & Konnerth, A. (1996). Long-term potentiation and functional synapse induction in developing hippocampus. *Nature*, *381*(6577), 71.

Eroglu, Çagla et al. (2009). "Gabapentin Receptor A2δ-1 Is a Neuronal Thrombospondin Receptor Responsible for Excitatory CNS Synaptogenesis." *Cell* 139(2): 380–92.

Eroglu, Cagla, and Ben A. Barres. (2010). "Regulation of Synaptic Connectivity by Glia." *Nature* 468(7321): 223–31.

Ethell, Iryna M. et al. (2001). "EphB/Syndecan-2 Signaling in Dendritic Spine Morphogenesis." *Neuron* 31(6): 1001–13.

Filosa, Alessandro et al. (2009). "Neuron-Glia Communication via EphA4/Ephrin-A3 Modulates LTP through Glial Glutamate Transport." *Nature Neuroscience* 12(10): 1285–92. http://dx.doi.org/10.1038/nn.2394.

Garrett, A. M., and J. A. Weiner. (2009). "Control of CNS Synapse Development by -Protocadherin-Mediated Astrocyte-Neuron Contact." *Journal of Neuroscience* 29(38): 11723–31. http://www.jneurosci.org/cgi/doi/10.1523/JNEUROSCI.2818-09.2009.

Goldshmit, Yona, Samuel McLenachan, and Ann Turnley. (2006). "Roles of Eph Receptors and Ephrins in the Normal and Damaged Adult CNS." *Brain Research Reviews*.

Grunwald, Ilona C. et al. (2004). "Hippocampal Plasticity Requires Postsynaptic EphrinBs." *Nature Neuroscience*.

Hama, Hiroshi, Chikako Hara, Kazuhiko Yamaguchi, and Atsushi Miyawaki. (2004). "PKC Signaling Mediates Global Enhancement of Excitatory Synaptogenesis in Neurons Triggered by Local Contact with Astrocytes." *Neuron* 41(3): 405–15.

Henderson, Jeffrey T. et al. (2001). "The Receptor Tyrosine Kinase EphB2 Regulates NMDA-Dependent Synaptic Function." *Neuron* 32(6): 1041–56.

Henkemeyer, Mark et al. (2003). "Multiple EphB Receptor Tyrosine Kinases Shape Dendritic Spines in the Hippocampus." *Journal of Cell Biology* 163(6): 1313–26.

Higashimori, H. et al. (2016). "Selective Deletion of Astroglial FMRP Dysregulates Glutamate Transporter GLT1 and Contributes to Fragile X Syndrome Phenotypes In Vivo." *Journal of Neuroscience* 36(27): 7079–94. http://www.jneurosci.org/cgi/doi/10.1523/JNEUROSCI.1069-16.2016.

Isaac, John T.R., Roger A. Nicoll, and Robert C. Malenka. (1995). "Evidence for Silent Synapses: Implications for the Expression of LTP." *Neuron* 15(2): 427–34.

Jacobs, Shelley, Meera Nathwani, and Laurie C. Doering. (2010). "Fragile X Astrocytes Induce Developmental Delays in Dendrite Maturation and Synaptic Protein Expression." *BMC Neuroscience* 11: 1–11.

Kayser, M. S., A. C. McClelland, E. G. Hughes, and M. B. Dalva. (2006). "Intracellular and Trans-Synaptic Regulation of Glutamatergic Synaptogenesis by EphB Receptors." *Journal of Neuroscience* 26(47): 12152–64. http://www.jneurosci.org/cgi/doi/10.1523/JNEUROSCI.3072-06.2006.

Kucukdereli, Hakan et al. (2011). "Control of Excitatory CNS Synaptogenesis by Astrocyte-Secreted Proteins Hevin and SPARC." *Proceedings of the National Academy of Sciences of the United States of America* 108(32): E440-9. http://www.pnas.org/content/108/32/E440.

Lauterbach, Jenny, and Rüdiger Klein. (2006). "Release of Full-Length EphB2 Receptors from Hippocampal Neurons to Cocultured Glial Cells." *The Journal of neuroscience : the official journal of the Society for Neuroscience* 26(45): 11575–81.

Liebl, Daniel J, Carol J Morris, Mark Henkemeyer, and Luis F Parada. (2002). *MRNA Expression of Ephrins and Eph Receptor Tyrosine Kinases in the Neonatal and Adult Mouse Central Nervous System*.

Lioy, Daniel T. et al. (2011). "A Role for Glia in the Progression of Rett-Syndrome." *Nature* 475(7357): 497–500. http://dx.doi.org/10.1038/nature10214.

Luo, Liqun, and Dennis D.M. O'Leary. (2005). "AXON RETRACTION AND DEGENERATION IN DEVELOPMENT AND DISEASE." *Annual Review of Neuroscience*.

Maletic-Savatic, M. et al. (1999). "Rapid Dendritic Morphogenesis in CA1 Hippocampal Dendrites Induced by Synaptic Activity." *Science* 283(5409): 1923–27. http://www.ncbi.nlm.nih.gov/pubmed/10082466%0Ahttp://www.sciencemag.org/cgi/doi/10.1126/science.283.5409.1923.

Miles, Richard et al. (1996). "Differences between Somatic and Dendritic Inhibition in the Hippocampus." *Neuron*.

Murai, Keith K. et al. (2003). "Control of Hippocampal Dendritic Spine Morphology through Ephrin-A3/EphA4 Signaling." *Nature Neuroscience* 6(2): 153–60.

Nikolakopoulou, Angeliki M. et al. (2016). "Astrocytic Ephrin-B1 Regulates Synapse Remodeling Following Traumatic Brain Injury." *ASN Neuro*.

Nolt, M. J. et al. (2011). "EphB Controls NMDA Receptor Function and Synaptic Targeting in a Subunit-Specific Manner." *Journal of Neuroscience* 31(14): 5353–64. http://www.jneurosci.org/cgi/doi/10.1523/JNEUROSCI.0282-11.2011.

Oberheim, N. A. et al. (2009). "Uniquely Hominid Features of Adult Human Astrocytes." *Journal of Neuroscience*.

Paolicelli, Rosa C et al. (2011). "Synaptic Pruning by Microglia Is Necessary for Normal Brain Synaptic Pruning by Microglia Is Necessary for Normal Brain Development." *Science* 333(September): 1456–59.

Sloniowski, Slawomir, and Iryna M. Ethell. (2012). "Looking Forward to EphB Signaling in Synapses." *Seminars in Cell and Developmental Biology*.

Spacek, J. (2004). "Trans-Endocytosis via Spinules in Adult Rat Hippocampus." *Journal of Neuroscience*.

Stevens, Beth et al. (2007). "The Classical Complement Cascade Mediates CNS Synapse Elimination." *Cell* 131(6): 1164–78.

Takasu, Mari A et al. (2002). "Modulation of NMDA Receptor-Dependent Calcium Influx and Gene Expression through EphB Receptors." *Science* 295(5554): 491–95. http://www.ncbi.nlm.nih.gov/pubmed/11799243.

Ullian, E. M., S. K. Sapperstein, K. S. Christopherson, and B. A. Barres. (2001). "Control of Synapse Number by Glia." *Science* 291(5504): 657–61.

Wang, Yan et al. (2005). "Induction of Ephrin-B1 and EphB Receptors during Denervation-Induced Plasticity in the Adult Mouse Hippocampus." *European Journal of Neuroscience* 21(9): 2336–46.

Xu, Nan Jie, and Mark Henkemeyer. (2012). "Ephrin Reverse Signaling in Axon Guidance and Synaptogenesis." *Seminars in Cell and Developmental Biology*.

Yasumatsu, N. et al. (2008). "Principles of Long-Term Dynamics of Dendritic Spines." *Journal of Neuroscience*.

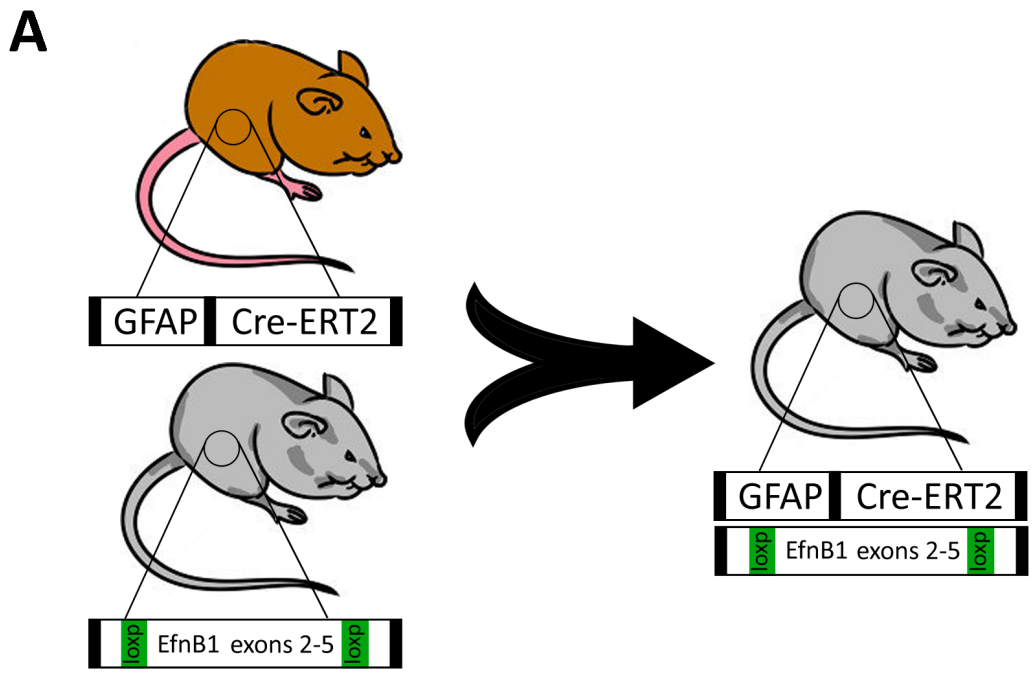

B

Tamoxifen:
Intraperitoneal injections daily for 7 consecutive days
200ml (5mg/ml; 1:9 ethanol/ sunflower seed oil solution)

Day 0 **Day 7** **Day 14**

P 72-80

Perfuse and collect coronal hippocampal sections:
IHC: vGlut1/ PSD95/ GAD65/ PV
Dendritic spine analysis (Thy1-GFP)

Collect synaptosomes
Western Blots: GluA1, GluA2/3, PSD95, GAPDH

Behavior tests
Fear conditioning

Figure 2.1

Figure 2.1. Tamoxifen mediated astrocytic ephrin-B1 KO mouse model.

(A) ERT2-Cre^{GFAP} male mice were crossed with *ephrin-B1* $^{flox/y}$ female mice for ERT2-Cre^{GFAP}*ephrin-B1* $^{flox/y}$ littermates. (B) Adult male ERT2-Cre^{GFAP} and ERT2-Cre^{GFAP}*ephrin-B1* $^{flox/y}$ mice (P90 –P110) were intraperitoneally injected with 1 mg of tamoxifen once a day for 7 consecutive days. Immunohistochemistry, spine labeling, synaptosome isolation, and behavior tests were performed 14 d after first injection.

Figure 2.2

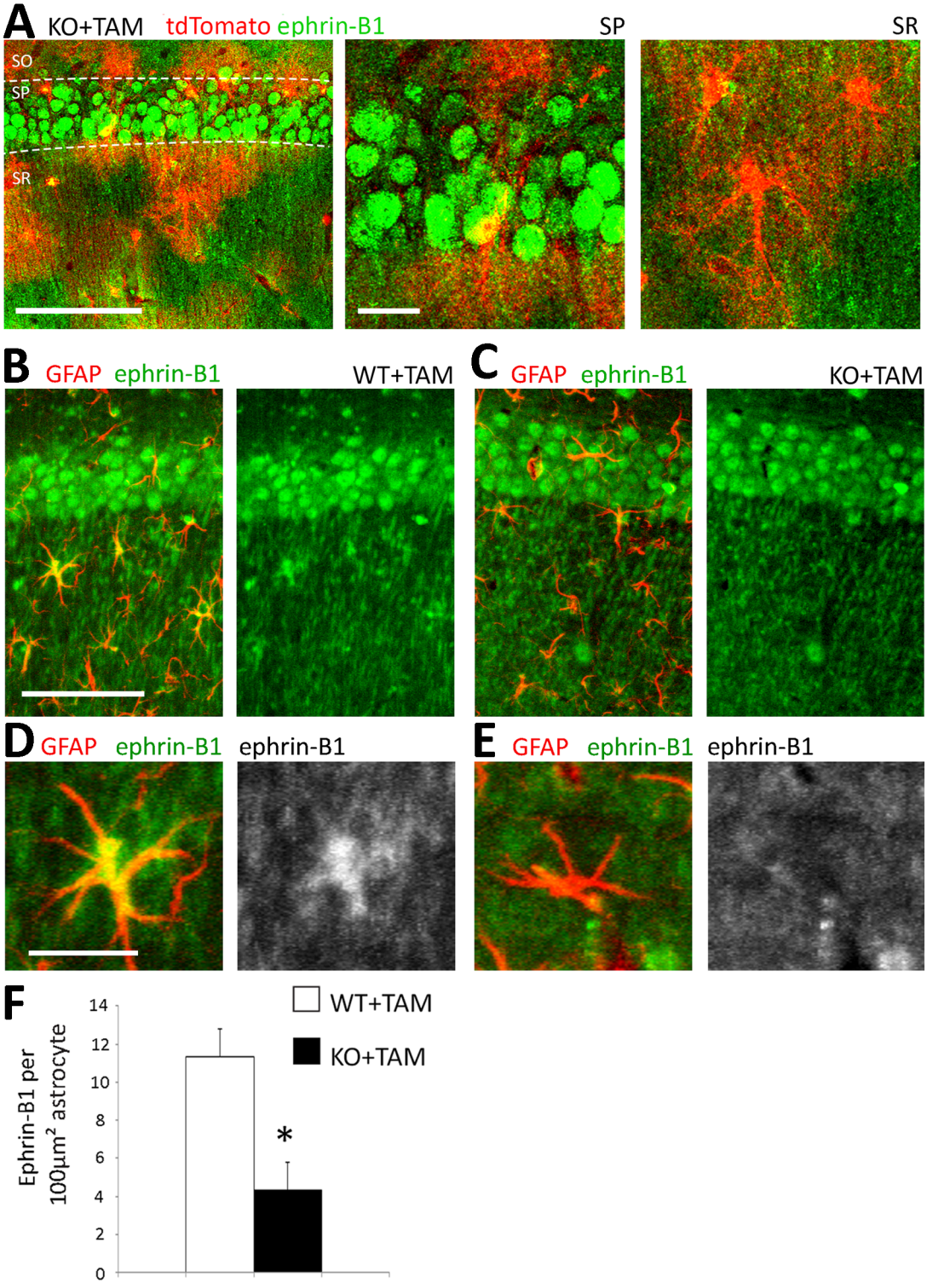
A
KO+TAM
tdTomato ephrin-B1
SO
SP
SR
SP
SR
B
GFAP ephrin-B1
WT+TAM
C
GFAP ephrin-B1
KO+TAM
D
GFAP ephrin-B1
ephrin-B1
E
GFAP ephrin-B1
ephrin-B1
F
WT+TAM
KO+TAM
Ephrin-B1 per 100µm² astrocyte
14
12
10
8
6
4
2
0
*

Figure 2.2. Ephrin-B1 ablation in CA1 hippocampal astrocytes.

(A) Max projection confocal images of the CA1 hippocampus in tamoxifen-injected ERT2-Cre$^{GFAP}{}_{stop}{}^{\text{flox}}{}_{tdTomato}$ mice show tdTomato expression in astrocytes of SR, but not in CA1 neurons of the SP area. Ephrin-B1 immunoreactivity was detected in cell bodies (green, SP) and dendrites (green, SR) of CA1 neurons but not in tdTomato-positive astrocytes (red). Low-magnification. Scale bars: 100 μ□m; high-magnification, 20 μm. (B,C) Max projection confocal images show GFAP (red) and ephrin-B1 (green) immunoreactivity in the CA1 hippocampus. Scale bar, 100 μm. (D, E) High-magnification images show ephrin-B1 immunoreactivity in astrocytes of WT□+TAM but not KO+TAM mice. Ephrin-B1 is detected in dendrites of CA1 neurons verifying that deletion of ephrin-B1 is specific to astrocytes. Scale bar, 25 μm. (F) Astrocytic ephrin-B1 immunoreactivity was significantly reduced in the hippocampus of KO+TAM compared with WT+TAM mice (n =3 mice, t-test, *p=□0.05). Graphs show mean values and error bars represent SEM.

Figure 2.3

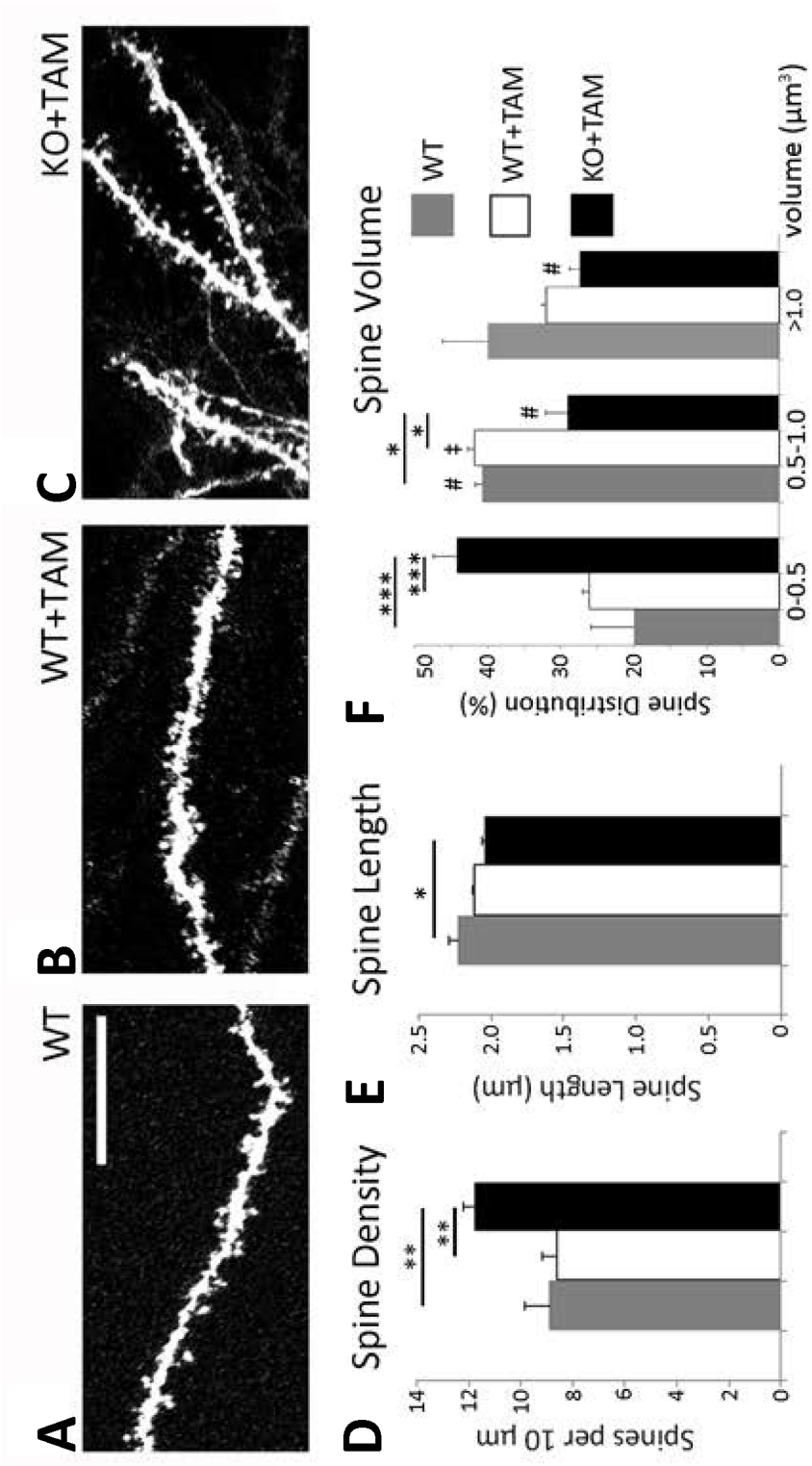
A
WT
B
WT+TAM
C
KO+TAM
D
Spine Density
Spines per 10 µm
E
Spine Length
Spine Length (µm)
F
Spine Distribution (%)
Spine Volume
WT
WT+TAM
KO+TAM
0-0.5
0.5-1.0
>1.0
volume (µm³)

Figure 2.3. Synaptogenic effects of astrocyte-specific deletion of ephrin-B1 in the CA1 hippocampus.

(A–C) Max projection confocal images of DiI-labeled dendrites of CA1 neurons in the SR area of CA1 hippocampus of WT, WT+TAM, and KO+TAM adult mice. Scale bar, 5 μm. (D–F) Graphs show the average number of dendritic spines per 10 μm dendrite (D), average spine length (E) and spine volume (F). There is a significant 36% increase in average dendritic spine density in KO+TAM mice compared with WT and WT+TAM mice; error bars represent SEM (n = 3– 6 mice, WT: 8.91 □± 0.93 WT+TAM: 8.65 ± 0.51 vs KO+TAM: 11.77 ± 0.46; $F_{(2,98)} = 9.199$, p =0.0002; one-way ANOVA, Tukey's *post hoc* test, $^{**}p = 0.01$). A significant two fold increase in the proportion of dendritic spines with smaller heads (volume 0 – 0.5 μm ^{3}) and a decrease in percentage of mature spines with volume 0.5–1.0 μm ^{3} are observed in KO+TAM group compared with WT and WT+TAM groups (n = 3– 6 mice, $F_{(14,45)} = 36.19$, $p = 0.0001$ and $F = 7.701$ p = 0.05, respectively; two-way ANOVA followed by Tukey's *post hoc*, $^{*}p = 0.05$, $^{***}p$ = 0.001). WT and WT+TAM groups exhibit a significantly higher proportion of spines with larger heads (volume 0.5–1.0 μm ^{3}) than the spines with smaller heads (volume 0 – 0.5 μm ^{3}; n = 3– 6 mice, one-way ANOVA, Tukey's *post hoc* test, #$p = 0.05$, ‡$p = 0.001$, $F = 4.462$). KO+TAM group shows a significantly lower proportion of spines with larger heads (volume 0.5–1.0 μm ^{3} and □1.0 μm ^{3}) than spines with smaller heads (volume 0 – 0.5 μm ^{3}; n = 3– 6 mice, one-way ANOVA, Tukey's *post hoc* test, #$p = 0.05$, $F = 4.462$).

Graphs show mean values and error bars represent SEM.

Figure 2.4

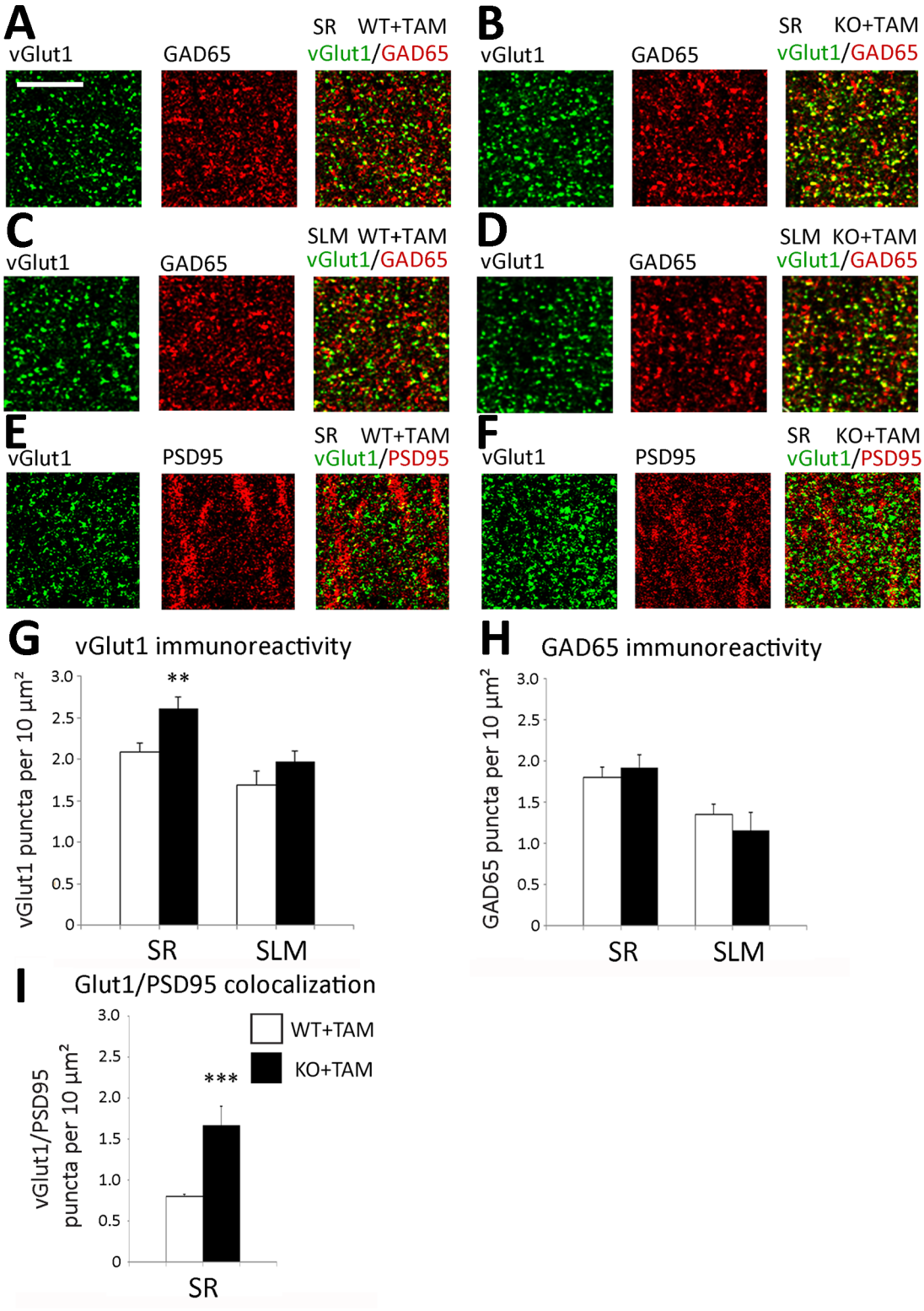
A
vGlut1
GAD65
SR WT+TAM
vGlut1/GAD65
B
vGlut1
GAD65
SR KO+TAM
vGlut1/GAD65
C
vGlut1
GAD65
SLM WT+TAM
vGlut1/GAD65
D
vGlut1
GAD65
SLM KO+TAM
vGlut1/GAD65
E
vGlut1
PSD95
SR WT+TAM
vGlut1/PSD95
F
vGlut1
PSD95
SR KO+TAM
vGlut1/PSD95
G
vGlut1 immunoreactivity
vGlut1 puncta per 10 µm²
3.0
2.5
2.0
1.5
1.0
0.5
0
**
SR
SLM
H
GAD65 immunoreactivity
GAD65 puncta per 10 µm²
3.0
2.5
2.0
1.5
1.0
0.5
0
SR
SLM
I
Glut1/PSD95 colocalization
vGlut1/PSD95 puncta per 10 µm²
3.0
2.5
2.0
1.5
1.0
0.5
0
***
WT+TAM
KO+TAM
SR

Figure 2.4. Astrocytic ephrin-B1 deletion increases glutamatergic synapses in the SR.

(A-D) Confocal images showing vGlut1 (green) and GAD65 (red) immunolabeling in SR (A,B) and SLM (C,D) areas of the CA1 hippocampus of WT+TAM (A,C) and KO+TAM (H, J) adult mice. Scale bar, 50 μm. (E,F) Confocal images showing vGlut1 (green) and PSD95 (red) immunolabeling in SR area of the CA1 hippocampus of WT+TAM (E) and KO+TAM (F) adult mice. (G,H) Graphs show the density of vGlut1 and GAD65-positive puncta per 10 μm^2 of the SR and SLM areas in the CA1 hippocampus of WT+TAM and KO+TAM mice. (G) There is a significant 25% increase in vGlut1-positive puncta in SR but not SLM area of KO+TAM compared with WT+TAM group; error bars represent SEM (n = 3– 6 mice, WT+TAM: 2.09 ± 0.11 vs KO+TAM: 2.61 ± 0.14, $t_{(64)} = 2.89$, p= 0.0053, t test, $^{**}p = 0.01$). (H) There was no significant difference in the number of inhibitory GAD65- positive puncta between WT+TAM and KO+TAM mice (n = 3– 6 mice, WT+TAM: 1.68 ± 0.18 vs KO+TAM: 1.97 ± 0.13, $t_{(64)} \pm 1.124$, $p = 0.2654$, t test). (I) Graph shows the density of colocalized vGlut1 and PSD95-positive puncta per 10 μm^2 in the SR area of the CA1 hippocampus of WT+TAM and KO+TAM mice. There is a significant increase in vGlut1/PSD95 colocalization in KO+TAM compared with WT+TAM group, error bars represent SEM (n = 3 mice, WT+TAM: 0.800 ± 0.031 vs KO+TAM: 1.666 ± 0.232, $t_{(14)} = 4.198$, $p = 0.0009$, t test, $^{***}p = 0.001$). Graphs show mean values and error bars represent SEM.

Figure 2.5

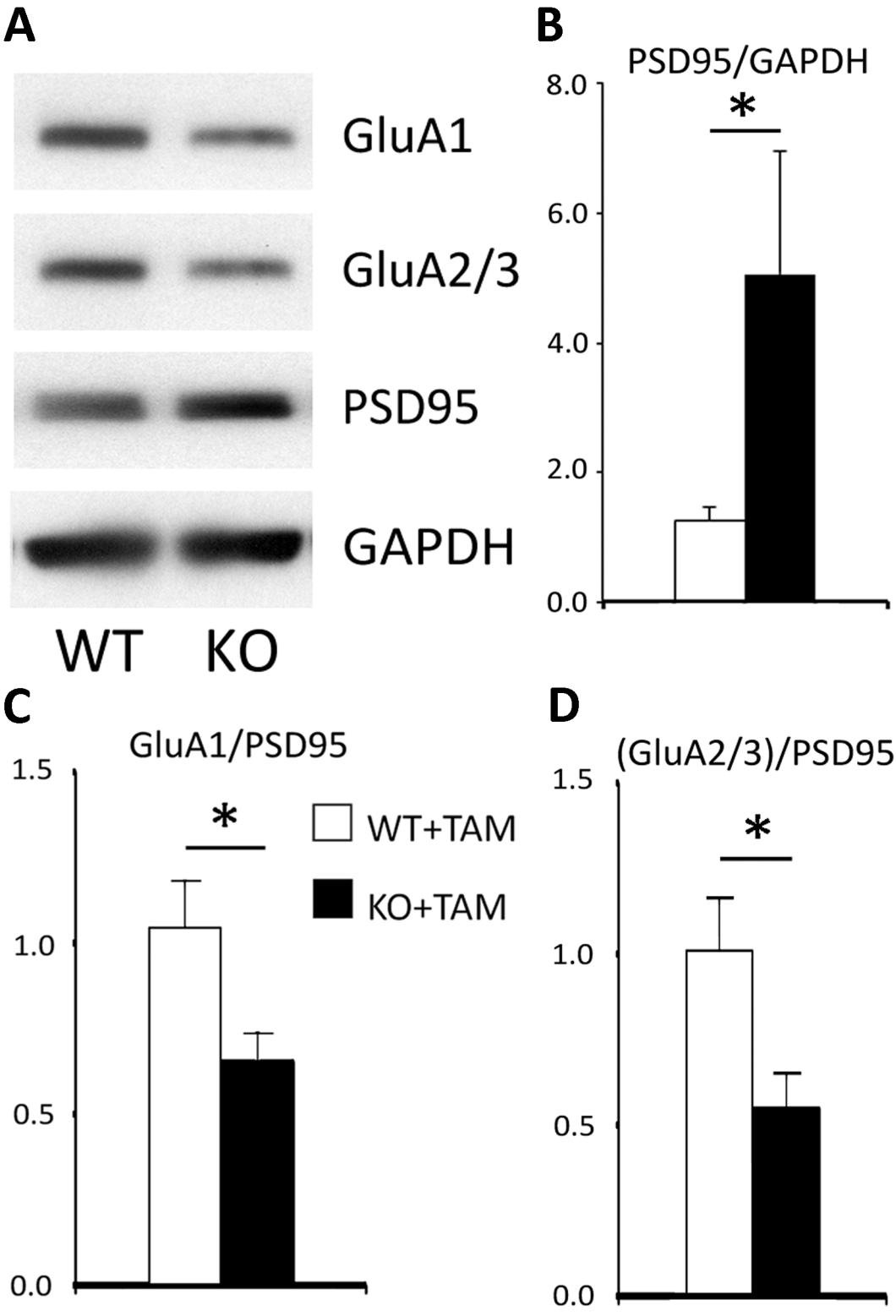
A
GluA1
GluA2/3
PSD95
GAPDH
WT
KO
B
PSD95/GAPDH
8.0
6.0
4.0
2.0
0.0
*
C
GluA1/PSD95
1.5
1.0
0.5
0.0
*
WT+TAM
KO+TAM
D
(GluA2/3)/PSD95
1.5
1.0
0.5
0.0
*

Figure 2.5. KO mice show deficits in synaptic AMPAR levels.

(A) Western blots show levels of AMPAR subunits (GluA1 and GluA2/3), PSD95 and GAPDH in synaptosomes isolated from the hippocampus of WT and KO mice. (B) There was a significant increase in synaptic PSD95 levels in naive KO compared with naive WT (WT+TAM: 1.252 ± 0.204 vs KO+TAM: 5.058 ± 1.895, $t_{(8)} = 2.505$, $p = 0.0366$). GluA1 and GluA2/3 levels were not significantly different between the groups (GluA1 WT+TAM: 1.168 ± 0.087 vs KO+TAM: 3.358 ± 1.309, $t_{(8)} = 2.104$, $p = 0.0685$; GluA2/3 WT+TAM: 1.118 ± 0.075 vs KO+TAM: 2.589 ± 1.010, $t_{(7)} = 1.65$, $p = 0.143$). However, there was a significant decrease in AMPAR/PSD95 ratio for synaptic (C) GluA1 (WT+TAM: 1.04 ± 0.13 vs KO+TAM: 0.65 ± 0.079, $t_{(8)} = 2.564$, $p = 0.0335$, *t* test) and (D) GluA2/3 subunits (WT+TAM: 1.01 ± 0.15 vs KO+TAM: 0.54 ± 0.09, $t_{(8)} = 2.687$, $p = 0.0276$). Graphs show mean values and error bars represent SEM.

Figure 2.6

A

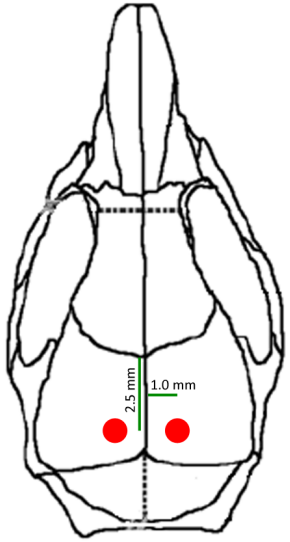

B

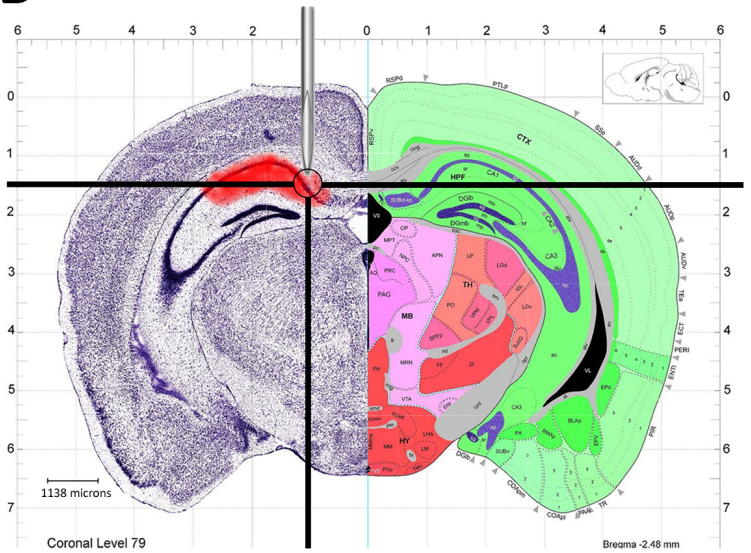

C

Concentrate AAV:

AAVtdTomato (1.16 × 10^{13} VP/ml)

AAVephrin-B1 (3.78 × 10^{13} VP/ml) + AAVtdTomato (1 µl of 2.32 × 10^{13} VP/ml)

Stereotactic AAV injection

Ketamine (80mg/kg) + Xylazine (10mg/kg)

Bilateral injections of 2ml viral solution

Day 0 **Day 7** **Day 14**

Buprenorphine (0.3ml)

Inject every 8h for 48h post surgery

P 72-80

Perfuse and collect coronal hippocampal sections:

IHC: vGlut1/ PSD95/ GAD65/ PV

Dendritic spine analysis (Thy1-GFP)

Collect synaptosomes

Western Blots: GluA1, GluA2/3, PSD95, GAPDH

Behavior tests

Fear conditioning

Figure 2.6. AAV mediated overexpression of astrocytic ephrin-B1 in the CA1 hippocampus.

(A) Diagram depicts coordinates (-2.5mm) from bregma and (-1.0mm) from midline where a craniotomy was preformed (red). (B) Injection depth (-1.2mm) and spread (red) of AAV virus two week after surgery. (C). Thy-1 GFP mice (P72-80) received bilateral hippocampal injections of 2µl AAVtdTomato (control) or 1µl AAVephrin-B1 + 1µl AAVtdTomato (OE), Immunohistochemistry, spine labeling, synaptosome isolation, and behavior tests were performed 14 d after first injection.

Figure 2.7

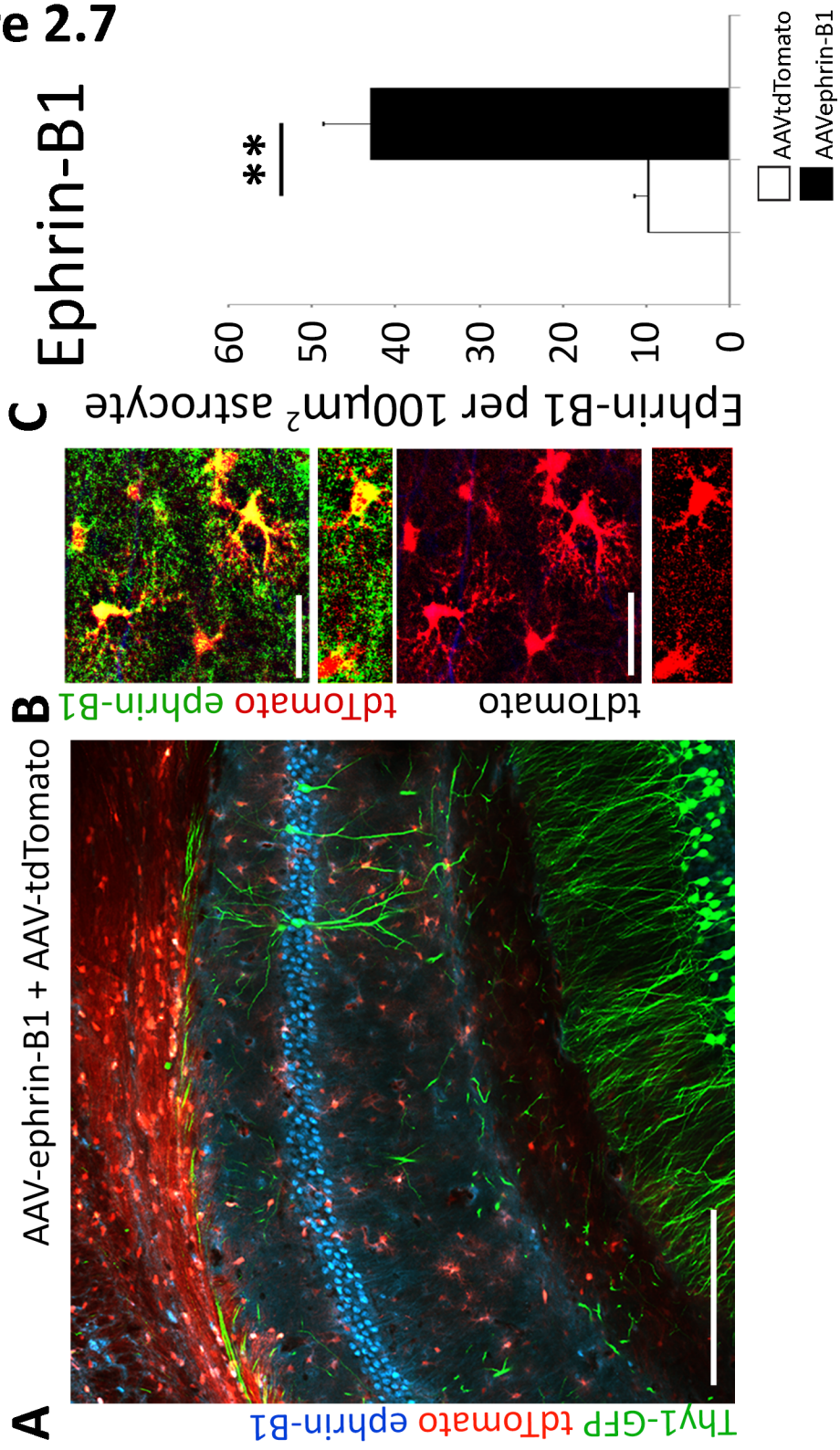
A
AAV-ephrin-B1 + AAV-tdTomato
Thy1-GFP tdTomato ephrin-B1
B
tdTomato
tdTomato ephrin-B1
C
Ephrin-B1
Ephrin-B1 per 100μm² astrocyte
0
10
20
30
40
50
60
**
AAVtdTomato
AAVephrin-B1

Figure 2.7. Overexpression of astrocytic ephrin-B1 in the adult mouse hippocampus.

(A) Confocal images showing GFP (green), tdTomato (red) and ephrin-B1 immunoreactivity (blue) in CA1 hippocampus of Thy1-EGFP adult mice injected with AAV-*GFAP-ephrinB1* + AAV-*GFAP-tdTomato*. Scale bar, 150 μm. (B) Confocal images of hippocampal astrocytes expressing tdTomato (red) and ephrin-B1 (green). Scale bar, 25 μm. (C) Graph shows ephrin-B1 immunoreactivity in astrocytes of AAV-*GFAP-tdTomato* (Control) or AAV-*GFAP-ephrinB1* + AAV-*GFAP-tdTomato* (ephrin-B1 OE) hippocampus. There is a significant increase in ephrin-B1 levels in hippocampal astrocytes of ephrin-B1 OE compared with control mice. Graph shows mean values and error bars represent SEM (n = 3 mice, 10 astrocytes per animal; ephrin-B1 OE: 42.930 ± 5.663 vs control: 9.678 ± 1.729; $t_{(4)} = 5.616$; $p = 0.0049$, t test, $^{**}p = 0.01$). Graphs show mean values and error bars represent SEM.

Figure 2.8

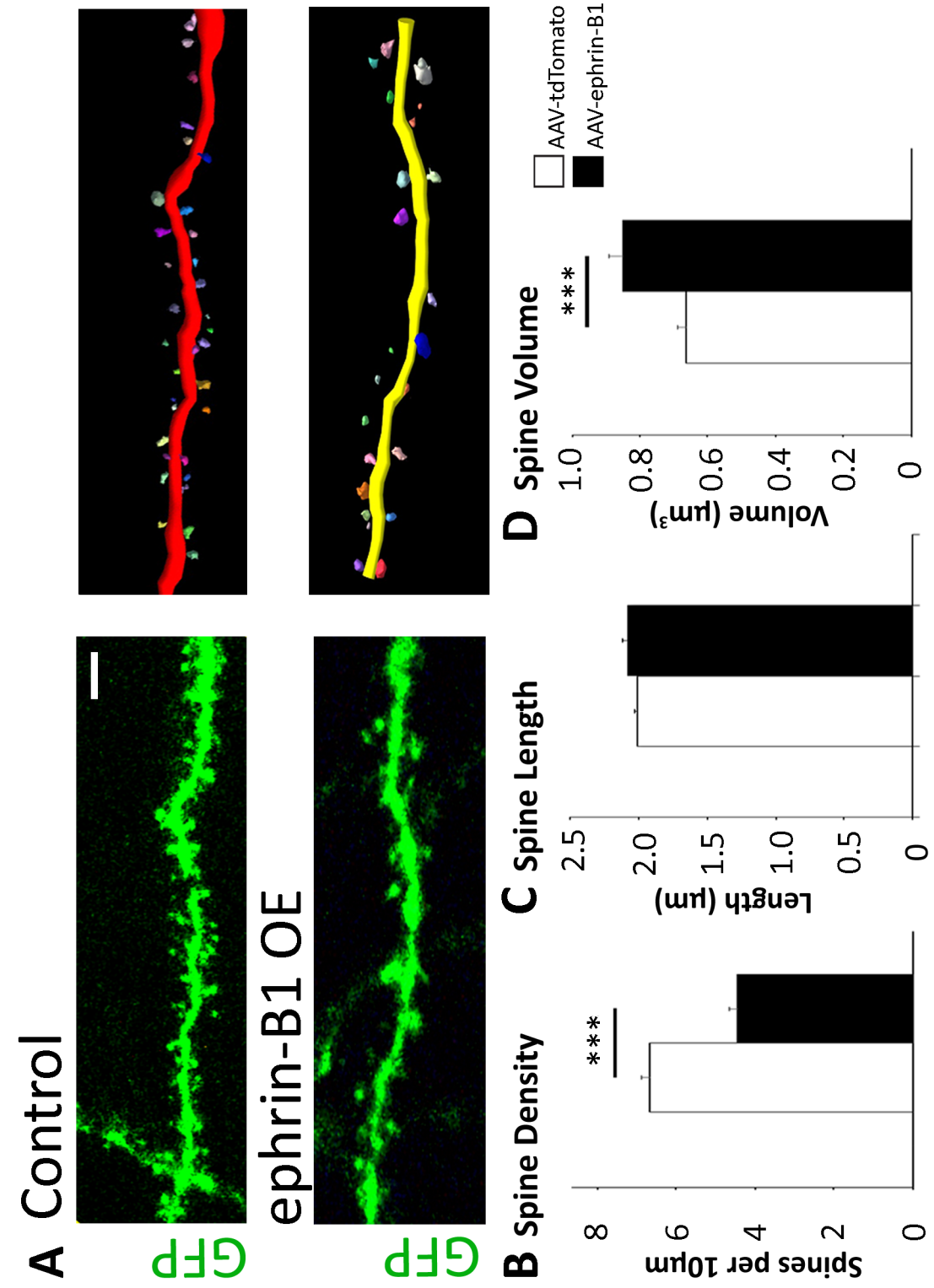
A Control
ephrin-B1 OE
GFP
GFP
B Spine Density
Spines per 10μm
***
C Spine Length
Length (μm)
D Spine Volume
Volume (μm³)
***
AAV-tdTomato
AAV-ephrin-B1

Figure 2.8. Astrocytic ephrin-B1 overexpression reduces immature dendritic spines number.

(A) Confocal images of Thy1-EGFP-expressing dendrites of CA1 neurons in control (AAV-tdTomato) or ephrin-B1 OE (AAV-ephrinB1+AAV-tdTomato) hippocampus with corresponding Neurolucida 360 rendering of the images. (B-D) Graphs show analysis of dendritic spine density (B), length (C), and average spine volume (D) in SR area of CA1 hippocampus of control and ephrin-B1 OE group. There is a significant 34% decrease in dendritic spine density (n = 81–92 dendrites, 3 mice per group; control: 6.675 ± 0.192 vs ephrin-B1 OE: 4.444 ± 0.187, $t_{(183)} = 8.305$, $p = 0.0001$, t test, ***$p = 0.001$) and a 28% increase in spine volume (n = 81–92 dendrites; 3 mice per group, control: 0.664 ± 0.024 vs ephrin-B1 OE: 0.851 ± 0.04, $t_{(171)} = 3.866$, $p = 0.0002$, t test, ***$p = 0.001$) without changes to spine length (n = 81–92 dendrites, 3 mice per group; control: 2.007 ± 0.021 vs ephrin-B1 OE: 2.080 ± 0.033, $t_{(185)} = 1.785$, $p = 0.0758$, t test). Graphs show mean values and error bars represent SEM.

Figure 2.9

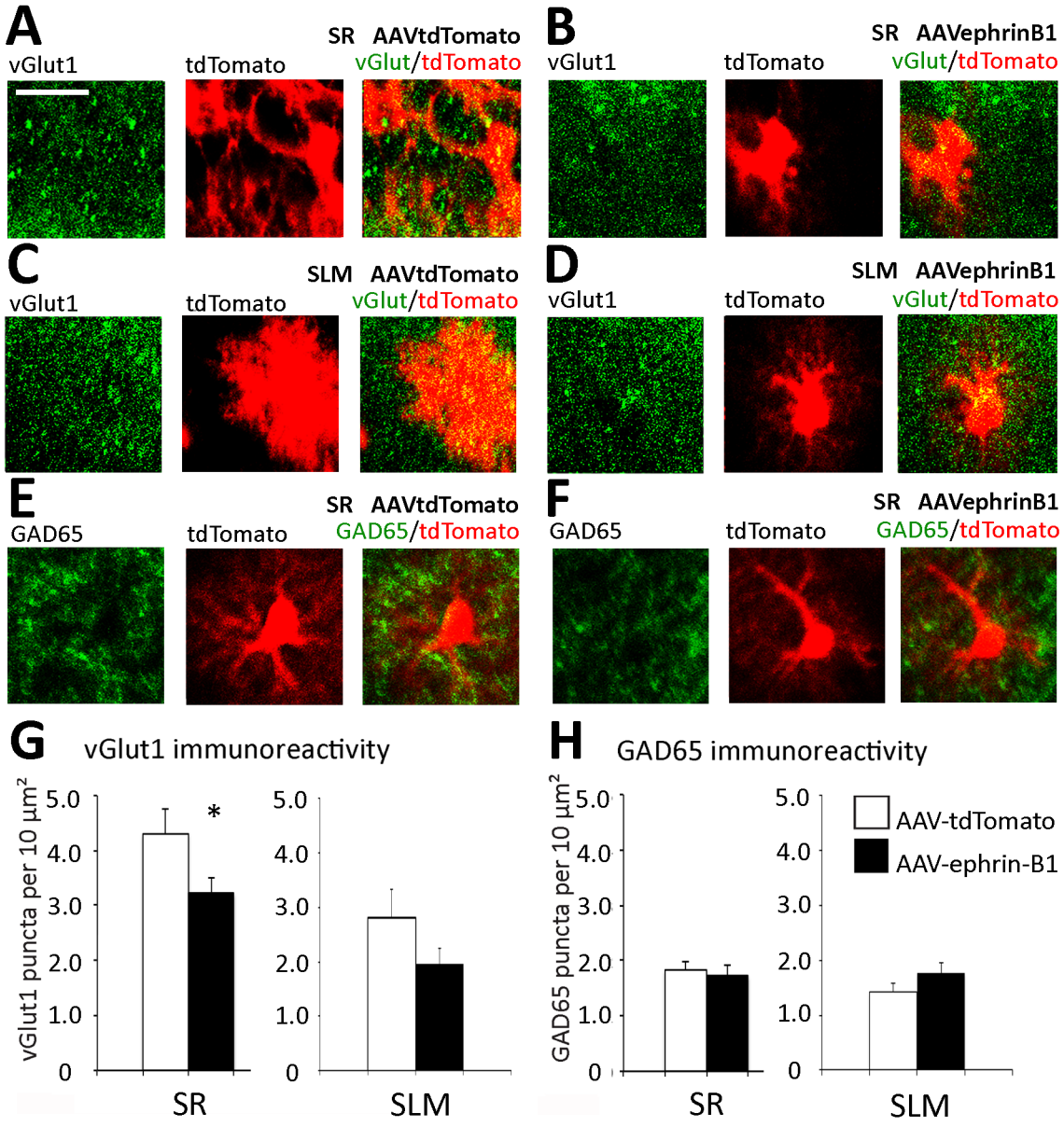
A
vGlut1
tdTomato
SR AAVtdTomato
vGlut/tdTomato
B
vGlut1
tdTomato
SR AAVephrinB1
vGlut/tdTomato
C
vGlut1
tdTomato
SLM AAVtdTomato
vGlut/tdTomato
D
vGlut1
tdTomato
SLM AAVephrinB1
vGlut/tdTomato
E
GAD65
tdTomato
SR AAVtdTomato
GAD65/tdTomato
F
GAD65
tdTomato
SR AAVephrinB1
GAD65/tdTomato
G
vGlut1 immunoreactivity
vGlut1 puncta per 10 µm²
5.0
4.0
3.0
2.0
1.0
0
*
SR
SLM
H
GAD65 immunoreactivity
GAD65 puncta per 10 µm²
AAV-tdTomato
AAV-ephrin-B1
SR
SLM

Figure 2.9. Overexpression of astrocytic ephrin-B1 reduces the number of glutamatergic synapse.

(A-D) Confocal images showing vGlut1 (green) and tdTomato (red) immunolabeling in SR (A,B) and SLM (C,D) areas of the CA1 hippocampus of AAV-*GFAP-tdTomato* (A,C,E) and AAV-*GFAP-ephrinB1* + AAV-*GFAP-tdTomato* (*B,D,F*) adult mice. Scale bar, 50 μm. (E, F) Confocal images showing GAD65 (green) and tdTomato (red) immunolabeling in SR area of the CA1 hippocampus of AAV-*GFAP-tdTomato* (E) and AAV-*GFAP-ephrinB1* + AAV-*GFAP-tdTomato* (F) adult mice. (G,H) Graphs show the density of vGlut1 (A-D) and GAD65-positive (E,F) puncta per 10 μm^2 of the SR area in the CA1 hippocampus of Thy1-EGFP adult mice injected with AAV-*GFAP-tdTomato* (Control) or AAV-*GFAP-ephrinB1* + AAV-*GFAP-tdTomato* (ephrin-B1 OE). There is a significant 25% decrease in vGlut1-positive puncta in the SR of ephrin-B1 OE group compared with WT group (n = 5 mice; control: 4.30 ± 0.446 vs ephrin-B1 OE: 3.22 ± 0.297, $t_{(58)} = 2.016$, $p = 0.0484$, t test, $^*p = 0.05$). Graphs show mean values and error bars represent SEM.

Figure 2.10

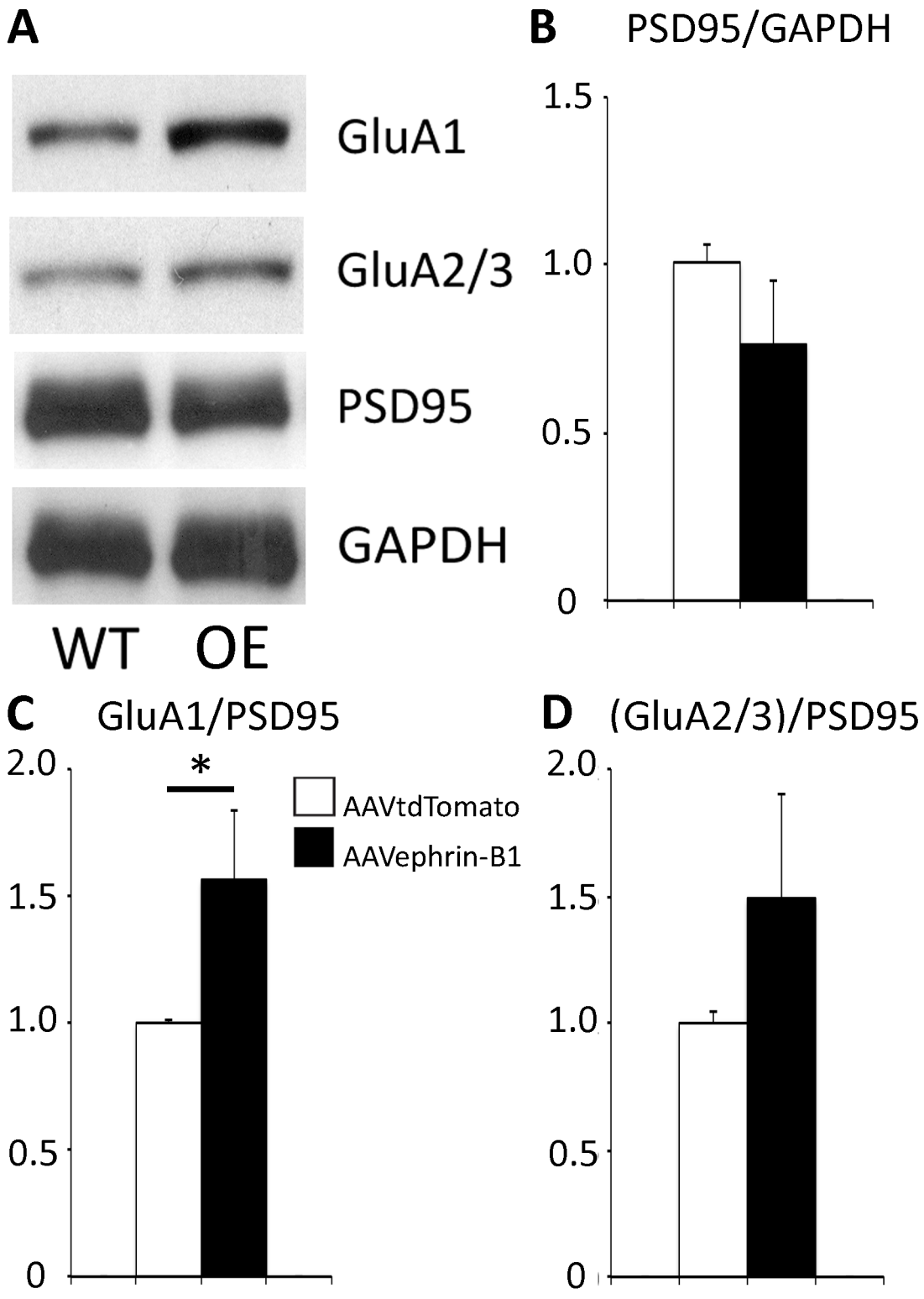
A
GluA1
GluA2/3
PSD95
GAPDH
WT
OE
B
PSD95/GAPDH
1.5
1.0
0.5
0
C
GluA1/PSD95
*
AAVtdTomato
AAVephrin-B1
2.0
1.5
1.0
0.5
0
D
(GluA2/3)/PSD95
2.0
1.5
1.0
0.5
0

Figure 2.10. Overexpression of ephrin-B1 increases synaptic GluA1 levels.

(A) Western blots show levels of AMPAR subunits (GluA1 and GluA2/3), PSD95 and GAPDH in synaptosomes isolated from the hippocampus of Control and OE mice. (B) PSD95 levels in naive KO compared with naive WT (AAV-*GFAP-tdTomato*: 1.008 ± 0.049 vs AAV-*GFAP-ephrinB1* + AAV-*GFAP-tdTomato*: 0.763 ± 0.191, $t_{(6)} = 1.229$, $p = 0.1307$). There was a significant increase in AMPAR/PSD95 ratio for synaptic (C) GluA1 (AAV-*GFAP-tdTomato*: 0.999 ± 0.013 vs AAV-*GFAP-ephrinB1* + AAV-*GFAP-tdTomato*: 1.564 ± 0.273, $t_{(6)} = 2.068$, $p = 0.0421$, *t* test). Decreases seen in GluA2/3 subunits were not significant (AAV-*GFAP-tdTomato*: 0.999 ± 0.043 vs AAV-*GFAP-ephrinB1* + AAV-*GFAP-tdTomato*: 1.491 ± 0.0425, $t_{(6)} = 1.24$, $p = 0.130$). Graphs show mean values and error bars represent SEM.

Figure 2.11

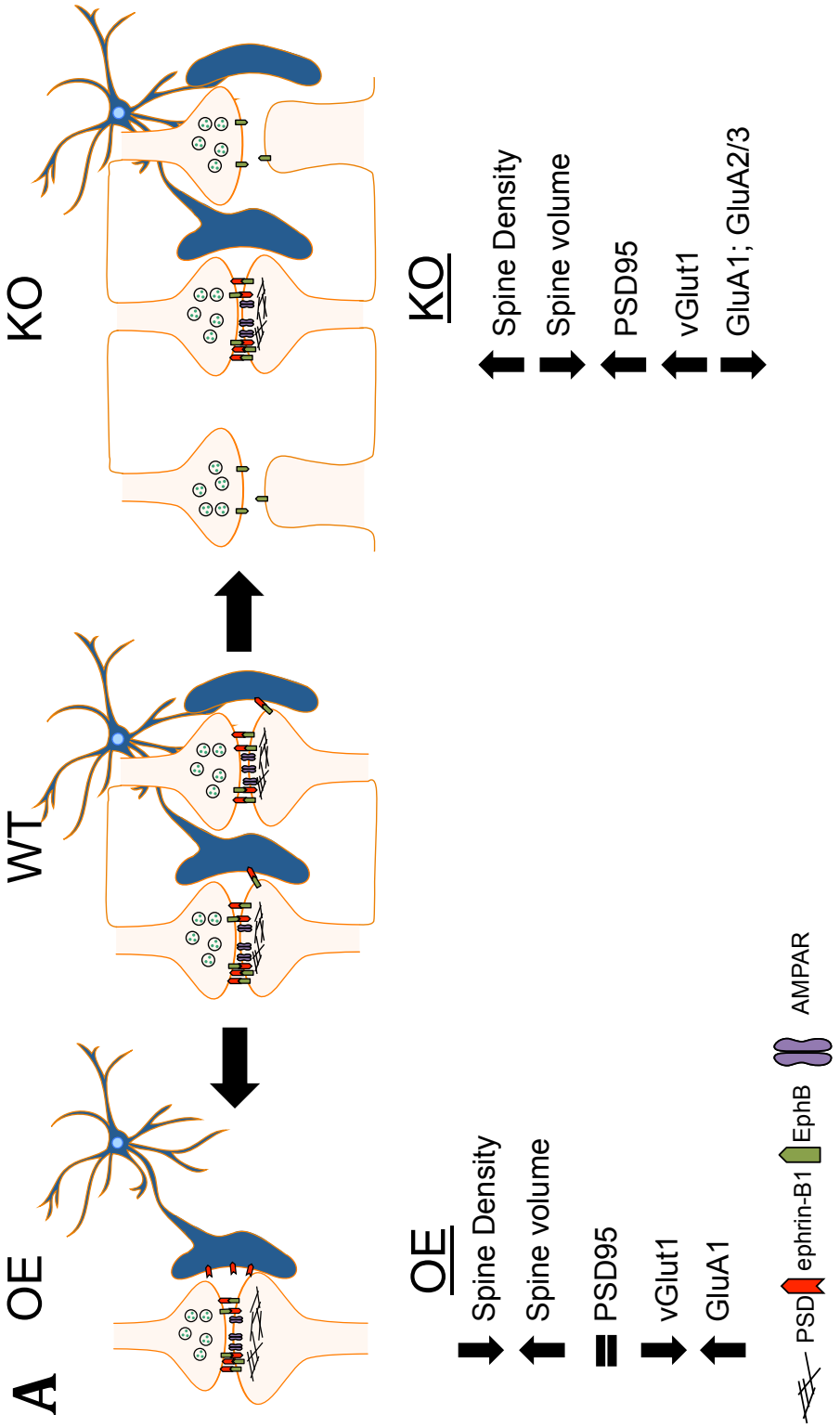
A
OE
WT
KO
OE
Spine Density
Spine volume
PSD95
vGlut1
GluA1
KO
Spine Density
Spine volume
PSD95
vGlut1
GluA1; GluA2/3
PSD
ephrin-B1
EphB
AMPAR

Figure 2.11. Synaptic effects of astrocytic ephrin-B1 ablation and overexpression. (A) Model of the synaptic effects of astrocytic deletion and overexpression of ephrin-B1. Deletion of astrocytic ephrin-B1 increased spine density, postsynaptic PSD95, and presynaptic vGlut1, while decreasing spine volume and synaptic AMPAR (GluA1; GluA2/3) levels. Overexpression of ephrin-B1 decreased dendritic spine density and presynaptic vGlut1, with an increased spine volume and synaptic GluA1 levels.

Chapter 3 – Role of astrocytic ephrin-B1 in hippocampal dependent learning and memory

Abstract

The hippocampus is necessary for the formation of new memories and is integral to life-long learning in adulthood. In fact, damage to the hippocampus leads to anterograde amnesia and impaired acquisition of new memories. Further, acquisition of associative memory requires the activation of excitatory pyramidal neurons and maturation of hippocampal synapses. During synaptic maturation postsynaptic dendritic spines increase in volume and integrate AMPARs into the synaptic membrane, increasing excitatory signal efficiency. EphB/ephrinB interactions are shown to promote synaptic maturation and stabilization, but most studies have focused on neuronal Eph/ephrins. Previously I demonstrated ablation of astrocytic ephrin-B1 increases, and in contrast overexpression decreases, immature synapse number in the SR region of the CA1 hippocampus in adult mice. Astrocytic ephrin-B1 mediated synapse elimination suggests hippocampal astrocytes may modulate memory formation and hippocampal dependent recall. Indeed, ablation of astrocytic ephrin-B1 enhanced contextual recall after fear conditioning. KO mice showed a 51% increase in dendritic spine density in activated neurons compared to non-activated WT pyramidal cells. However, activation of hippocampal neurons induces synaptic maturation in both KO and WT mice. Fear conditioning also increased vGlut1/PSD95 co-localization in KO mice, suggesting enhanced contextual recall is due to an increased number of mature excitatory connections in the CA1 hippocampus. Indeed deficits in synaptic AMPAR in naïve KO

mice are no longer seen in trained KO mice. Overexpression of astrocytic ephrin-B1 leads to deficits in contextual recall possibly as a result of a lack of available immature synapses prior to training. OE mice had fewer dendritic spines on activated neurons coinciding with decreased vGlut1/PSD95 co-localization indicating a reduced formation of new hippocampal synapses may underlie impaired fear conditioning.

These studies indicate that astrocytic ephrin-B1 may negatively regulate memory formation by eliminating immature synapses in the SR CA1 hippocampus, reducing potential sites for new memories in an activity dependent manner.

Introduction

Hippocampal circuits are well known for their role in the formation of new memories and life-long learning (Milner, Squire, & Kandel, 1998; Neves, Cooke, & Bliss, 2008). Hippocampal dependent learning requires the activation of CA1 pyramidal neurons (Strekalova et al., 2003), which promotes the growth and maturation of hippocampal synapses. In fact, maturation of dendritic spines through the recruitment of AMPAR and an increase in spine volume were shown to be activity dependent (Matsuo, Reijmers, & Mayford, 2008) and deletion of synaptic NMDARs in the CA1 hippocampus was reported to impact hippocampal dependent learning (Tsien & Huerta, 1996). In addition to promoting synapse formation, experience is also shown to modify hippocampal circuits through selective stabilization or removal of synapses (Lichtman and Colman 2000; Draft and Lichtman, 2009; Holtman and Svoboda et al., 2009).

Retention of high EphB receptor and ephrinB expression in the adult hippocampus (Grunwald et al., 2001; Liebl, Morris, Henkemeyer, & Parada, 2002) and trans-synaptic Eph/ephrinB interactions promoting postsynaptic dendritic spine maturation (Henderson et al., 2001; Henkemeyer, Itkis, Ngo, Hickmott, & Ethell, 2003; Kayser, McClelland, Hughes, & Dalva, 2006) indicates EphB/ephrinB interactions may affect hippocampal dependent memory formation by stabilizing new synaptic connections. Indeed, activation of EphA and EphB receptors are reported to increase associative memory in mice (Dines et al., 2015; Gerlai et al., 1999; Halladay, Tessarollo, Zhou, & Wagner, 2004; Willi et al., 2012). Interestingly, EphB2 activation increases both

short and long-term memory, though only long-term memory requires EphB2 kinase activity (Dines et al., 2015). While trans-synaptic EphB/ephrinB interactions enhance memory formation little is known about how astrocytic ephrin-B1 and neuronal EphB interactions modulate memory. I previously reported astrocytic ephrin-B1 as a negative regulator of immature synapses in the CA1 hippocampus. As a result, this raises the possibility of astrocytic ephrin-B1 modifying hippocampal dependent memory by reducing the population of available immature sites for new memory formation.

Hippocampal dependent memory formation also requires input from local inhibitory neurons. In fact, ablation of $GABA_A$ receptor α5 subunit increased contextual recall (Crestani et al., 2002; Yee et al., 2004) and enhanced spatial learning in mice (Collinson et al., 2002). Enhanced parvalbumin (PV) interneuron activity also diminished contextual recall after fear extinction suggesting activation of PV interneurons may lead to memory loss (Çalişkan et al., 2016). In contrast, in another study interneurons in CA3 hippocampus expressing high levels of PV were shown to receive higher excitatory input following fear conditioning and play a role in memory consolidation (Donato et al. 2013; Donato et al. 2015). High-PV expressing interneurons also exhibit a higher excitatory to inhibitory input ratio compared to low-PV expressing interneurons (Donato et al., 2015). Although astrocytic ablation and overexpression of ephrin-B1 does not affect GAD65 inhibitory sites in the CA1 hippocampus, ephrin-B1 may regulate excitatory input on inhibitory neurons increasing inhibitory activity.

Studies presented here show astrocytic ephrin-B1 mediated elimination of immature synapses inhibits hippocampal dependent memory formation. Fear conditioning tests demonstrated enhanced contextual recall in KO mice most likely the result of the maturation of excess immature synapses observed in naïve KO as compared to WT mice. After fear conditioning both WT and KO mice showed a significant increase in dendritic spine density on activated c-Fos-positive neurons as compared to c-Fos-negative neurons. Dendritic spines on activated neurons also showed an increase in spine volume in both WT and KO mice, indicating excess immature synapses in KO mice mature during fear conditioning. Indeed, KO mice had a 30% increase in vGlut1/PSD95 co-localization compared to WT mice suggesting an increase in the number of functional synapses. In addition, trained KO mice had no difference in synaptic AMPAR levels compared to trained WT mice suggesting excess immature synapses observed in naïve KO mice mature during fear conditioning. OE of astrocytic ephrin-B1 inhibited contextual recall and OE mice had fewer dendritic spines on activated neurons coinciding with a 25% reduction in vGlut1/PSD95 co-localization as compared to trained WT mice. Our results suggest that fear conditioning promoted the recruitment of AMPAR in WT but not OE synapses, probably due to a lack of immature synapses in OE mice. These studies implicate astrocytic ephrin-B1 as a negative regulator of synapse formation in the hippocampus during learning, therefore regulating contextual memory formation.

Material and Methods

Ethics statement

All animal care protocols and procedures were approved by the UC Riverside Animal Care & Use Program, which is accredited by AAALAC International, and animal welfare assurance number A3439-01 is on file with the Office of Laboratory Animal Welfare (OLAW).

Mice

B6.Cg-Tg(*GFAP*-cre/ERT2)505Fmv/J (ERT2-Cre^{GFAP}, RRID: IMSR_JAX:012849) male mice were crossed with 129S-*Efnb1*^{tm1Sor}/J female mice (*ephrin-B1*$^{flox/+}$, RRID: IMSR_JAX:007664) to obtain ERT2-Cre^{GFAP}*ephrin-B1*$^{flox/y}$ (KO), or ERT2-Cre^{GFAP} (WT) male mice (Fig. 2.1 A). Adult WT and KO littermates received tamoxifen intraperitoneally (IP; 1 mg in 5 mg/ml of 1:9 ethanol/sunflower seed oil solution) once a day for 7 consecutive days (Fig. 2.1B). We did not detect any changes in ephrin-B1 levels in astrocytes or neurons in ERT2-Cre^{GFAP}*ephrin-B1*$^{flox/y}$ non-injected or injected with sunflower seed oil without tamoxifen as previously reported (Nikolakopoulou et al., 2016). Ephrin-B1 immunoreactivity was analyzed in ERT2-Cre^{GFAP}*ephrin-B1*$^{flox/y}$ (KO) and ERT2-Cre^{GFAP} (WT) mice (Fig. 2.2 A-F). Astrocyte-specific Cre expression was confirmed in tamoxifen-treated ERT2-Cre^{GFAP} using Rosa-CAG-LSL-tdTomato reporter mice (CAG-tdTomato, RRID:IMSR_JAX:007909; Fig. 2.2 A). Ephrin-B1 immunoreactivity was observed in cell bodies and dendrites of CA1 neurons but not hippocampal astrocytes of tamoxifen-treated KO mice (Fig. 2.2 B-C).

There were no changes in ephrin-B1 levels in astrocytes and neurons of untreated and tamoxifen-treated WT animals. Genotypes were confirmed by PCR analysis of genomic DNA isolated from mouse-tails. Mice were maintained in an AAALAC accredited facility under 12-h light/dark cycle and fed standard mouse chow. All mouse studies were done according to NIH and Institutional Animal Care and Use Committee guidelines.

Stereotaxic micronjections

To induce expression of ephrin-B1 and tdTomato in hippocampal astrocytes we used adeno-associated viruses (AAV7) containing *AAV7.GfaABC1D.ephrin-B1.SV40* or *AAV7.GfaABC1D.tdTomato.SV40*, respectively (both obtained from UPenn Vector Core, http://www.med.upenn.edu/gtp/vectorcore). Viral titers were 7.56 X 10^{12} viral particles (VP)/ml for AAV7.GfaABC1D.ephrin-B1.SV40 (AAV-ephrin-B1) and 4.46 X 10^{12} VP/ml for AAV7.GfaABC1D.tdTomato.SV40 (AAV-tdTomato). VP were further concentrated with Amicon ultra-0.5 centrifugal filter (UFC505024, Sigma-Aldrich) pretreated with 0.1% Pluronic F-68 non-ionic surfactant (24040032, Thermofisher). VP were stereotaxically injected into the dorsal hippocampus of adult postnatal day (P) 70-90 C57BL/6 or Thy1-EGFP mice as follows. Mice were anesthetized by intraperitoneal injections (IP) of ketamine/xylazine mix (80 mg/kg ketamine and 10 mg/kg xylazine). Adequate anesthesia was assessed by paw pad pinch test, respiratory rhythm, righting reflex, and/or loss of corneal reflex. Animals received craniotomies (1 mm in diameter) and stereotaxic injections were performed at 2.5 mm posterior to bregma, 1.0 mm lateral to midline, and 1.2 mm from the pial surface (Fig. 2.6 A-B). Control mice were bilateral

injected with 2 μl of 1.16 X 10^{13} VP/ml AAV7.GfaABC1D.tdTomato.SV40 and experimental animals received 1 μl of 3.78 X 10^{13} VP/ml AAV7,GfaABC1D.ephrin-B1.SV40 + 1 μl of 2.32 X 10^{13} VP/ml AAV7.GfaABC1D.tdTomato.SV40. Post-surgery mice received 0.3 ml of buprenorphine by subcutaneous injection every 8 h for 48 h as needed for pain and animals were alowed to recover for 14 days prior to fear conditioning tests and/or immunohistochemistry (Fig. 2.6C). Coronal sections selected for analysis were determined by hippocampal specific tdTomato expression (Fig. 2.6B).

Fear conditioning test

Hippocampal dependent contextual learning was assessed using a fear-conditioning paradigm as previously described (Anagnostaras et al., 2001). Two contexts were used to test contextual memory. Context A consisted of an 18 X 18 cm rectangular clear plexiglass box with 16-grated steel bars on the bottom. All trials under context A were under white light and the scent of Quatricide TB. Context B consisted of a cylinder with a diameter of 15 cm and a height of 20 cm with 2.5 X 2.5 cm checkered black and white walls. All trials in context B were under altered light with fresh litter and the scent of Windex. Animals were acclimated in behavioral room for 30 min before each day of testing, and handled for 2 min for 5 days prior to subsequent testing. On day one the test mouse was placed in context A and allowed to habituate to the chamber for 10 min, 1 h after context A mice were habituated to context B for 10 min. The mouse was removed and separated from its home cage until all mice in that cage were habituated to both contexts. 16 h after context habituation, test mice were trained to associate an

unconditioned stimulus (US; 0.6 mA scrambled foot shock) with a conditioned stimulus (CS; 9 kHz, 70 dB tone) in context A. Test mice were placed in context A and given 3 minutes for habituation, followed by a 30 s tone (CS), which co-terminated with a 2 s foot shock (US). The CS-US pairing occurred five times, with a pseudorandom interval between pairings. 24 h after the training session animals were tested for their associated memory of the context (in context A) and of the CS tone (in context B). For contextual recall, mice were placed in context A for 5 min with no sound and returned to home cage for 1 h before testing context B. For tone recall test mice were placed in context B for a total of 6 min with the CS tone playing for the final 3 min. For extinction of contextual memory 24 h after tone recall mice were placed in context A for 10 min for four consecutive days. For memory reactivation, 1 h after the final extinction training mice were placed in context B for a total of 6 min with the CS tone playing for the final 3 min. For contextual memory renewal, mice were placed in context A for 5 min 1 h after memory reactivation. Freezing behavior was measured as a percentage of time freezing using TopScan Software. GraphPad Prism 6 software (RRID: SCR_002798) was used to preform a one-way ANOVA followed by Tukey's post hoc analysis or t-test when appropriate, data represent mean ± SEM.

Immunohistochemistry

Animals were anesthetized with isoflurane and transcardially perfused first with 0.9% NaCl followed by fixation with 4% paraformaldehyde in 0.1 M phosphate-buffered saline (PBS), pH 7.4. Brains were post-fixed overnight with 4% paraformaldehyde in 0.1

M PBS and 100 μm coronal brain sections were cut with a vibratome. Excitatory presynaptic boutons were labeled by immunostaining against vesicular glutamate transporter 1 (vGlut1) using rabbit anti-vGlut1 antibody (0.25 mg/ml, Invitrogen Cat# 482400, RRID: AB_2533843), postsynaptic sites were identified with mouse anti-postsynaptic density-95 (PSD95) antibody (1.65 μg/ml, Invitrogen Cat# MA1-045, RRID: AB_325399). Inhibitory sites were detected with mouse anti-glutamic acid decarboxylase 65 (GAD65) antibody (10 μg/ml, BD Pharmingen Cat# 559931, RRID: AB_397380). Ephrin-B1 levels were detected by immunostaining with goat anti-ephrin-B1 antibody (20 μg/ml, R&D Systems Cat# AF473, RRID: AB_2293419). Activated neurons were detected with ant-c-fos antibodies (40 μg/ml, Invitrogen Cat# PA1-37437, RRID: AB_1073599). Secondary antibodies used were Alexa Fluor 594-conjugated donkey anti-mouse IgG (4 mg/ml, Molecular Probes Cat# A-21203, RRID: AB_141633), Alexa Fluor 647-conjugated donkey anti-rabbit IgG (4 mg/ml, Molecular Probes Cat# A-31573, RRID: AB_2536183), Alexa Fluor 647-conjugated donkey anti-goat IgG (4 mg/ml, Molecular Probes Cat# A-21447, RRID: AB_141844), or Alexa Fluor 488-conjugated donkey anti-goat IgG (4 mg/ml, Molecular Probes Cat# A-11055, RRID: AB_2534102). Sections were mounted on slides with Vectashield mounting medium containing DAPI (Vector Laboratories Inc. Cat# H-1200, RRID: AB_2336790).

Confocal Imaging and Analysis

Confocal images of the stratum radiatum (SR) and stratum lacunosum-moleculare (SLM) layers of CA1 hippocampus were taken with a Leica SP2 and Zeiss 880 confocal laser-

scanning microscope. A series of high-resolution optical sections (1,024 x 1,024-pixel format) were captured with a 20x or 63x water-immersion objective (1.2 numerical aperture) and 1x zoom at 1-μm step intervals (z-stack of 10 optical sections). All images were acquired under identical conditions. Each z-stack was collapsed into a single image by projection, converted to a tiff file, encoded for blind analysis, and analyzed using Image J Software. Three adjacent projections from SR were analyzed per each hippocampus from at least three animals/group. Cell area, integrated fluorescent intensity, and cell perimeter were determined for each GFAP-positive and ephrinB1-positive cell (100–300 astrocytes, z-stacks at least 10 optical images, 5–11 brain slices, 3–4 mice per group). For the analysis of vGlut1, GAD65, and PSD95 immunolabeling, at least six sequential images were captured for selected area at 1-μm step intervals, each image in the series was threshold-adjusted to identical levels (0-160 intensity) and puncta (0.5-10 μm^2) were measured using ImageJ software (RRID: nif-0000-30467). Cell body and dendritic labeling were excluded from the analysis. Three adjacent areas from SR and SLM were imaged and analyzed per each hippocampus from at least three animals/group. Statistical analysis was performed with one-way ANOVA followed by Tukey post-hoc analysis using GraphPad Prism 6 software (RRID: SCR_002798), data represent mean ± standard error of the mean (SEM).

Dendritic spine analysis

Animals were anesthetized with isoflurane and transcardially perfused with 4% paraformaldehyde in 0.1 M PBS, pH 7.4. Brains were post-fixed for 2 h in 4%

paraformaldehyde in 0.1 M PBS and 100 μm coronal sections were cut with a vibratome. Dendritic spines were labeled using a DiOlistic approach (Henkemeyer et al., 2003). Tungsten particles coated with fluorescent lipophilic dye 1,1'-dioctadecyl-3,3,3',3'-tetramethyl-indocarbocyanine perchlorate (DiI, D282, Molecular Probes) was delivered by helium-powered ejection (Bio-Rad Helios Gene Gun System) into hippocampal slices. Labeled neurons were imaged using a LSM 510 Carl Zeiss confocal microscope. 10-15 DiI-labeled neurons were randomly selected per group and dendrites were imaged using a 63x objective (1.2 NA), 1x zoom. Three-dimensional fluorescent images were created by the projection of each z stack containing 50-100 high-resolution optical serial sections (1,024 x 1,024-pixel format) taken at 0.5 μm intervals in the X-Y plane. Quantifications of the spine density (spines per 10 μm dendrite), lengths (μm), and volumes (μm^3) were carried out using Neurolucida 360 software (MicroBrightField RRID: SCR_001775). Statistical analysis was performed with one-way ANOVA followed by Tukey post-hoc analysis using GraphPad Prism 6 software (Graphpad Prism, RRID: SCR_002798), data represent mean ± SEM.

Synaptosome Purification

Synaptosome purification was performed as previously described (Hollingsworth et al., 1985). Hippocampal tissues from adult WT or EphB1,2,3 KO mice were homogenized in 1 ml synaptosome buffer (124 mM NaCl, 3.2 mM KCl, 1.06 mM KH_2PO_4, 26 mM $NaHCO_3$, 1.3 mM $MgCl_2$, 2.5 mM $CaCl_2$, 10 mM Glucose, 20 mM HEPES). Homogenates were filtered through a 100 μm nylon net filter (NY1H02500, Millipore)

and 5 μm nylon syringe filter (SF15156, Tisch International). Homogenate flow through was collected and synaptosomes were spun down at 10,000 g, 4°C, for 30 min. Synaptosomes were resuspended in 800 μl synaptosome buffer. To confirm synaptosome enrichment, levels of synapsin-1, PSD95, and histone deacetylase (HDAC I) were analyzed in tissue homogenates and synaptosome fractions with western blot analysis. Synaptosomes for engulfment assays were also stained with 5% (w/v) DiI (D282, Molecular Probes) in DMSO for 10 min.

Western Blot Analysis

Tissue homogenate or purified synaptosome samples were centrifuged at 10,000 g, 4°C, for 30 min, pellets were re-suspended in lysis buffer (50 mM Tris, 100 mM NaCl, 2% TritonX-100, 10 mM EDTA,) containing 2% protease inhibitor cocktail (P8340, Sigma-Aldrich) and incubated for 2 h at 4°C. Samples were added to 2X Laemmli Buffer (S3401, Sigma-Aldrich) and run on an 8-16% Tris-Glycine Gel (EC6045BOX, Invitrogen). Protein samples were transferred onto a nitrocellulose blotting membrane (10600007, GE Healthcare). Blots were blocked with 5% milk in TBS (10 mM Tris, 150 mM NaCl, pH 8.0) followed by immunostaining with mouse anti-PSD95 (1.65 μg/ml, Invitrogen Cat# MA1-045, RRID: AB_325399), rabbit anti-GluA1 (1:100, Millipore Cat# AB1504, RRID: AB_2113602), rabbit anti-GluA2/3 (0.1 μg/ml, Millipore Cat# AB1506, RRID: AB_90710), rabbit anti-HDAC I (0.40 μg/ml, Santa Cruz Biotechnologies Cat# sc-7872, RRID: AB_2279709), rabbit anti-synapsin-1 (0.2 μg/ml, Millipore Cat# AB1543P, RRID: AB_90757), or mouse anti-GAPDH (0.2 μg/ml,

Thermo Fisher Scientific Cat# 39-8600, RRID:AB_2533438) antibodies in 0.1% tween 20/TBS at 4^{o}C for 16 h. Secondary antibodies used were HRP conjugated donkey anti-mouse IgG (Jackson ImmunoResearch Cat#715-035-150, RRID: AB_2340770) or HRP conjugated goat anti-rabbit IgG (Jackson ImmunoResearch Cat# 111-035-003, RRID: AB_2313567). Blots were incubated in ECL 2 Western Blotting Substrate (Pierce Cat# 80196) and a signal was collected with CL-XPosure film (34090, Pierce). Band density was analyzed by measuring band and background intensity using Adobe Photoshop CS5.1 software (RRID: SCR_014199). Statistical analysis was performed with a one-way ANOVA followed by Tukey post-hoc analysis using GraphPad Prism 6 software (RRID: SCR_002798), data represent mean ± SEM.

Results

Contextual memory is enhanced in astrocyte specific ephrin-B1 KO mice following fear conditioning.

As immature synapses are preferential sites for spine enlargement (Matsuzaki et al., 2004), I next tested whether ablation of astrocytic ephrin-B1 enhanced contextual hippocampal-dependent learning using a fear-conditioning test. WT, WT+TAM and KO+TAM mice were trained to associate an electric shock with a tone in context A. Their ability to recall the context and tone was then tested by measuring the amount of time freezing in context A without tone (context recall) and in context B with a tone (tone recall) respectively (Fig. 3.1 A). A significant 30% increase in freezing during contextual recall was observed in KO+TAM (66.95 ± 3.77) mice as compared to WT (54.29 ± 5.90) and WT+TAM (Fig 3.1E; 51.15 ± 5.68; $F_{(4,146)} = 3.601$, $p = 0.05$) mice. WT+TAM and KO+TAM mice were tested for fear extinction after fear conditioning (Fig. 3.2 A-E). KO+TAM (63.56 ± 10.25) mice also showed a significant 78% increase in contextual memory renewal following fear memory extinction and reactivation compared to WT+TAM (Fig 3.2 E; 38.51 ± 8.34; $t_{(7)} = 2.534$ $p = 0.047$) mice.

Maturation of excess dendritic spines in ephrin-B1 KO mice is activity dependent.

Coronal hippocampal sections from WT+TAM and KO+TAM mice perfused 1h after context A recall and stained for c-fos to distinguish activated (c-fos+) from non-activated (c-fos -) neurons (Fig. 3.3 A,B). Dendritic spines were labeled with DiO and measured using Neurolucida 360 software to determine spine density (C), length (D), and

average spine volume (E) in WT+TAM and KO+TAM mice (Fig. 3.3 C-E). Activated (c-fos-positive) CA1 pyramidal neurons had a significant increase in dendritic spine density in KO+TAM (c-fos (+): 15.98 ± 0.78; c-fos (-): 12.42 ± 0.98) compared to a smaller but significant increases observed in WT+TAM (c-fos (+): 12.99 ± 0.608; c-fos (-): 10.60 ± 0.86; $F_{(1,41)} = 12.52$, $p = 0.001$) mice. Activated neurons also showed an increase in average spine volume compared to c-fos negative cells (WT+TAM c-fos (-): 0.471 ± 0.007; WT+TAM c-fos (+): .555 ± 0.028; KO+TAM c-fos (-): 0.440 ± 0.015; KO+TAM c-fos +: 0.533 ± 0.017; $F_{(2,26)} = 9.606$, $p = 0.0008$). The results suggest astrocytic ephrin-B1 negatively regulates learning-induced dendritic spine formation in the adult hippocampus as greater increases are seen in activated KO neurons compared to activated WT cells.

Astrocyte specific ephrin-B1 deletion increases synapse formation after fear conditioning.

To determine if KO mice have an increased number of synaptic connections in the CA1 hippocampus after fear-conditioning coronal hippocampal sections were stained for presynaptic vGlut1 and the postsynaptic PSD95 (Fig. 3.4A-D). A 34% increase in vGlut1/PSD95 co-localization was seen in trained KO+TAM (2.678 ± 0.116) compared to trained WT+TAM (Fig. 3.4F; 1.999 ± 0.215; $t_{(29)} = 2.828$, $p = 0.008$) mice. Surprisingly, no differences were seen in vGlut1-positive puncta in trained WT+TAM (3.549 ± 0.173) and KO + TAM (Fig 3.4E; KO+TAM: 3.601 ± 0.1753; $t_{(29)} = 0.213$, $p = 0.833$) mice. Increases in co-localization may be due to an increased number of PSD95-

positive puncta seen in trained KO+TAM (5.592 ± 0.088) compared to trained WT+TAM (Fig. 3.4F; WT+TAM: 4.727 ± 0.425; $t_{(32)}$= 2.104, p = 0. 043, t test). The results suggest excess synapse formation in KO mice may contribute to enhanced contextual recall.

Fear conditioning promotes AMPAR recruitment in KO synapses.

Hippocampal tissues were collected following context recall and synaptosomes were assessed for AMPAR and PSD95 levels (Fig. 3.5A). In contrast to reduced levels of synaptic AMPAR in naïve KO mice as compared to WT (chapter 2), we observed similar synaptic levels of AMPAR subunits GluA1 (Fig. 3.5C; WT+TAM: 1.003 ± 0.007 vs KO+TAM: 0.918 ± 0.091, $t_{(12)}$ =0.6931 p=0.505, t-test) and GluA2/3 (Fig. 3.5D; WT+TAM: 1.032 ± 0.062 vs KO+TAM: 0.799 ± 0.106; $t_{(12)}$ =1.537, p=0.152, t-test) in the hippocampus of trained WT and KO mice, suggesting that immature synapses may recruit more AMPARs in KO mice following training. Levels of PSD95 were also similar in trained KO+TAM and WT+TAM groups (Fig. 3.5B; WT+TAM: 1.073 ± 0.191 vs KO: 1.517 ± 0.509, $t_{(9)}$ = 0.7545, p= 0.4698), most likely due to increased number of synapses in WT mice following training.

The results suggest that the excess immature synapses observed following astrocyte-specific loss of ephrin-B1 in adult mice most likely mature following learning contributing to enhanced contextual memory.

Ablation of astrocytic ephrin-B1 has no effect on inhibitory circuits in the CA1 hippocampus during fear conditioning.

Hippocampal sections were stained for GAD65 following training and memory recall to determine differences in inhibitory circuits in the CA1 hippocampus (Fig. 3.6 A). No significant differences were seen in GAD65-positve puncta between WT+TAM and KO+TAM mice in the SR of the CA1 hippocampus (Fig 3.6E; WT+TAM: 1.036 ± 0.103; KO+TAM: 1.247 ± 0.150; $t_{(32)}$ ± 1.159, $p = 0.255$) or SLM (WT+TAM: 1.452 ± 0.219; KO+TAM 1.784 ± 0.230; $t_{(32)} = 1.159$, $p = 0.306$). To determine if astrocytic ephrin-B1 regulates excitatory inputs on inhibitory cells hippocampal sections were stained for vGlut1 and PV (Fig. 3.6 C, D) in naïve (C) and trained (D) mice. No significant differences were seen in the number of vGlut1-positive presynaptic sites per 100μm^2 PV interneuron between WT and KO mice before (Fig. 3.6 F; WT+TAM: 1.780 ± 0.088 vs KO+TAM: 1.968 ± 0.084; $t_{(520)} = 1.536$, $p = 0.125$) or after (Fig 3.6 G; WT+TAM: 1.280 ± 0.070 vs KO+TAM: 1.451 ± 0.083; $t_{(663)} = 1.516$ $p = 0.114$) fear conditioning. Astrocytic ephrin-B1 shows no effect on inhibitory circuits in the CA1 suggesting enhanced contextual recall in KO mice is due to changes in excitatory circuits.

Contextual memory is deficient in astrocyte specific ephrin-B1 overexpressing mice following fear conditioning.

To determine if overexpression (OE) of ephrin-B1 in adult hippocampal astrocytes also affected hippocampal-dependent learning, we examined contextual memory acquisition and recall using a fear-conditioning paradigm. 14 days post-injection, mice were trained to associate an electric shock with a tone in context A (Fig. 3.7A-G). Their ability to recall context and tone association was then tested 24 h after the

training by measuring mouse freezing-time in context A without tone (context recall, Fig. 3.7E) and in context B with a tone (tone recall), respectively (Fig. 3.7G). We found no differences between control and astrocytic ephrin-B1 OE groups during the training (Fig. 3.7D), but a significant reduction in freezing was observed during contextual recall in astrocytic ephrin-B1 OE mice (22.23 ± 5.12) as compared to control mice (Fig. 3.7E; 35.14 ± 2.11, $t_{(7)}$ =2.534 p=0.039, t-test). It appears that freezing time of astrocytic ephrin-B1 OE mice during contextual recall 24 h after training (22.23 ± 5.12) was not significantly different from their freezing time during initial habituation to the context A before the training (14.85 ± 2.11). In contrast, control mice expressing tdTomato retained fear memory of context A and were freezing more 24 h after training (35.14 ± 2.11) than during habituation (16.68 ± 0.28, $t_{(8)}$ =8.673, p=0.0004, t-test).

Overexpression of astrocytic ephrin-B1 inhibits activity dependent dendritic spine formation.

Coronal hippocampal sections from AAV-tdTomato and AAV-ephrinB1 Thy1-GFP mice were perfused 1h after context A recall and stained for c-fos to detect activated neuron (Fig. 3.8A,B). Dendritic spines were measured using Neurolucida 360 software to determine spine density (C), length (D), and average spine volume (E) in AAV-tdTomato and AAV-ephrinB1 mice (Fig. 3.8C-E). Similar to WT mice, in AAV-tdTomato mice activated neurons showed a slight 28% increase in dendritic spine density in activated c-fos+ neurons as compared to c-fos- neurons (c-fos (-): 7.168 ± 0.555; c-fos (+): 9.167 ± 0.680). However overexpression of ephrin-B1 inhibited activity dependent dendritic

spine formation in AAV-ephrinB1 mice (Fig 3.8C; c-fos (+): 7.48 ± 0.797; c-fos (-): 7.843; $F_{(1,41)} = 1.795$, $p = 0.162$). In addition, activated c-fos+ neurons in both AAV-tdTomato (0.641 ± 0.018) and AAV-ephrin-B1 (0.665 ± 0.022) showed an increase in spine volume compared to c-fos negative cells (Fig. 3.8F; AAV-tdTomato: 0.540 ± 0.029; AAV-ephrin-B1 0.595 ± 0.020; $F_{(3,45)} = 6.085$, $p = 0.0014$). The results suggest deficits in contextual recall may be due to a loss of available immature dendritic spines on activated CA1 hippocampal pyramidal neurons.

Astrocytic ephrin-B1 regulates post-synaptic sites during memory formation.

Hippocampal excitatory connections were determined by co-localization of presynaptic vGlut1 and postsynaptic PSD95 in the SR and SLM of the CA1 hippocampus following their training in the fear conditioning test (Fig. 3.9A-D). No difference were observed in vGlut1 positive puncta between trained AAV-tdTomato (5.736 ± 0.275) and AAV-ephrinB1 (Fig 3.9G; 5.352 ± 0.1588, $t_{(32)} = 1.120$, $p = 0.159$, *t* test). However, a 25% reduction in vGlut1/PSD95 co-localization was seen in trained AAV-ephrinB1 (2.036 ± 0.232) compared to trained AAV-tdTomato (Fig. 3.9I; 2.719 ± 0.158; $t_{(32)} = 2.433$, $p = 0.022$, *t* test). Although not significant a 15% decrease in total PSD95 puncta is also seen in trained ephrin-B1 OE mice (Fig. 3.9H; (AAV-tdTomato: 5.600 ± 0.336; AAV-ephrinB1: 4.835 ± 0.148; $t_{(32)} = 2.084$, $p = 0.078$, *t* test). Inhibitory connections were detected by staining hippocampal sections for GAD65 (Fig. 3.9E, F). No significant differences were seen in GAD65 staining between trained AAV-tdTomato (1.550 ±

0.080) and AAV-ephrinB1 (1.450 ± 0.077) mice. Reduced formation of synapses after fear conditioning may be the cause of contextual recall deficits in ephrinB1 OE mice. However, no significant differences were seen between trained WT and OE mice in synaptic GluA1 (Fig. 3.10C; AAV-tdTomato: 1.006 ± 0.063 vs AAV-ephrinB1: 1.251 ± 0.161, $t_{(8)} = 1.637$, $p = 0.140$, *t* test) of GluA2/3 (Fig. 3.10D; AAV-tdTomato: 1.007 ± 0.065 vs AAV-ephrinB1: 0.757 ± 0.238, $t_{(8)} = 1.221$, $p = 0.257$, *t* test). Astrocytic ephrin-B1 may affect the formation of new synapses during memory formation without influencing their maturation.

Discussion

Hippocampal excitatory neurons play an integral role in associative memory formation, in particular activation of CA1 pyramidal neurons is observed during contextual recall in mice (Ji & Maren, 2008). Activity dependent maturation of hippocampal synapses during memory formation promotes structural changes to dendritic spines (Knott, Holtmaat, Wilbrecht, Welker, & Svoboda, 2006; Lichtman & Colman, 2000; Draft & Lichtman, 2009; Holtmaat & Svoboda, 2009) and increases synaptic AMPA receptor levels (Matsuo et al., 2008). Activity dependent synapse maturation in the hippocampus suggests immature dendritic spines are potential sites for new memory formation (Matsuzaki et al., 2004). Our goal was to investigate the role of astrocyte specific ephrin-B1 in regulating CA1 hippocampal synapse during contextual memory formation.

Activation of neuronal EphB receptors facilitates dendritic spine formation and maturation (Dalva *et al.*, 2000; Grunwald *et al.*, 2001) and increases contextual recall (Dines *et al.,*2015). However, previously reported results demonstrate that astrocytic ephrin-B1 induces the elimination of immature synapses decreasing the availability of potential sites for memory formation. Indeed, astrocytic ephrin-B1 KO mice showed an increase in contextual recall following fear conditioning as compared to WT mice. In addition, we observed a two-fold increase in contextual memory reactivation following extinction, suggesting the formation of long-lasting connections in astrocytic ephrin-B1 KO hippocampus. In contrast, contextual recall was impaired in mice overexpressing astrocytic ephrin-B1, possibly due to the removal of EphB expressing immature synapses

by astrocytes overexpressing ephrin-B1. Activation of hippocampal neurons during learning was analyzed by detecting cFos immunoreactivity and promoted dendritic spine maturation in both KO and WT mice compared to non-activated c-Fos negative cells. Activated neurons in KO mice had a significant increase in dendritic spine density, which suggests astrocytic ephrin-B1 mediated regulation of synapses is activity dependent. A 30% increase in pre- and postsynaptic co-localization in the SR region of the CA1 hippocampus in trained KO mice as compared to trained WT mice indicates dendritic spines in KO mice are making functional synaptic connections contributing to enhanced memory formation. OE of astrocytic ephrinB1 inhibited activity dependent synaptogenesis as compared to AAV-tdTomato (WT) mice possibly due to increased elimination of newly formed immature synapses. A 25% decrease in pre- and postsynaptic co-localization in trained OE mice as compared to trained WT mice suggests reductions in the number of immature synapses in naïve OE mice reduces the number of potential sites for new memory formation during memory formation. Surprisingly, deletion and overexpression of astrocytic ephrin-B1 had no effect on the number of glutamatergic presynaptic sites after fear conditioning. However, an 18% increase of postsynaptic sites in trained KO mice and a 15% decrease in trained OE mice as compared to trained WT mice confirms that astrocytic ephrin-B1 regulates the elimination of postsynaptic sites, which is also observed following learning. In contrast, synaptic AMPA receptor levels were similar in KO and WT mice following fear conditioning suggesting maturation of excess immature synapses during memory formation in KO mice. Increased synaptic GluA1 levels seen in naïve OE mice as

compared to naïve WT were not observed following fear conditioning probably due to additional recruitment of AMPAR in WT but not OE mice following training.

Inhibitory circuits in hippocampal interneurons also contribute to memory formation and contextual recall. A partial deletion of $GABA_A$ receptor α5 subunit leads to similar increases in contextual recall during fear conditioning (Crestani et al., 2002; Yee et al., 2004) and a complete deletion enhances spatial learning (Collinson et al., 2002). In addition an inverse agonist to α5 subunit increases spatial learning (Sternfeld et al., 2004; Chambers et al., 2004). As $GABA_A$ receptor α5 subunit is highly expressed on hippocampal pyramidal neurons (Pirker et al., 2000; Rudolph & Mohler, 2006), changes in inhibitory cell activity may be involved in enhanced recall in KO and deficits in OE mice. However, after deletion or overexpression of astrocytic ephrin-B1 we observed no differences in GAD65 positive sites in the hippocampus of naïve and trained mice, no differences were also seen in the number of glutamatergic synapses on PV-positive inhibitory interneurons in KO mice compared to WT mice before and after fear conditioning.

The studies presented here suggest astrocytic ephrin-B1 regulates excitatory connections in the CA1 hippocampus by eliminating immature synapses during contextual memory formation in an activity dependent manner (Fig. 3.11A). In addition astrocytic ephrin-B1-mediated regulation of synapses appears to be specific to excitatory synapses. We propose that astrocytic ephrin-B1 is involved in the elimination of hippocampal synapses by astrocytes, which reduces the number of site available for new memory acquisition.

References

Çalişkan, G., Müller, I., Semtner, M., Winkelmann, A., Raza, A. S., Hollnagel, J. O., … Meier, J. C. (2016). Identification of Parvalbumin Interneurons as Cellular Substrate of Fear Memory Persistence. *Cerebral Cortex*. https://doi.org/10.1093/cercor/bhw001

Collinson, N., Kuenzi, F. M., Jarolimek, W., Maubach, K. A., Cothliff, R., Sur, C., … Rosahl, T. W. (2002). *Enhanced Learning and Memory and Altered GABAergic Synaptic Transmission in Mice Lacking the 5 Subunit of the GABA A Receptor*.

Crestani, F., Keist, R., Fritschy, J.-M., Benke, D., Vogt, K., Prut, L., … Rudolph, U. (2002). Trace fear conditioning involves hippocampal 5 GABAA receptors. *Proceedings of the National Academy of Sciences*. https://doi.org/10.1073/pnas.142288699

Dines, M., Grinberg, S., Vassiliev, M., Ram, A., Tamir, T., & Lamprecht, R. (2015). The roles of Eph receptors in contextual fear conditioning memory formation. *Neurobiology of Learning and Memory*, *124*, 62–70. https://doi.org/10.1016/j.nlm.2015.07.003

Donato, F., Rompani, S. B., & Caroni, P. (2013). Parvalbumin-expressing basket-cell network plasticity induced by experience regulates adult learning. *Nature*, *504*(7479), 272.

Donato, F., Chowdhury, A., Lahr, M., & Caroni, P. (2015). Early- and Late-Born Parvalbumin Basket Cell Subpopulations Exhibiting Distinct Regulation and Roles in Learning. *Neuron*. https://doi.org/10.1016/j.neuron.2015.01.011

Draft, R. W., & Lichtman, J. W. (2009). It's lonely at the top: winning climbing fibers ascend dendrites solo. *Neuron*, *63*(1), 6-8.

Gerlai, R., Shinsky, N., Shih, a, Williams, P., Winer, J., Armanini, M., … Phillips, H. S. (1999). Regulation of learning by EphA receptors: a protein targeting study. *The Journal of Neuroscience : The Official Journal of the Society for Neuroscience*, *19*(21), 9538–49. Retrieved from http://www.ncbi.nlm.nih.gov/pubmed/10531456

Grunwald, I. C., Korte, M., Wolfer, D., Wilkinson, G. A., Unsicker, K., Lipp, H.-P., & Bonhoeffer, T. (2001). *Kinase-Independent Requirement of EphB2 Receptors in Hippocampal Synaptic Plasticity (E-LTP) require protein synthesis (reviewed in Impey et al duces a reduction in synaptic efficacy in the CA1 region*. *Neuron* (Vol. 32). Retrieved from http://www.neuron.org/cgi/content/full/

Halladay, A. K., Tessarollo, L., Zhou, R., & Wagner, G. C. (2004). Neurochemical and

behavioral deficits consequent to expression of a dominant negative EphA5 receptor. *Molecular Brain Research*. https://doi.org/10.1016/j.molbrainres.2004.01.005

Henderson, J. T., Georgiou, J., Jia, Z., Robertson, J., Elowe, S., Roder, J. C., & Pawson, T. (2001). The receptor tyrosine kinase EphB2 regulates NMDA-dependent synaptic function. *Neuron*, *32*(6), 1041–1056. https://doi.org/10.1016/S0896-6273(01)00553-0

Henkemeyer, M., Itkis, O. S., Ngo, M., Hickmott, P. W., & Ethell, I. M. (2003). Multiple EphB receptor tyrosine kinases shape dendritic spines in the hippocampus. *Journal of Cell Biology*, *163*(6), 1313–1326. https://doi.org/10.1083/jcb.200306033

Holtmaat, A., & Svoboda, K. (2009). Experience-dependent structural synaptic plasticity in the mammalian brain. *Nature Reviews Neuroscience*, *10*(9), 647.

Ji, J., & Maren, S. (2008). Differential roles for hippocampal areas CA1 and CA3 in the contextual encoding and retrieval of extinguished fear. *Learning and Memory*. https://doi.org/10.1101/lm.794808

Kayser, M. S., McClelland, A. C., Hughes, E. G., & Dalva, M. B. (2006). Intracellular and Trans-Synaptic Regulation of Glutamatergic Synaptogenesis by EphB Receptors. *Journal of Neuroscience*, *26*(47), 12152–12164. https://doi.org/10.1523/JNEUROSCI.3072-06.2006

Knott, G. W., Holtmaat, A., Wilbrecht, L., Welker, E., & Svoboda, K. (2006). Spine growth precedes synapse formation in the adult neocortex in vivo. *Nature Neuroscience*. https://doi.org/10.1038/nn1747

Lichtman, J. W., & Colman, H. (2000). Synapse elimination and indelible memory. *Neuron*. https://doi.org/10.1016/S0896-6273(00)80893-4

Liebl, D. J., Morris, C. J., Henkemeyer, M., & Parada, L. F. (2002). *mRNA Expression of Ephrins and Eph Receptor Tyrosine Kinases in the Neonatal and Adult Mouse Central Nervous System*.

Matsuzaki, Masanori, Naoki Honkura, Graham CR Ellis-Davies, and Haruo Kasai. "Structural basis of long-term potentiation in single dendritic spines." *Nature* 429, no. 6993 (2004): 761.

Matsuo, N., Reijmers, L., & Mayford, M. (2008). Spine-Type – Specific Recruitment of Newly Synthesized AMPA Receptors with Learning. *Science*, (February), 1104–1108.

Milner, B., Squire, L., & Kandel, E. (1998). Cognitive Neuroscience and the Study of Memory. *Neuron*, *20*, 445–468. https://doi.org/10.1016/S0896-6273(00)80987-3

Neves, G., Cooke, S. F., & Bliss, T. V. P. (2008). Synaptic plasticity, memory and the hippocampus - a neural network aproach to causality. *Nature Reviews Neuroscience*, *9*(January 2008), 65–75. https://doi.org/nrn2303 [pii] 10.1038/nrn2303

Strekalova, T., Zörner, B., Zacher, C., Sadovska, G., Herdegen, T., & Gass, P. (2003). Memory retrieval after contextual fear conditioning induces c-Fos and JunB expression in CA1 hippocampus. *Genes, Brain and Behavior*, *2*(1), 3–10. https://doi.org/10.1034/j.1601-183X.2003.00001.x

Tsien, J. Z., & Huerta, P. T. (1996). *The Essential Role of Hippocampal CA1 NMDA Receptorâ€"Dependent Synaptic Plasticity in Spatial Memory*. *CELL* (Vol. 87). https://doi.org/10.1016/S0092-8674(00)81827-9

Willi, R., Winter, C., Wieske, F., Kempf, A., Yee, B. K., Schwab, M. E., & Singer, P. (2012). Loss of EphA4 impairs short-term spatial recognition memory performance and locomotor habituation. *Genes, Brain and Behavior*. https://doi.org/10.1111/j.1601-183X.2012.00842.x

Yee, B. K., Hauser, J., Dolgov, V. V., Keist, R., Möhler, H., Rudolph, U., & Feldon, J. (2004). GABAAreceptors containing the α5 subunit mediate the trace effect in aversive and appetitive conditioning and extinction of conditioned fear. *European Journal of Neuroscience*. https://doi.org/10.1111/j.1460-9568.2004.03642.x

Figure 3.1

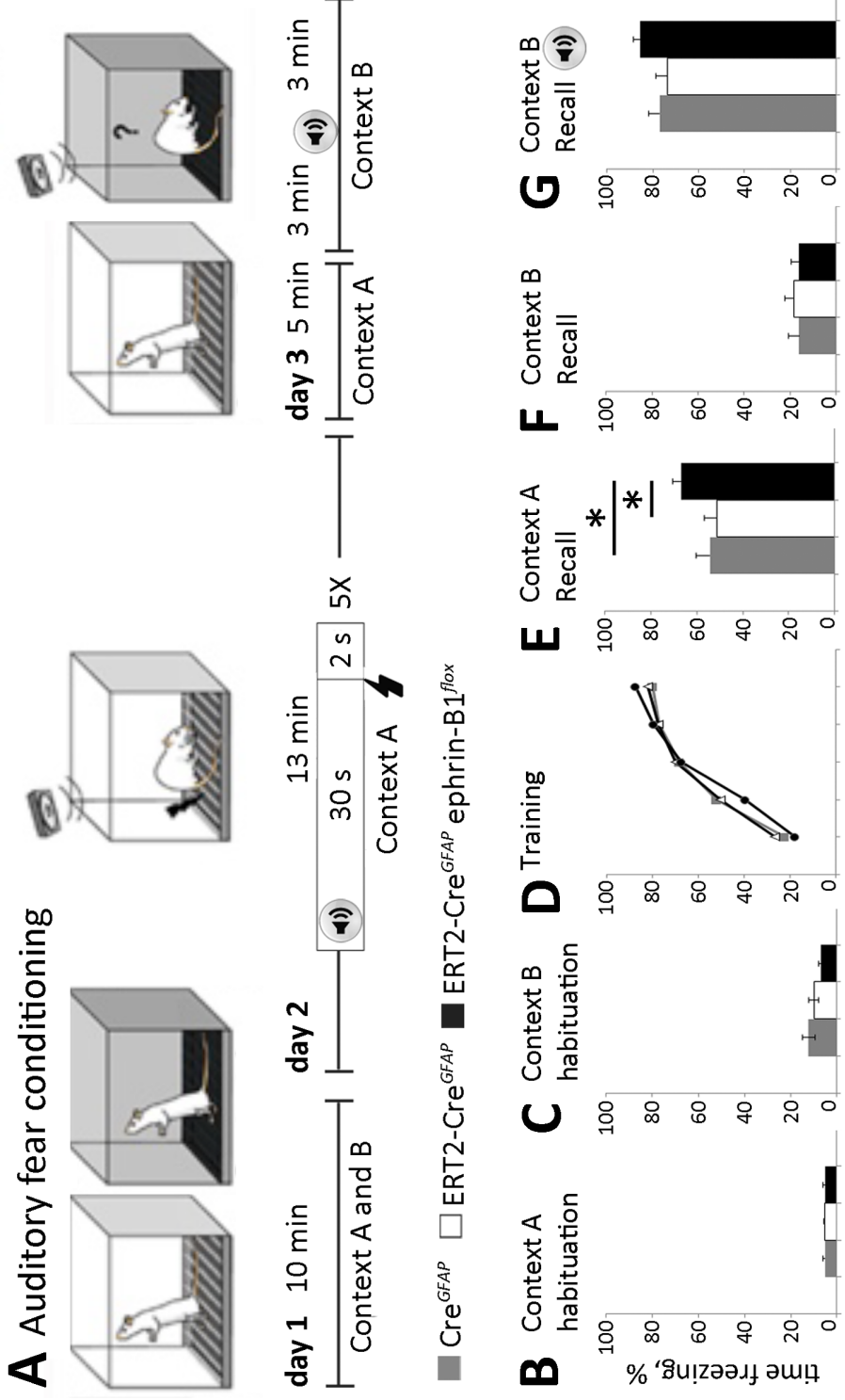
A Auditory fear conditioning
day 1 10 min
Context A and B
day 2
13 min
30 s
2 s
5X
Context A
day 3 5 min
Context A
3 min
3 min
Context B
Cre^GFAP
ERT2-Cre^GFAP
ERT2-Cre^GFAP ephrin-B1^flox
B Context A habituation
C Context B habituation
D Training
E Context A Recall
F Context B Recall
G Context B Recall
time freezing, %
0
20
40
60
80
100
*
*

Figure 3.1. Performance of astrocytic ephrin-B1 KO mice is improved in contextual fear conditioning test.

(A) Schematic depiction of fear conditioning test. Mice were habituated to contexts A and B for 10 min on day 1. On day 2 mice were placed in Context A and received 5 random 0.7 mA foot shocks for 2 s after a 30 s tone at 70 Hz, training the mice to associate the tone with the foot shock. On day 3 mice were placed in Context A for 5 min, 1 h later mice were placed in Context B for 6 min and exposed to a 70 dB tone for the last 3 min. (B-G) Graphs show the percentage of time that mice freeze during each trial, including Context A habituation (B), Context B habituation (C), Context A training (D), Context A recall (E), Context B without (F), and with tone (G) KO□TAM mice show higher freezing than WT and WT+TAM mice during Context A recall. Graphs show mean values and error bars represent SEM (n = □20 –21 mice per group, two-way ANOVA followed by Bonferroni multiple-comparison post-test; $F_{(4,146)} = 3.601$ *p □= 0.05). Graphs show mean values and error bars represent SEM.

Figure 3.2

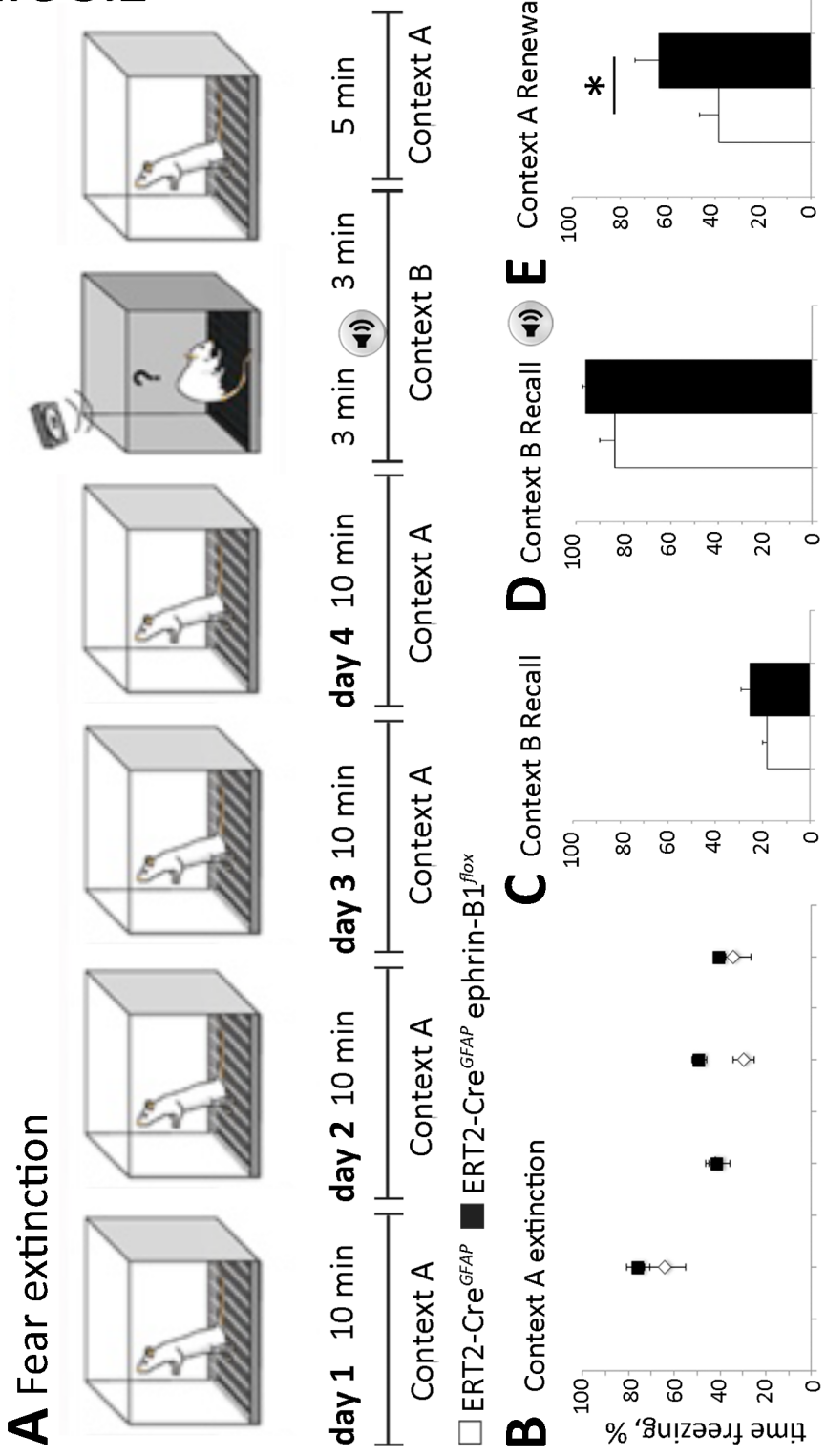
A Fear extinction
day 1 10 min
Context A
day 2 10 min
Context A
day 3 10 min
Context A
day 4 10 min
Context A
3 min
Context B
3 min
Context A
5 min
ERT2-Cre^GFAP
ERT2-Cre^GFAP ephrin-B1^flox
B Context A extinction
time freezing, %
Day 1
Day 2
Day 3
Day 4
C Context B Recall
D Context B Recall
E Context A Renewal
*

Figure 3.2 Astrocytic ephrin-B1 KO mice have improved contextual renewal after a contextual fear extinction test.

(A) Schematic depiction of fear extinction test. After fear conditioning mice were placed context A for 10 min on day 1-3. On day On day 4 mice were placed in Context A for 10 min, 1 h later mice were placed in Context B for 6 min and exposed to a 70 dB tone for the last 3 min. 1 h later mice were placed in Context A for 5 min. (B-E) Graphs show the percentage of time that mice freeze during extinction in Context A (B) Context B recall without tone (C), memory reactivation in Context B with a tone (D), and memory renewal in Context A (E). KO+TAM mice show higher freezing than WT+TAM mice during memory renewal in Context A. Graphs show mean values and error bars represent SEM (n =3- 5 mice per group, t test; *p = 0.05 $t_{(7)}$ = 2.534 p=0.05). Graphs show mean values and error bars represent SEM.

Figure 3.3

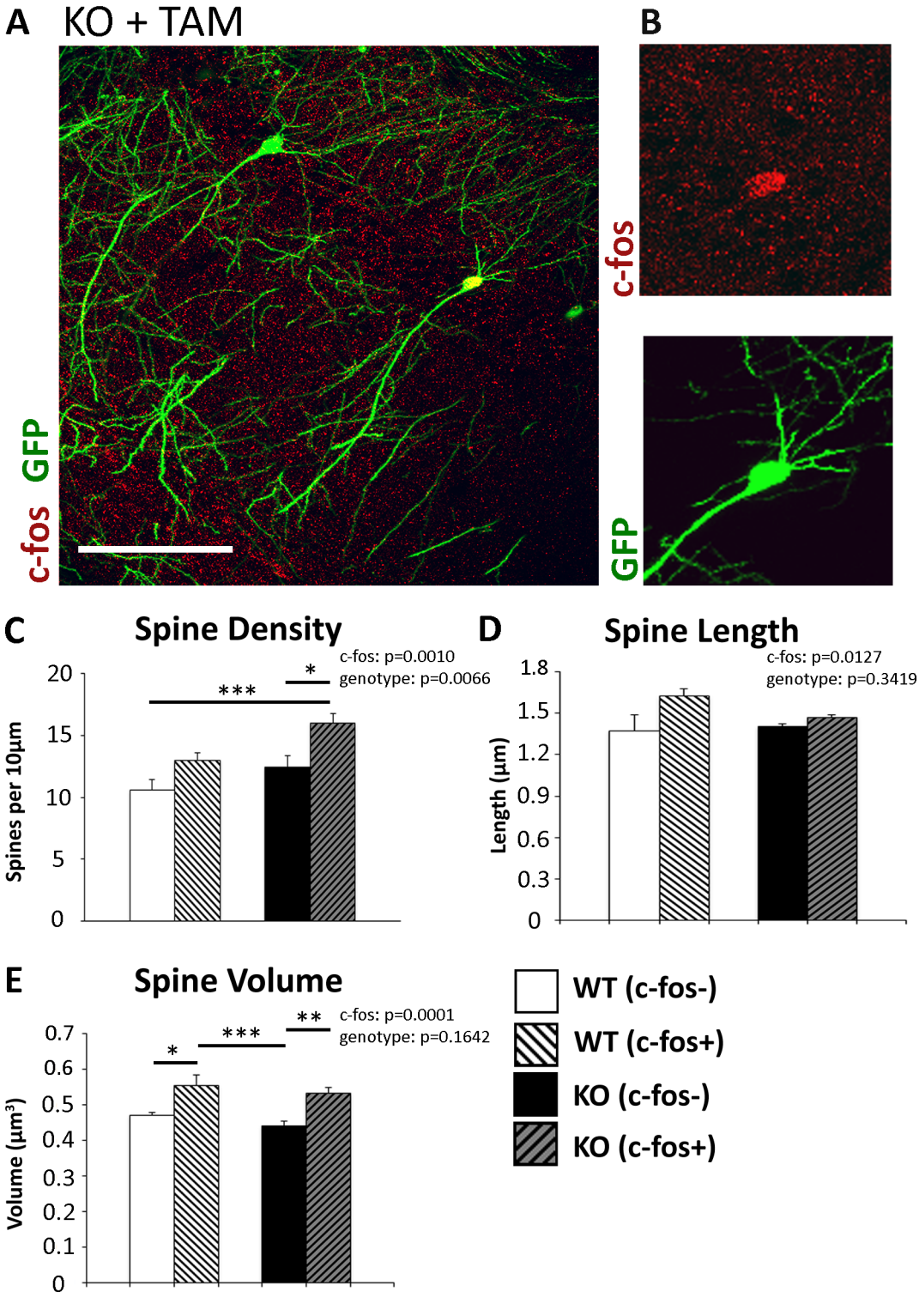
A KO + TAM
B
c-fos
GFP
c-fos
GFP
C
Spine Density
c-fos: p=0.0010
genotype: p=0.0066
***
*
Spines per 10µm
20
15
10
5
0
D
Spine Length
c-fos: p=0.0127
genotype: p=0.3419
Length (µm)
1.8
1.5
1.2
0.9
0.6
0.3
0
E
Spine Volume
c-fos: p=0.0001
genotype: p=0.1642
*
***
**
Volume (µm³)
0.7
0.6
0.5
0.4
0.3
0.2
0.1
0
WT (c-fos-)
WT (c-fos+)
KO (c-fos-)
KO (c-fos+)

Figure 3.3. Excess dendritic spines in KO mice mature during fear conditioning.

(A) Confocal image showing DiO (green) labeled neurons, c-fos (red) in CA1 hippocampus of KO+TAM adult mice. Scale bar, 150 μm. (B, C) Magnified image of c-fos-positive (red) Thy-1GFP (green) CA1 pyramidal neuron. (C–F) Graphs show the average number of dendritic spines per 10μm dendrite (C), average spine length (D), and average spine volume (E). (C) There is a significant 51% increase in average dendritic spine density in c-fos positive KO+TAM neurons compared with and c-fos negative WT+TAM mice; error bars represent SEM (n = 3– 6 mice, WT+TAM c-fos (+): 10.597 ± 0.862 vs KO+TAM c-fos (-): 15.98 ± 0.781; $F_{(1,41)} = 12.52$, p =0.001; one-way ANOVA, Tukey's *post hoc* test, ***p = 0.001). A significant decrease in the proportion of dendritic spines with smaller heads (volume 0 – 0.5 μm^3) was seen in c-fos positive neurons compared c-fos negative in both WT+TAM (n = 3– 6 mice, $F_{(1,126)} = 8.369$, p = 0.0001; two-way ANOVA followed by Tukey's *post hoc*, *p = 0.05, ***p = 0.001). Graphs show mean values and error bars represent SEM.

Figure 3.4

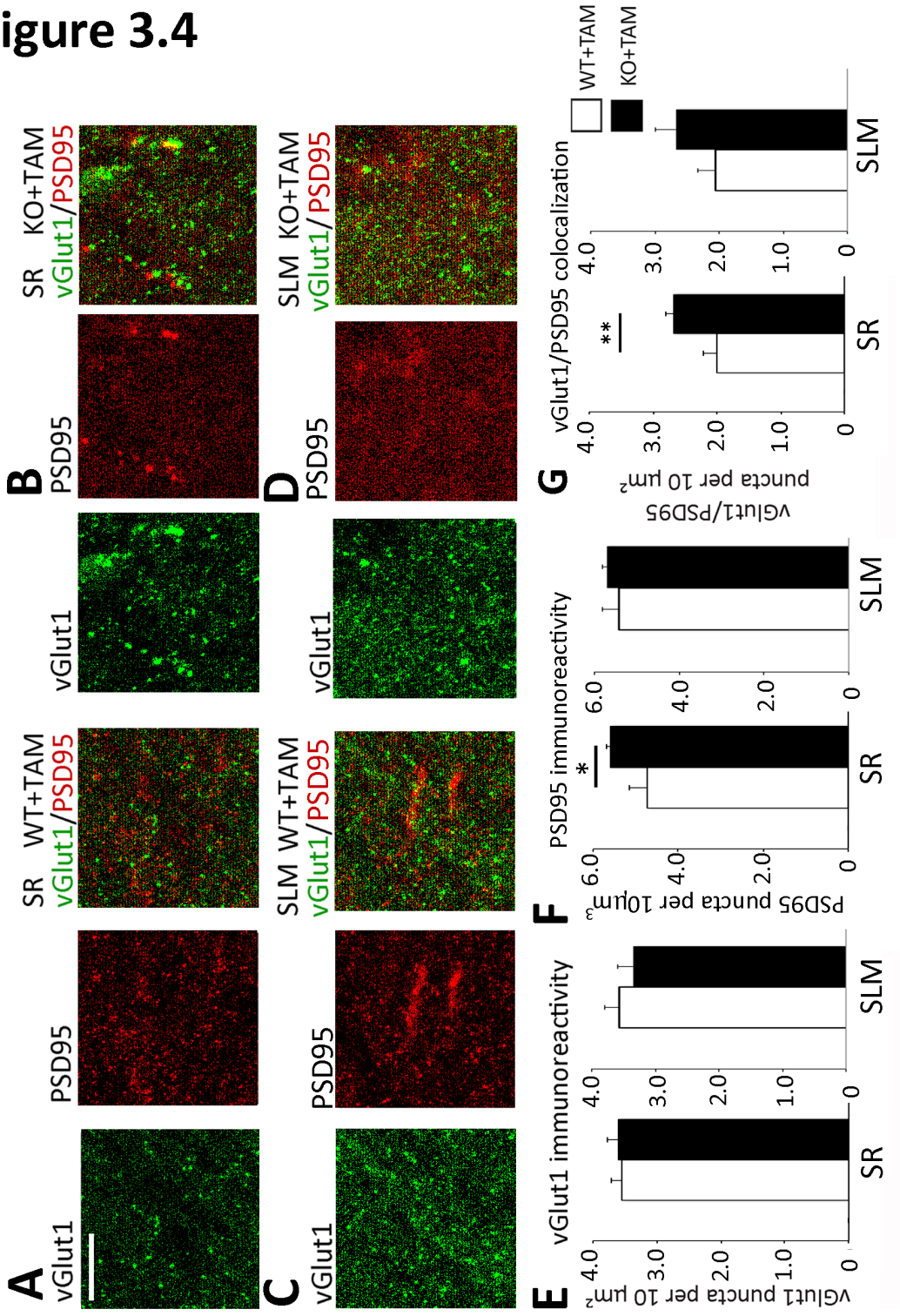
A
vGlut1
PSD95
SR WT+TAM
vGlut1/PSD95
B
vGlut1
PSD95
SR KO+TAM
vGlut1/PSD95
C
vGlut1
PSD95
SLM WT+TAM
vGlut1/PSD95
D
vGlut1
PSD95
SLM KO+TAM
vGlut1/PSD95
E
vGlut1 immunoreactivity
vGlut1 puncta per 10 μm²
SR
SLM
F
PSD95 immunoreactivity
PSD95 puncta per 10μm³
*
SR
SLM
G
vGlut1/PSD95 colocalization
vGlut1/PSD95 puncta per 10 μm²
**
WT+TAM
KO+TAM
SR
SLM

Figure 3.4. Ablation of astrocytic ephrin-B1 increases synapse formation after fear conditioning.

(A-D) Confocal images showing vGlut1 (green) and PSD95 (red) immunolabeling in SR (A,B) and SLM (C,D) areas of the CA1 hippocampus of WT+TAM (A,C) and KO+TAM (B,D) adult mice after fear conditioning. Scale bar, 50 μm. (E,F) Graphs show the density of vGlut1-positive (E), PSD95-postive (F) and vGlut1/PSD95 co-localized (G) puncta per 10 μm^2 of the SR and SLM areas in the CA1 hippocampus of WT+TAM and KO+TAM mice. There is no significant difference in vGlut1- positive puncta between WT+TAM and KO+TAM mice (n = 3– 6 mice, WT+TAM: 3.549 ± 0.173 vs KO+TAM: 3.601 ± 0.1753, $t_{(29)} = 0.213$, $p = 0.833$, t test). However, KO+TAM mice had a significant 18% increase in PSD95 positive puncta (WT+TAM: 4.727 ± 0.425; KO+TAM: 5.592 ± 0.088; $t_{(32)} = 2.104$, $p = 0.043$, t test) and a 34% increase in vGlut1/PSD95 co-localization (n = 3– 6 mice, WT+TAM: 1.999 ± 0.215 vs KO+TAM: 2.678 ± 0.116, $t_{(29)} = 2.828$, $p = 0.008$, t test) in the SR CA1. Graphs show mean values and error bars represent SEM.

Figure 3.5

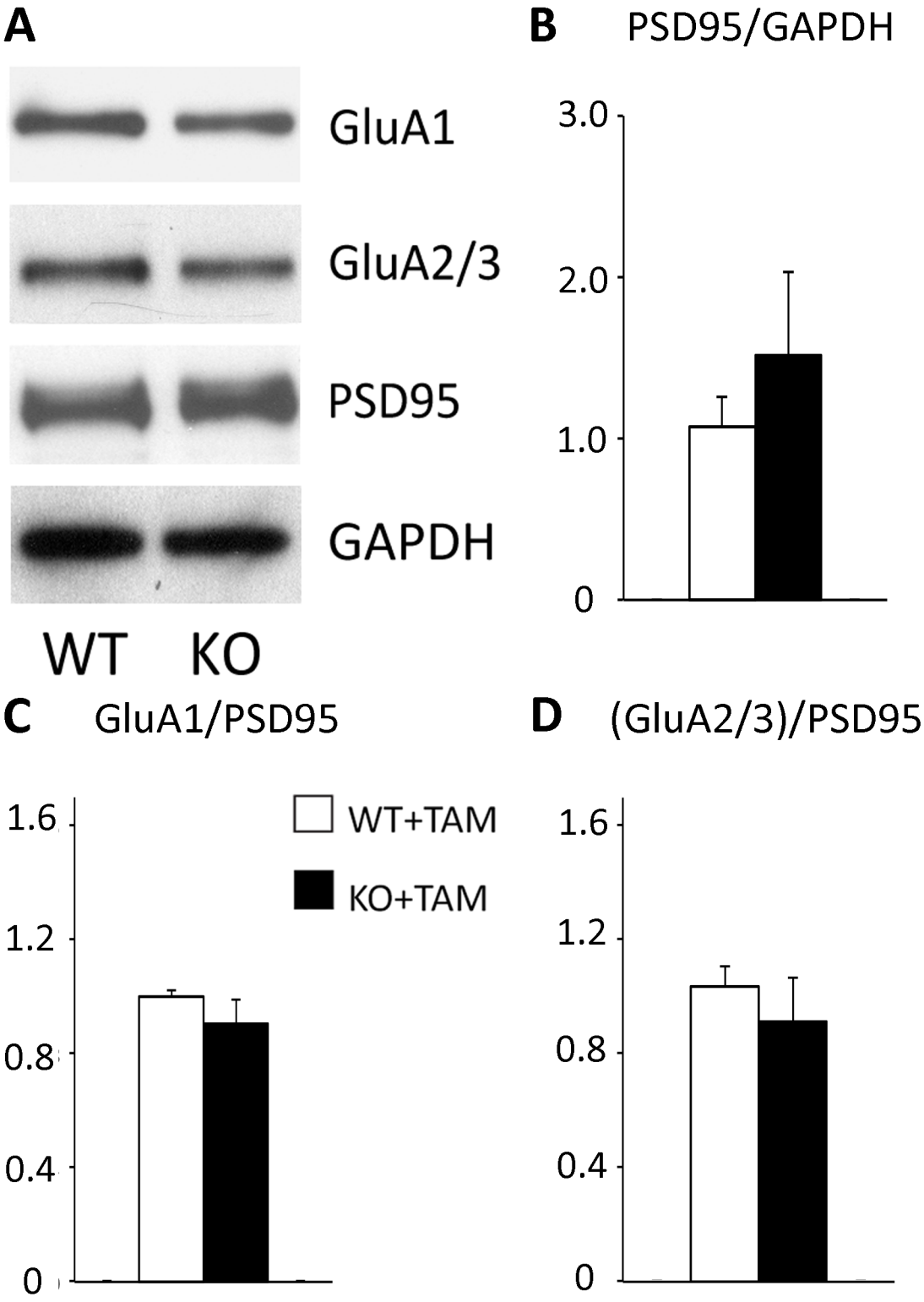
A
GluA1
GluA2/3
PSD95
GAPDH
WT
KO
B
PSD95/GAPDH
3.0
2.0
1.0
0
C
GluA1/PSD95
WT+TAM
KO+TAM
1.6
1.2
0.8
0.4
0
D
(GluA2/3)/PSD95
1.6
1.2
0.8
0.4
0

Figure 3.5. Fear conditioning promotes synaptic AMPAR recruitment in KO mice.

(A) Western blots show levels of AMPAR subunits (GluA1 and GluA2/3), PSD95 and GAPDH in synaptosomes isolated from the hippocampus of WT and KO mice 1h after context A recall. (B-D) Graphs show ratios of synaptic GluA1 or GluA2/3 levels to PSD95 levels and PSD95 to GAPDH ratios. Following training, PSD95 levels were similar between KO+TAM and WT+TAM (WT+TAM: 1.073 ± 0.191 vs KO: 1.517 ± 0.509, $t_{(9)} = 0.7545$, $p = 0.4698$). There were also similar levels of AMPAR (GluA1 WT+TAM: 1.059 ± 0.167 vs KO+TAM: 1.380 ± 0.428, $t_{(9)} = 0.647$, $p = 0.534$, *t* test; GluA2/3 WT+TAM: 1.105 ± 0.213 vs KO+TAM: 1.890 ± 0.885, $t_{(9)} = 0.788$, $p = 0.451$, *t* test) and AMPAR/PSD95 ratios (GluA1: WT+TAM: 1.003 ± 0.007 vs KO+TAM: 0.918 ± 0.091, $t_{(12)} = 0.6931$ $p = 0.505$, *t* test; GluA2/3: WT+TAM: 1.032 ± 0.062 vs KO+TAM: 0.799 ± 0.106; $t_{(12)} = 1.537$, $p = 0.152$, *t* test). Graphs show mean values and error bars represent SEM.

Figure 3.6

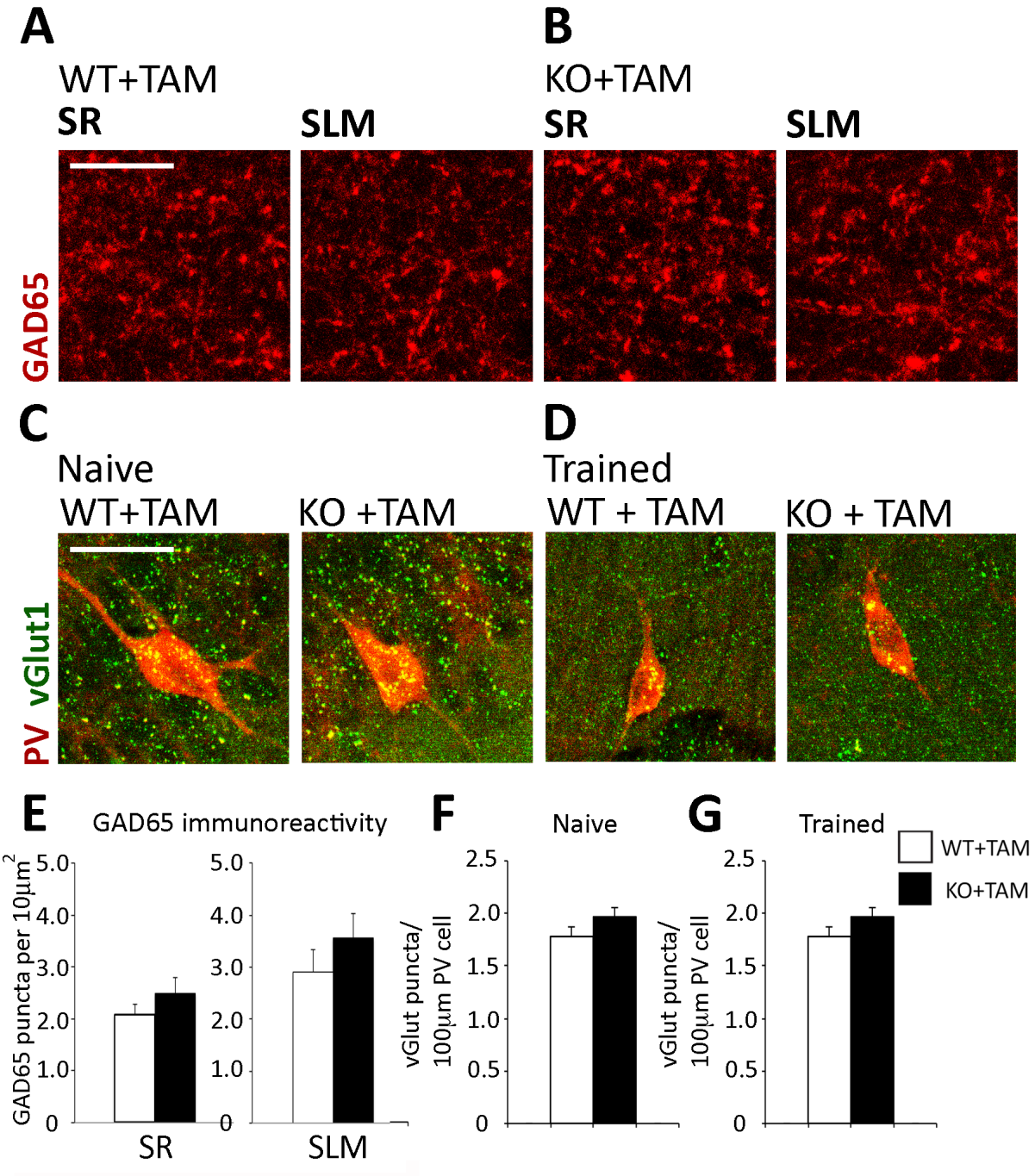
A
WT+TAM
SR
SLM
B
KO+TAM
SR
SLM
GAD65
C
Naive
WT+TAM
KO +TAM
D
Trained
WT + TAM
KO + TAM
PV vGlut1
E
GAD65 immunoreactivity
GAD65 puncta per 10μm2
5.0
4.0
3.0
2.0
1.0
0
SR
SLM
F
Naive
vGlut puncta/ 100μm PV cell
2.5
2.0
1.5
1.0
0.5
0
G
Trained
WT+TAM
KO+TAM

Figure 3.6. Astrocytic ephrin-B1 deletion does not effect inhibitory circuits during fear conditioning.

(A, B) Confocal images showing GAD65 (red) immunolabeling in SR and SLM areas of the CA1 hippocampus of WT+TAM (A) and KO+TAM (B) adult mice after fear conditioning. (C, D) Confocal images showing vGlut1 (green) and PV (red) immunolabeling in the CA1 hippocampus of WT+TAM and KO+TAM adult mice before (C) and after (D) fear conditioning. Graphs show immunoreactivity of GAD65 (E) and vGlut1-positive puncta per 100μm PV cell in naïve (F) and trained (G) mice. There was no significant difference in the number of inhibitory GAD65-positive puncta between WT+TAM and KO+TAM mice in the SR (n = 3– 6 mice, WT+TAM: 1.036 ± 0.103 vs KO+TAM: 1.247 ± 0.150, $t_{(32)}$ ± 1.159, p = 0.255, t test) or SLM (n = 3– 6 mice, WT+TAM: 1.452 ± 0.219 vs KO+TAM: 1.784 ± 0.230, $t_{(29)}$ = 0.1254, p = 0.306, t test). There was also no significant difference in vGlut1 co-localization with PV cell in naïve (n = 250-300 cells, WT+TAM: 1.780 ± 0.088 vs KO+TAM: 1.968 ± 0.084, $t_{(520)}$ =1.536, p = 0.125, t test) or trained (n = 250-300 cells, WT+TAM: 1.280 ± 0.070 vs KO+TAM: 1.451 ± 0.083, $t_{(663)}$ = 1.516, p = 0.114, t test). Graphs show mean values and error bars represent SEM.

Figure 3.7

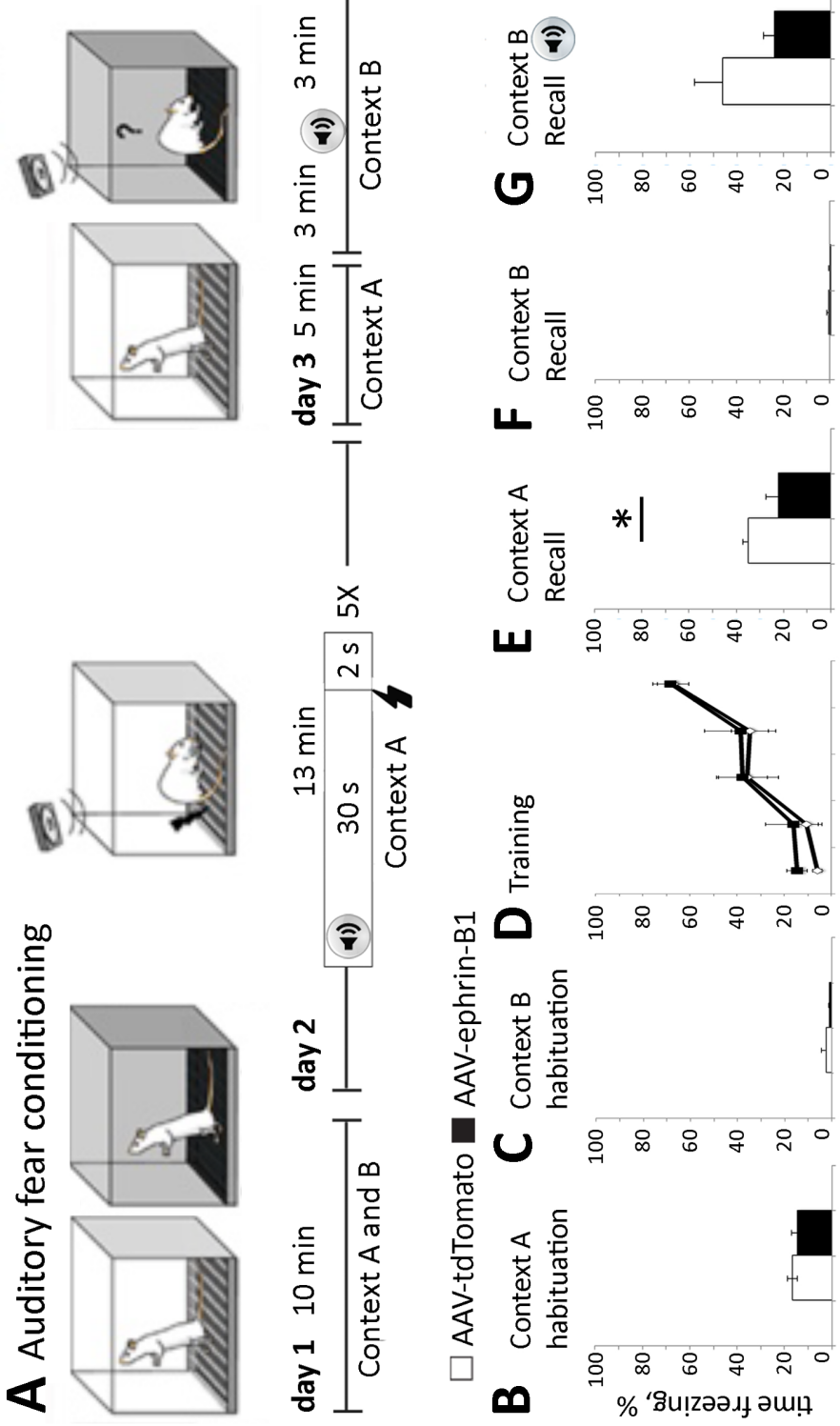
A Auditory fear conditioning
day 1 10 min
Context A and B
day 2
13 min
30 s
2 s
5X
Context A
day 3 5 min
Context A
3 min
Context B
3 min
AAV-tdTomato
AAV-ephrin-B1
B Context A habituation
C Context B habituation
D Training
E Context A Recall
F Context B Recall
G Context B Recall
time freezing, %
100
80
60
40
20
0
*

Figure 3.7. Mice over expressing astrocytic ephrin-B1 showed deficits in contextual recall.

(A) Schematic depiction of fear conditioning test. Mice were habituated to contexts A and B for 10 min on day 1. On day 2 mice were placed in Context A and received 5 random 0.7 mA foot shocks for 2 s after a 30 s tone at 70 Hz, training the mice to associate the tone with the foot shock. On day 3 mice were placed in Context A for 5 min, 1 h later mice were placed in Context B for 6 min and exposed to a 70 dB tone for the last 3 min. (B-G) Graphs show the average mouse freezing during each trial, including Context A habituation (B), Context B habituation (C), Context A training (D), Context A recall (E), Context B without (F) and with tone (G). Ephrin-B1 OE mice show reduced freezing compared with WT mice during Context A recall (n = 5 mice per group, astrocytic ephrin-B1 OE: 22.23 ± 5.12 vs control: 35.14 ± 2.11, $t_{(7)} = 2.534$ $p = 0.039$, t test, *$p = 0.05$). However, freezing time of astrocytic ephrin-B1 OE mice during initial habituation to Context A before training and during contextual recall 24 h after training was not significantly different (astrocytic ephrin-B1 OE Context A habituation: 14.85 ± 2.11 vs astro-ephrin-B1 OE Context A recall: 22.23 ± 5.12). In contrast, control mice expressing tdTomato retained Context A fear memory and were freezing more 24 h after training than during habituation (n = 5 mice per group, tdTomato control Context A habituation: 16.68 ± 0.28 vs tdTomato control Context A recall: 35.14 ± 2.1, $t_{(8)} = 8.673$, $p = 0.0004$, t test). Graphs show mean values and error bars represent SEM.

Figure 3.8

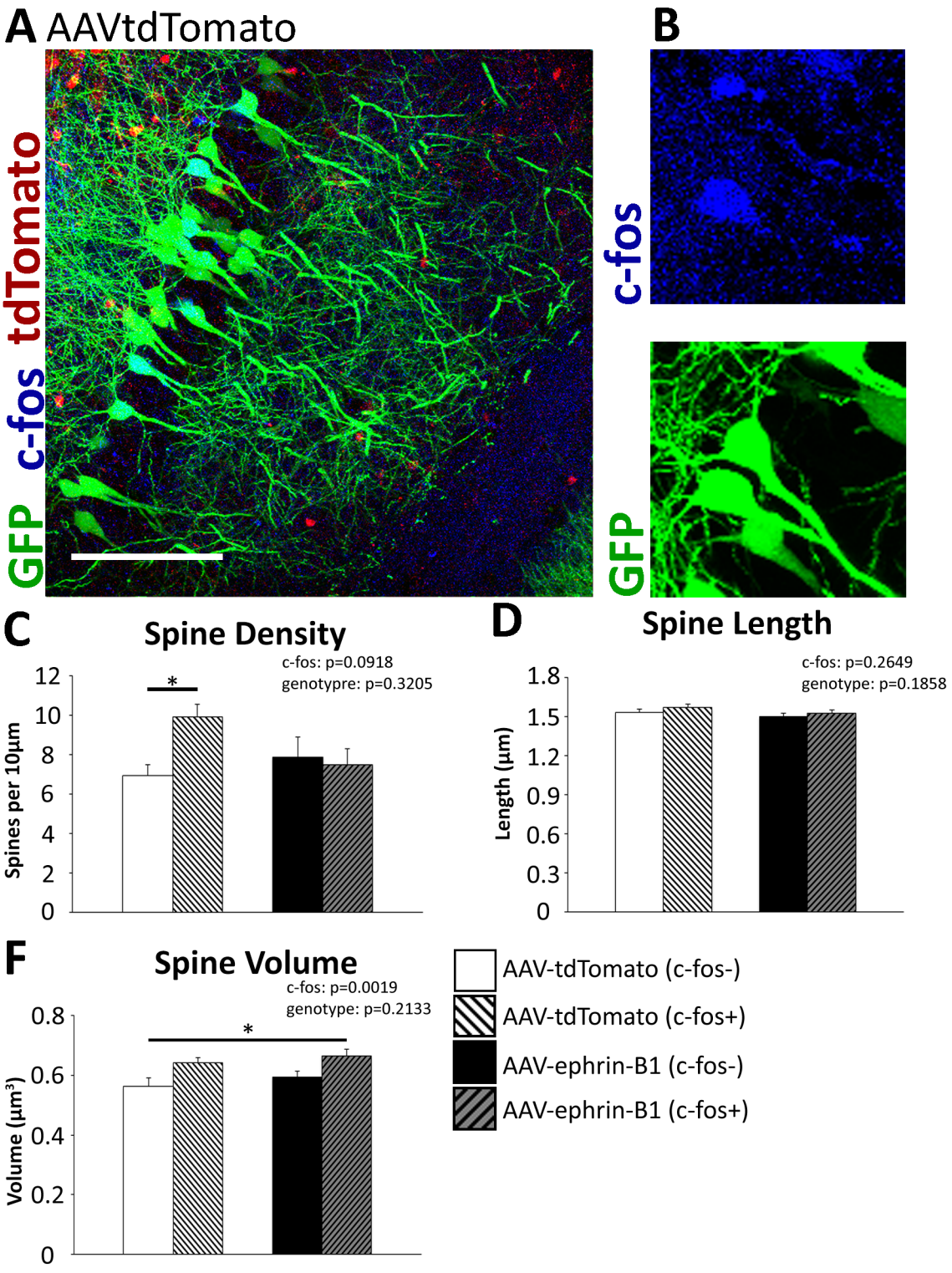
A AAVtdTomato
GFP c-fos tdTomato
B
c-fos
GFP
C
Spine Density
c-fos: p=0.0918
genotypre: p=0.3205
Spines per 10µm
12
10
8
6
4
2
0
*
D
Spine Length
c-fos: p=0.2649
genotype: p=0.1858
Length (µm)
1.8
1.5
1.2
0.9
0.6
0.3
0
F
Spine Volume
c-fos: p=0.0019
genotype: p=0.2133
Volume (µm³)
0.8
0.6
0.4
0.2
0
*
AAV-tdTomato (c-fos-)
AAV-tdTomato (c-fos+)
AAV-ephrin-B1 (c-fos-)
AAV-ephrin-B1 (c-fos+)

Figure 3.8. Overexpression of astrocytic ephrin-B1 inhibits activity dependent dendritic spine formation.

(A) Confocal images of the CA1 hippocampus Thy1-EGFP (green), c-fos (blue),and tdTomato (red) scale bar = 100μm. (B) Magnified images of c-fos-positive (blue) Thy-1 GFP (green) pyramidal neurons. (C) There was no significant difference in average dendritic spine density in c-fos positive KO+TAM neurons compared with and c-fos-negative WT+TAM mice; error bars represent SEM (n = 3– 6 mice, KO+TAM c-fos (+) : 7.168 ± 0.555 vs WT+TAM c-fos (-): 7.476 ± 0.797; $F_{(5,156)} = 0.0213$, p =0.001; one-way ANOVA, Tukey's *post hoc* test, ***p = 0.001). A significant decrease in the proportion of dendritic spines with smaller heads (volume 0 – 0.5 μm^3) in c-fos negative AAV-tdTomato and c-fos positive neurons compared c-fos negative AAV-tdTomato (n = 3– 6 mice, $F_{(5,156)} = 120.9$, $p = 0.0001$; two-way ANOVA followed by Tukey's *post hoc*, *p = 0.05,). Graphs show mean values and error bars represent SEM.

Figure 3.9

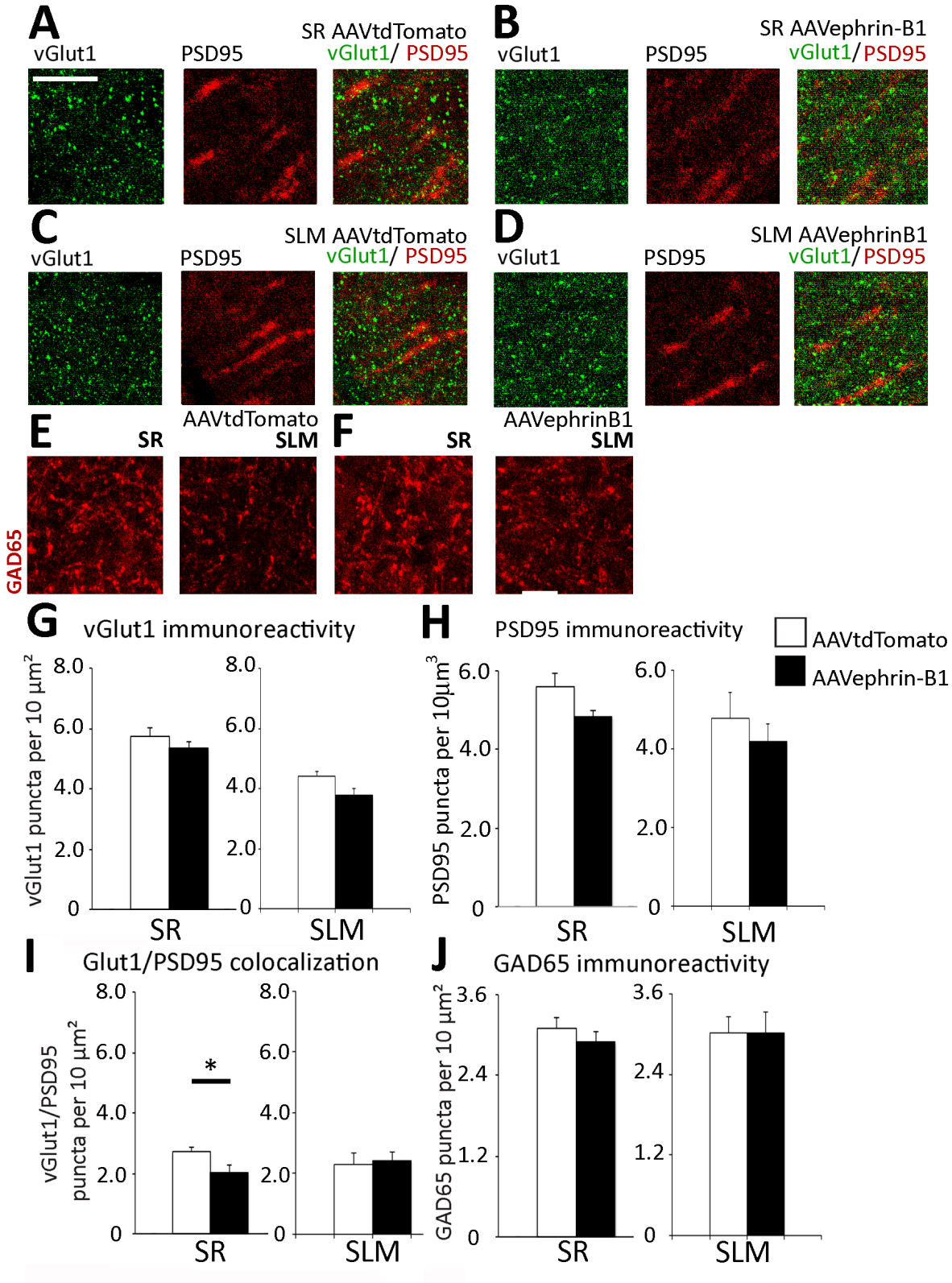
A
vGlut1
PSD95
SR AAVtdTomato
vGlut1/ PSD95
B
vGlut1
PSD95
SR AAVephrin-B1
vGlut1/PSD95
C
vGlut1
PSD95
SLM AAVtdTomato
vGlut1/ PSD95
D
vGlut1
PSD95
SLM AAVephrinB1
vGlut1/PSD95
E
SR
AAVtdTomato
SLM
F
SR
AAVephrinB1
SLM
GAD65
G
vGlut1 immunoreactivity
vGlut1 puncta per 10 µm²
8.0
6.0
4.0
2.0
0
SR
SLM
H
PSD95 immunoreactivity
PSD95 puncta per 10µm³
AAVtdTomato
AAVephrin-B1
6.0
4.0
2.0
0
SR
SLM
I
Glut1/PSD95 colocalization
vGlut1/PSD95 puncta per 10 µm²
*
8.0
6.0
4.0
2.0
0
SR
SLM
J
GAD65 immunoreactivity
GAD65 puncta per 10 µm²
3.6
2.4
1.2
0
SR
SLM

Figure 3.9 Astrocytic ephrin-B1 OE decreases excitatory synapse formation after fear conditioning.

(A-D) Confocal images showing vGlut1 (green) and PSD95 (red) immunolabeling in SR (A,B) and SLM (C,D) areas of the CA1 hippocampus of AAV-tdTomato (A,C) and AAV-ephrinB1 (B,D) adult mice1h after fear conditioning. (E,F) Confocal images showing GAD65 (red) Scale bar, 50 μm. (G-J) Graphs show the density of vGlut1-positive (G), PSD95-positive (H), vGlut1/PSD95 co-localized (I), and GAD65-positive (J) puncta per 10 μm^2 of the SR and SLM areas in the CA1 hippocampus of AAV-tdTomato and AAV-ephrinB1 mice. There is no significant difference in vGlut1-positive puncta between AAV-tdTomato and AAV-ephrinB1 mice (n = 3– 6 mice, AAV-tdTomato: 5.736 ± 0.275 vs AAV-ephrinB1: 5.352 ± 0.1588, $t_{(32)}$ ± 1.120, p = 0.2709, t test). AAV-ephrinB1 mice had a 15% decrease in PSD-95 puncta (AAV-tdTomato: 5.600 ± 0.336; AAV-ephrinB1: 4.835 ± 0.148; $t_{(32)}$ = 2.084, p = 0. 0453, t test) AAV-ephrinB1 mice had a significant 25% decrease in vGlut1/PSD95 co-localization (n = 3– 6 mice, AAV-tdTomato: 2.719 ± 0.158 vs AAV-ephrinB1: 2.036 ± 0.232, $t_{(32)}$ = 2.433, p = 0. 021, t test). No significant differences were seen in GAD65 staining. Graphs show mean values and error bars represent SEM.

Figure 3.10

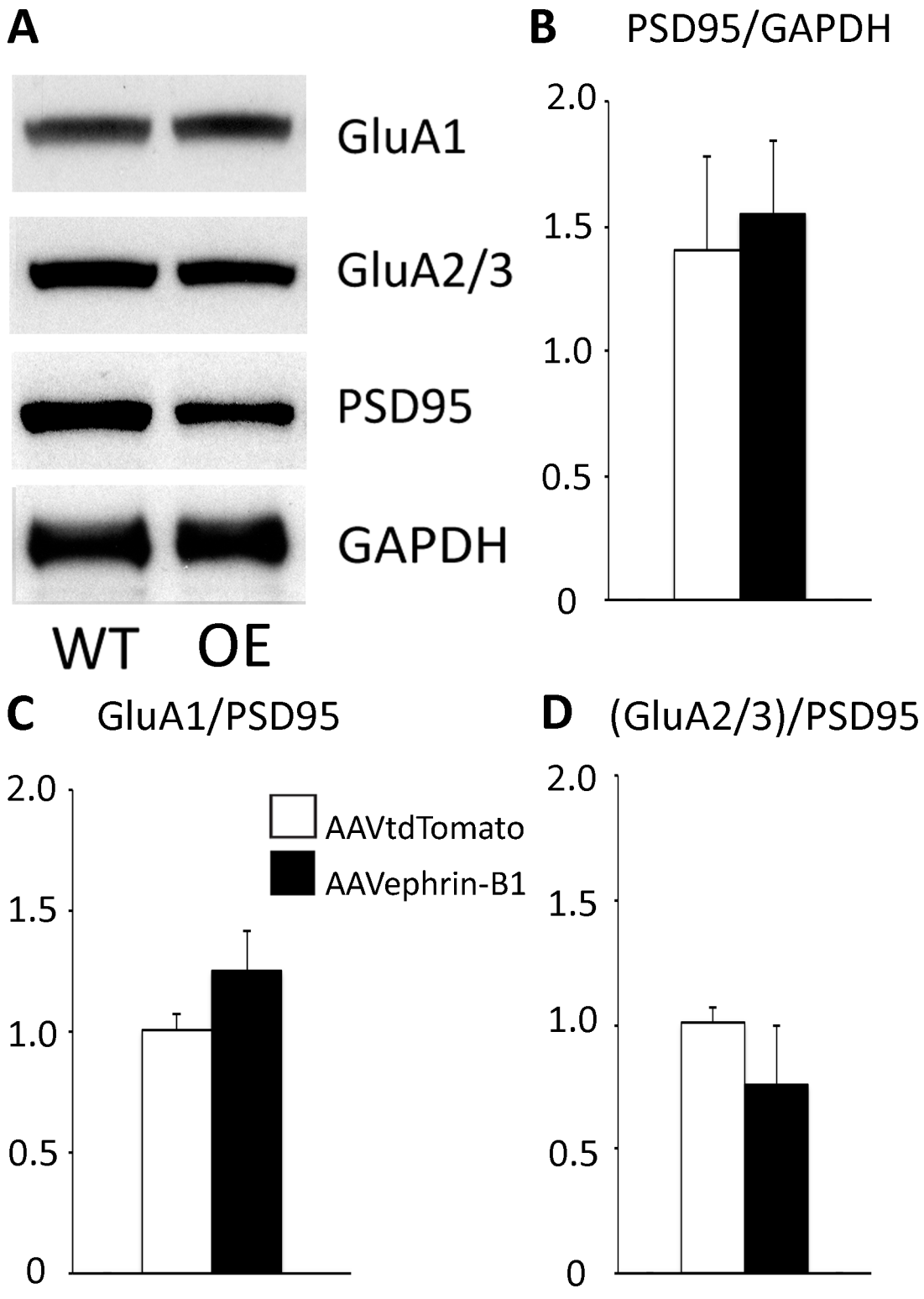
A
GluA1
GluA2/3
PSD95
GAPDH
WT
OE
B
PSD95/GAPDH
2.0
1.5
1.0
0.5
0
C
GluA1/PSD95
AAVtdTomato
AAVephrin-B1
2.0
1.5
1.0
0.5
0
D
(GluA2/3)/PSD95
2.0
1.5
1.0
0.5
0

Figure 3.10. Astrocytic ephrin-B1 OE and Control mice show no differences in synaptic AMPAR after fear conditioning.

(A) Western blots show levels of AMPAR subunits (GluA1 and GluA2/3), PSD95 and GAPDH in synaptosomes isolated from the hippocampus of Control and OE mice 1h after context A recall. (B-D) Graphs show ratios of synaptic GluA1 or GluA2/3 levels to PSD95 levels and PSD95 to GAPDH ratios. There were also similar levels of AMPAR/PSD95 ratios (GluA1; AAV-tdTomato: 1.006 ± 0.063 vs AAV-ephrinB1: 1.251 ± 0.161, $t_{(8)} = 1.637$ $p = 0.140$, *t* test; GluA2/3 AAV-tdTomato: 1.007 ± 0.065 vs AAV-ephrinB1: 0.757 ± 0.238, $t_{(8)} = 1.221$, $p = 0.1285$, *t* test). Graphs show mean values and error bars represent SEM.

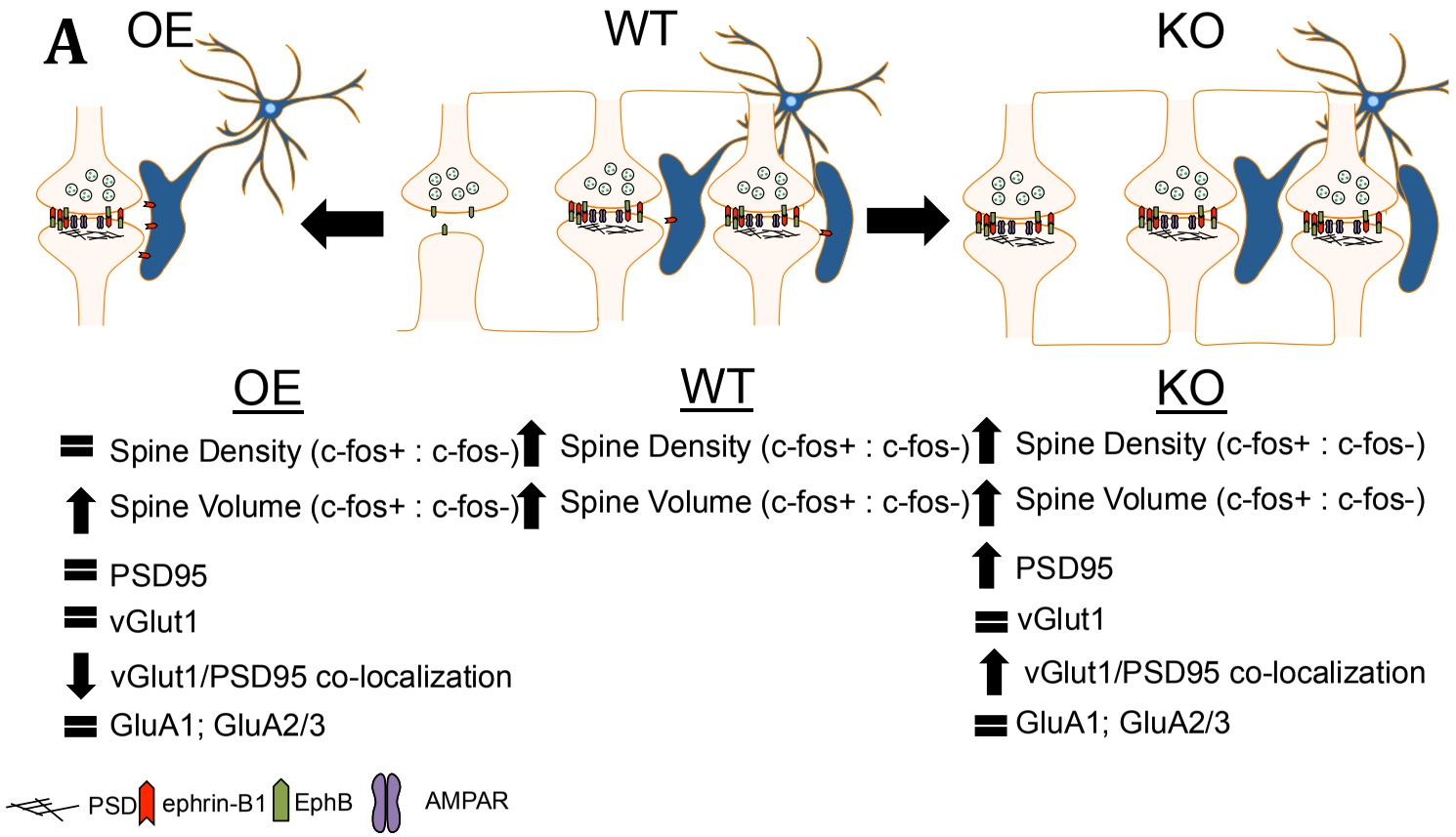
A
OE
WT
KO
OE
Spine Density (c-fos+ : c-fos-)
Spine Volume (c-fos+ : c-fos-)
PSD95
vGlut1
vGlut1/PSD95 co-localization
GluA1; GluA2/3
WT
Spine Density (c-fos+ : c-fos-)
Spine Volume (c-fos+ : c-fos-)
KO
Spine Density (c-fos+ : c-fos-)
Spine Volume (c-fos+ : c-fos-)
PSD95
vGlut1
vGlut1/PSD95 co-localization
GluA1; GluA2/3
PSD
ephrin-B1
EphB
AMPAR

Figure 3.11

Figure 3.11. Astrocytic ephrin-B1 mediated regulation of synapses during fear conditioning.

(A). Model of the synaptogenic effects of ephrin-B1 deletion and overexpression in astrocytes after fear conditioning. Ablation of astrocytic ephrin-B1 saw activity dependent increases in dendritic spine density and volume. In addition to PSD95 puncta, vGlut1/PSD95 co-localization was increased in KO mice. Overexpression of ephrin-B1 inhibited activity dependent increases in dendritic spine density and saw decreased vGlut1/PSD95 co-localization.

Chapter 4- Ephrin-B1 mediates synaptosome engulfment in primary hippocampal astrocytes.

Abstract

Previously presented *in vivo* studies implicate astrocyte specific ephrin-B1 as a negative regulator for immature synapses in the adult CA1 hippocampus. Deletion of astrocytic ephrin-B1 leads to an increase in AMPA silent immature excitatory synapses that mature during fear conditioning leading to enhancing contextual recall in KO mice. In contrast, overexpression of astrocytic ephrin-B1 in the hippocampus results in fewer immature synapses contributing to reduced contextual recall, and OE mice had fewer excitatory connections after fear conditioning suggesting memory formation was inhibited by the lack of available immature synapses. How hippocampal astrocytes eliminate immature synapses, however, is still unclear. Our *in vitro* experiments suggest neuronal EphB receptors may be an "eat me" signal for synapse elimination by trans-phagocytosis in hippocampal astrocytes. In fact, inhibition of ephrin-B1 reverse signaling reduces synaptosome engulfment by hippocampal astrocytes, and a deletion of neuronal EphB receptors impairs the ability of astrocytes expressing functional ephrin-B1 to engulf synaptosomes *in vitro*.

Introduction

Many astrocyte-secreted factors are involved in promoting synaptogenesis (Christopherson et al., 2005; Eroglu et al., 2009; Ullian, Sapperstein, Christopherson, & Barres, 2001) and promote synaptic AMPAR recruitment (Allen et al., 2012). Despite robust synaptogenic effects from secreted proteins, neurons treated with ACM had fewer synapses than neurons co-cultured with astrocytes (Christopherson et al., 2005), indicating that contact mediated factors play a role in synapse formation. In fact, astrocytic integrins and γ-Protocadherins promotes synaptogenesis through contact mediated signaling (Garrett & Weiner, 2009; Hama, Hara, Yamaguchi, & Miyawaki, 2004). EM microscopy showing neuronal debris within astrocytic endosomes also implicates astrocytes in synaptic pruning in the adult hippocampus by trans-phagocytosis. Indeed, primary astrocytes are shown eliminate synapses from RGCs through trans-phagocytosis utilizing the MEGF10 and MERTK pathways (Chung et al., 2013). A specific signal for synapse elimination in astrocytes, however, is still unknown. Here I propose neuronal EphB receptors as a potential "eat me" signal for synapse elimination through the activation of ephrin-B1 and trans-phagocytosis by hippocampal astrocytes.

Eph/ephrin signaling play various roles in proper CNS formation and maintenance, and are associated with both cell repulsion and adhesion. Trans-synaptic EphB/ephrinB interactions promote are also shown to promote formation and stabilization of synapses (Klein, 2009; Pasquale, 2005). EphB2 signaling contributes to dendritic spine maturation by inducing reorganization of the actin cytoskeleton through the activation of Rho-family GTPases. EphB2 association with interesectin-1 and N-WASP increases actin

polymerization by activating the Cdc42 (Irie & Yamaguchi, 2002). In addition, EphB2 activation stimulates dendritic spine formation by Rac1 activation through Rho-GEF protein Kalirin (Penzes et al., 2003). Although EphB/ephrinB are involved in synaptic maturation and stabilization, EphB induced actin remodeling can also promote cell repulsion during axon guidance (Egea & Klein, 2007; Goldshmit, McLenachan, & Turnley, 2006; Pasquale, 2008). EphB1 stimulation promotes the internalization of ephrin-B1 ligand through clatherin mediated endocytosis (Parker et al., 2004) and the disassembly of F-actin by recruiting adaptor protein Grb4 SH2 domain (Cowan & Henkemeyer, 2001) which contributes to detachment during cell repulsion (Zimmer, Palmer, Köhler, & Klein, 2003). Debris from EphB expressing cells can also be found in endosomes of ephrinB expressing cells immediately after cell repulsion (Marston, Dickinson, & Nobes, 2003). Astrocytic ephrin-B1 may utilize similar pathways as seen in cell repulsion to eliminate immature synapses. Indeed, Neuronal ephrin-B1 activation promotes endocytosis of neuronal exosomes expressing EphB2 by increasing Tiam1 and Tiam2 activity leading to actin reorganization (Gaitanos *et al.,* 2016)

Our *in vivo* studies suggest astrocytic ephrin-B1 may be an "eat me" signal from synaptic EphB receptors leading to the elimination of the synapse possibly by increasing RhoGTPase activity.

Materials and Methods

Astrocyte cultures

Astrocytes were isolated from Cre^{GFAP}*ephrin-B1*$^{flox/y}$ or WT mouse hippocampi at postnatal day 0 (P0)-P1 as previously described (Barker et al., 2008). Hippocampi were treated with 0.1% trypsin/EDTA solution for 25 min at 37°C, and mechanically dissociated. Cells were plated on cell culture flasks and cultured in DMEM containing 10% FCS and 1% pen-strep, under 10% CO2 atmosphere at 37°C. To enrich astrocyte cultures (>95% astrocytes) cells were shaken after 4 days in *vitro* (DIV) for 1 h. After shaking, the medium was removed and cells were washed twice with 0.1 M PBS (pH 7.4). Cells were then treated with 0.1% trypsin/EDTA solution for 20 min at 37°C and plated on 10-cm Petri dishes with DMEM containing 10% FBS. Once confluent astrocytes were detached with trypsin and plated on six-well plates at a density of 330,000 cells per plate and cultured for 2 days before being transfected with *pEGFP,* *pEGFP* and *pcDNA-ephrin-B1*, or *pEGFP* and *pcDNA-Cre* plasmids using Lipofectamine according to the manufacturer's instructions (Invitrogen, 11668-019).

Ephrin-B1 Mutants

Mutagenesis was carried out using QuikChange Lighting Multi Site-Directed Mutagenesis Kit (Catalog No. 210513, Agilent Technologies, Santa Clara, CA) to generate ephrin-B1Y294F, ephrin-B1Y310F and ephrin-B1Y294F/Y310F mutants by changing tyrosine (TAC) at positions 294 and 310 to phenylalanine (TTC) using *pcDNA* plasmid containing mouse *ephrin-B1* cDNA (Fig 4.1B).

Synaptosome Purification

Synaptosome purification was performed as previously described (Hollingsworth et al., 1985). Hippocampal tissues from adult WT or EphB1,2,3 KO mice were homogenized in 1 ml synaptosome buffer (124 mM NaCl, 3.2 mM KCl, 1.06 mM KH_2PO_4, 26 mM $NaHCO_3$, 1.3 mM $MgCl_2$, 2.5 mM $CaCl_2$, 10 mM Glucose, 20 mM HEPES). Homogenates were filtered through a 100 μm nylon net filter (NY1H02500, Millipore) and 5 μm nylon syringe filter (SF15156, Tisch International). Homogenate flow through was collected and synaptosomes were spun down at 10,000 g, 4^{o}C, for 30 min. Synaptosomes were resuspended in 800 μl synaptosome buffer. To confirm synaptosome enrichment, levels of synapsin-1, PSD95, and histone deacetylase (HDAC I) were analyzed in tissue homogenates and synaptosome fractions with western blot analysis. Synaptosomes for engulfment assays were also stained with 5% (w/v) DiI (D282, Molecular Probes) in DMSO for 10 min.

Engulfment Assay

Astrocytes were isolated as described above. 14 DIV astrocytes were plated onto poly-D-lysine (0.5 mg/ml) coated coverslips at 50,000 cells per coverslip and maintained at 37^{o}C 10% CO_2. Astrocytes were transfected 24 h after plating with *pcDNA-eGFP, pcDNA-eGFP + pcDNA3-ephrin-B1, pcDNA-eGFP + pcDNA3-ephrin-B1Y294F, pcDNA-eGFP + pcDNA3-ephrin-B1Y310F*, or *pcDNA-eGFP + pcDNA3-ephrin-B1Y294/310F* using Lipofectamine 2000 (Invitrogen; 11668-027). Isolated synaptosomes (see synaptosome purification) were added to astrocyte cultures and incubated for 2-4 h at 37^{o}C 10% CO_2.

Astrocytes were washed with 0.1 M PBS (16 mM NaH_2PO_4, 96 mM Na_2HPO_4, 137 mM NaCl), followed by fixation for 30 min with 2% paraformaldehyde in 0.1 M PBS. Cultures were immunostained (see immunohistochemistry) against ephrin-B1 and imaged using a Zeiss 510 confocal microscope (see Confocal Imaging and Analysis). In brief, astrocytes were randomly selected per group and imaged using a 63x objective (1.2 NA) and 1x zoom. A series of 3-5 high-resolution optical sections (1024x1024) were taken at 0.5 μm-interval in the X-Y plane. Synaptosome engulfment was determined by measuring integrated density of DiI-labeled synaptosomes associated with GFP-expressing astrocytes using ImageJ Software. Statistical analysis was performed with a one-way ANOVA followed by Tukey post-hoc analysis using GraphPad Prism 6 software (RRID: SCR_002798), data represent mean ± SEM.

Results

Reverse signaling through ephrin-B1 regulates astrocyte engulfment of synaptosomes containing EphB receptors.

To determine whether ephrin-B1/EphB receptor interactions are responsible for astrocyte-mediated engulfment of pre-synaptic boutons, we tested the ability of astrocytes expressing ephrin-B1 to engulf synaptosomes. WT primary hippocampal astrocytes were transfected with loss-of-function ephrin-B1 mutant (Fig. 4.1B) 24h prior to engulfment assay. Astrocyte cultures were incubated for 2h with DiI labeled crude synaptosomes isolated from WT mouse hippocampi. Enrichment of synaptic proteins PSD95 and synapsin-1 in synaptosomes was confirmed by immunoblotting (Fig. 4.1A). Interestingly immunostaining indicated clustering of astrocytic ephrin-B1 around WT synaptosomes suggesting possible interactions between astrocytic ephrin-B1 and neuronal EphB receptors in synaptosomes (Fig. 4.2A). I observed a significant 69% decrease in synaptosome engulfment by astrocytes expressing ephrin-B1Y294F/Y310F mutant (5.04 ± 1.27) as compared to astrocytes expressing ephrin-B1 (Fig. 4.2B; 12.99 ± 2.40, $F_{(9,248)}$ =10.04, p=0.009, ANOVA). Partial loss-of-function mutants Y294F (6.2454 ± 1.356) and Y310F (4.852 ± 1.074) showed similar deficits in synaptosomes engulfment to Y294/310F expressing astrocytes. Our results show ephrin-B1 reverse signaling promotes synaptosome engulfment in astrocytes and requires phosphorylation of both tyrosine 294 and 310 on ephrin-B1.

Ephrin-B1 mediated synaptosome engulfment in astrocytes diminishes over time.

To investigate whether compensatory mechanisms increase synaptosome

engulfment over time, WT and loss-of-function astrocytes were incubated with DiI labeled synaptosomes for 4hr. Pro-longed incubation with synaptosomes did not increase engulfment in mutant astrocytes despite the presence of available free synaptosomes in culture (Fig. 4.3A). Astrocytes expressing WT ephrin-B1 (12.406 ± 3.841) maintained a 73% increase in synaptosome engulfment compared to Y294/310F (Fig. 4.3B; 4.532 ± 1.050; $F_{(4,162)}$ =2.436, p=0.049, ANOVA) mutants compared to a 69% increase during 2h incubation. Deficits in Y294/310F mutants demonstrate ephrin-B1 mediated synaptosome engulfment is not compensated for by other signaling mechanisms. Interestingly WT ephrin-B1 expressing astrocytes did not see an increase in synaptosome uptake from 2h (12.99 ± 2.40) to 4h (12.406 ± 3.841) possibly due to a lack of surface ephrin-B1 receptors which were probably internalized with synaptosomes early in the engulfment assay.

Neuronal EphB receptors are necessary for synaptosome engulfment in astrocytes.

To determine if neuronal EphB receptors trigger synaptosome engulfment in astrocytes synaptosomes were extracted from the hippocampi of EphB1,2,3 KO mice. WT ephrin-B1 and loss-of-function mutant expressing astrocytes were incubated with DiI labeled EphB1,2,3 KO synaptosome for 2h. Astrocyte expressing ephrin-B1 contained significantly more WT synaptosomes (12.99 ± 2.40) than synaptosomes lacking EphB1/2/3 receptors 2 h after the addition of synaptosomes (Fig. 4.2C; 2.11 ± 0.71, F(9,248) =10.04, p=0.000154, ANOVA), which indicates that synaptic EphB receptors are the trigger for ephrin-B1 mediated synapse elimination.

Discussion

Previously reported elimination of synapse could be due to engulfment of immature synapses during memory formation. While astrocytes are shown to prune neuronal synapses (Chung et al., 2013; Spacek, 2004), what triggers synapse engulfment by astrocytes is still unclear. Our *in vitro* studies indicate ephrin-B1 reverse signaling is necessary for synapse engulfment as loss-of-function mutants showed significant decreases in synaptosome engulfment in primary hippocampal astrocytes. Reduced synaptosome engulfment in full (Y294/310F) and partial (Y294F, Y310F) mutants indicates phosphorylation of ephrin-B1 is required for ephrin-B1 mediated synapse removal. Interestingly, synaptosome engulfment in astrocytes diminishes after 2h hour incubation. Activation induced internalization of ephrin-B1 (Parker et al., 2004) may deplete surface ephrin-B1 levels reducing astrocytes ability to uptake more synapses after initial engulfment. An observed association between ephrin-B1 and DiI labeled synaptosomes suggest engulfment of synaptosomes is accompanied by internalization of ephrin-B1. Inhibition of engulfment in EphB1,2,3 synaptosomes by WT ephrin-B1 astrocytes indicate EphB receptors are the neuronal trigger for ephrin-B1 mediated synapse removal by astrocytes. Synaptosome engulfment is likely mediated by ephrin-B1 stimulated actin remodeling as neuronal ephrin-B1 receptors were shown to increase Tiam1 and Tiam2 during exosome engulfment (Gaitanos *et al.,* 2016). Further studies into what mechanisms astrocytic ephrin-B1 utilizes during synaptosome engulfment may yield interesting results.

References

Allen, N. J., Bennett, M. L., Foo, L. C., Wang, G. X., Chakraborty, C., Smith, S. J., & Barres, B. A. (2012). Astrocyte glypicans 4 and 6 promote formation of excitatory synapses via GluA1 AMPA receptors. *Nature*, *486*(7403), 410–414. https://doi.org/10.1038/nature11059

Christopherson, K. S., Ullian, E. M., Stokes, C. C. A., Mullowney, C. E., Hell, J. W., Agah, A., … Barres, B. A. (2005). Thrombospondins are astrocyte-secreted proteins that promote CNS synaptogenesis. *Cell*. https://doi.org/10.1016/j.cell.2004.12.020

Chung, W. S., Clarke, L. E., Wang, G. X., Stafford, B. K., Sher, A., Chakraborty, C., … Barres, B. A. (2013). Astrocytes mediate synapse elimination through MEGF10 and MERTK pathways. *Nature*. https://doi.org/10.1038/nature12776

Cowan, C. A., & Henkemeyer, M. (2001). B-ephrin reverse signals, *413*(September).

Egea, J., & Klein, R. (2007). Bidirectional Eph-ephrin signaling during axon guidance. *Trends in Cell Biology*. https://doi.org/10.1016/j.tcb.2007.03.004

Eroglu, Ç., Allen, N. J., Susman, M. W., O'Rourke, N. A., Park, C. Y., Özkan, E., … Barres, B. A. (2009). Gabapentin Receptor α2δ-1 Is a Neuronal Thrombospondin Receptor Responsible for Excitatory CNS Synaptogenesis. *Cell*, *139*(2), 380–392. https://doi.org/10.1016/j.cell.2009.09.025

Gaitanos, T. N., Koerner, J., & Klein, R. (2016). Tiam–Rac signaling mediates trans-endocytosis of ephrin receptor EphB2 and is important for cell repulsion. *J Cell Biol*, jcb-201512010.

Garrett, A. M., & Weiner, J. A. (2009). Control of CNS Synapse Development by -Protocadherin-Mediated Astrocyte-Neuron Contact. *Journal of Neuroscience*, *29*(38), 11723–11731. https://doi.org/10.1523/JNEUROSCI.2818-09.2009

Goldshmit, Y., McLenachan, S., & Turnley, A. (2006). Roles of Eph receptors and ephrins in the normal and damaged adult CNS. *Brain Research Reviews*, *52*(2), 327–345. https://doi.org/10.1016/j.brainresrev.2006.04.006

Hama, H., Hara, C., Yamaguchi, K., & Miyawaki, A. (2004). PKC Signaling Mediates Global Enhancement of Excitatory Synaptogenesis in Neurons Triggered by Local Contact with Astrocytes. *Neuron*, *41*(3), 405–415. https://doi.org/10.1016/S0896-6273(04)00007-8

Irie, F., & Yamaguchi, Y. (2002). EphB receptors regulate dendritic spine development via intersectin, Cdc42 and N-WASP. *Nature Neuroscience*.

https://doi.org/10.1038/nn964

Klein, R. (2009). Bidirectional modulation of synaptic functions by Eph/ephrin signaling. *Nature Neuroscience*, *12*(1), 15–20. https://doi.org/10.1038/nn.2231

Marston, D. J., Dickinson, S., & Nobes, C. D. (2003). Rac-dependent trans-endocytosis of ephrinBs regulates Eph-ephrin contact repulsion. *Nature Cell Biology*. https://doi.org/10.1038/ncb1044

Parker, M., Roberts, R., Enriquez, M., Zhao, X., Takahashi, T., Pat Cerretti, D., … Chen, J. (2004). Reverse endocytosis of transmembrane ephrin-B ligands via a clathrin-mediated pathway. *Biochemical and Biophysical Research Communications*. https://doi.org/10.1016/j.bbrc.2004.07.209

Pasquale, E. B. (2005). Eph receptor signalling casts a wide net on cell behaviour. *Nature Reviews Molecular Cell Biology*, *6*(6), 462–475. https://doi.org/10.1038/nrm1662

Pasquale, E. B. (2008). Review Eph-Ephrin Bidirectional Signaling in Physiology and Disease, (Figure 1). https://doi.org/10.1016/j.cell.2008.03.011

Penzes, P., Beeser, A., Chernoff, J., Schiller, M. R., Eipper, B. A., Mains, R. E., & Huganir, R. L. (2003). Rapid induction of dendritic spine morphogenesis by trans-synaptic ephrinB-EphB receptor activation of the Rho-GEF kalirin. *Neuron*. https://doi.org/10.1016/S0896-6273(02)01168-6

Spacek, J. (2004). Trans-Endocytosis via Spinules in Adult Rat Hippocampus. *Journal of Neuroscience*, *24*(17), 4233–4241. https://doi.org/10.1523/JNEUROSCI.0287-04.2004

Ullian, E. M., Sapperstein, S. K., Christopherson, K. S., & Barres, B. A. (2001). Control of synapse number by glia. *Science*, *291*(5504), 657–661. https://doi.org/10.1126/science.291.5504.657

Zimmer, M., Palmer, A., Köhler, J., & Klein, R. (2003). EphB-ephrinB bi-directional endocytosis terminates adhesion allowing contact mediated repulsion. *Nature Cell Biology*. https://doi.org/10.1038/ncb1045

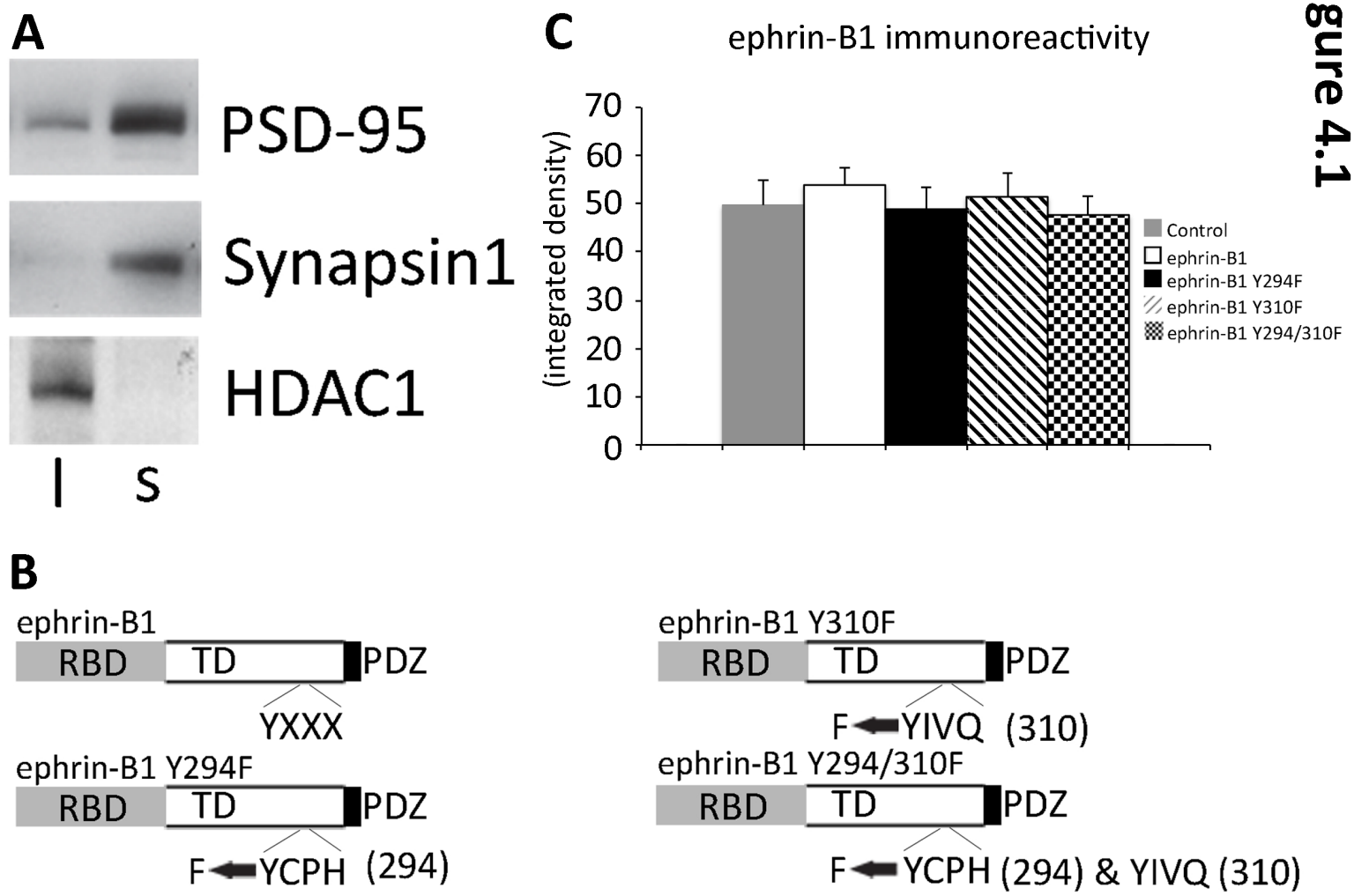
A
PSD-95
Synapsin1
HDAC1
I
S
C
ephrin-B1 immunoreactivity
(integrated density)
70
60
50
40
30
20
10
0
Control
ephrin-B1
ephrin-B1 Y294F
ephrin-B1 Y310F
ephrin-B1 Y294/310F
B
ephrin-B1
RBD
TD
PDZ
YXXX
ephrin-B1 Y294F
RBD
TD
PDZ
F YCPH (294)
ephrin-B1 Y310F
RBD
TD
PDZ
F YIVQ (310)
ephrin-B1 Y294/310F
RBD
TD
PDZ
F YCPH (294) & YIVQ (310)

Figure 4.1

Figure 4.1. Synaptosome isolation and loss-of-function ephrin-B1 mutants.

(A) Western blots showing enrichment of synaptic proteins (PSD95 and synapsin1) and a decrease in nuclear protein (HDAC1) in isolated synaptosomes. (B) Schematics of ephrin-B1 and ephrin-B1 mutants with tyrosine (Y) to phenylalanine (F) mutations. Graph shows ephrin-B1 immunoreactivity per 100 μm^2 primary hippocampal astrocytes treated with synaptosomes isolated form WT or mice. Graph shows that there are no significant differences in ephrin-B1 levels in primary astrocytes transfected with *pcDNA3ephrin-B1*, *pcDNA3ephrinB1Y294F*, *pcDNA3ephrinB1Y310F*, or *pcDNA3ephrinB1Y294/310F*. Graphs show mean values and error bars represent SEM (*n* = 28 –30 astrocytes, one-way ANOVA followed by Tukey's *post hoc* test).

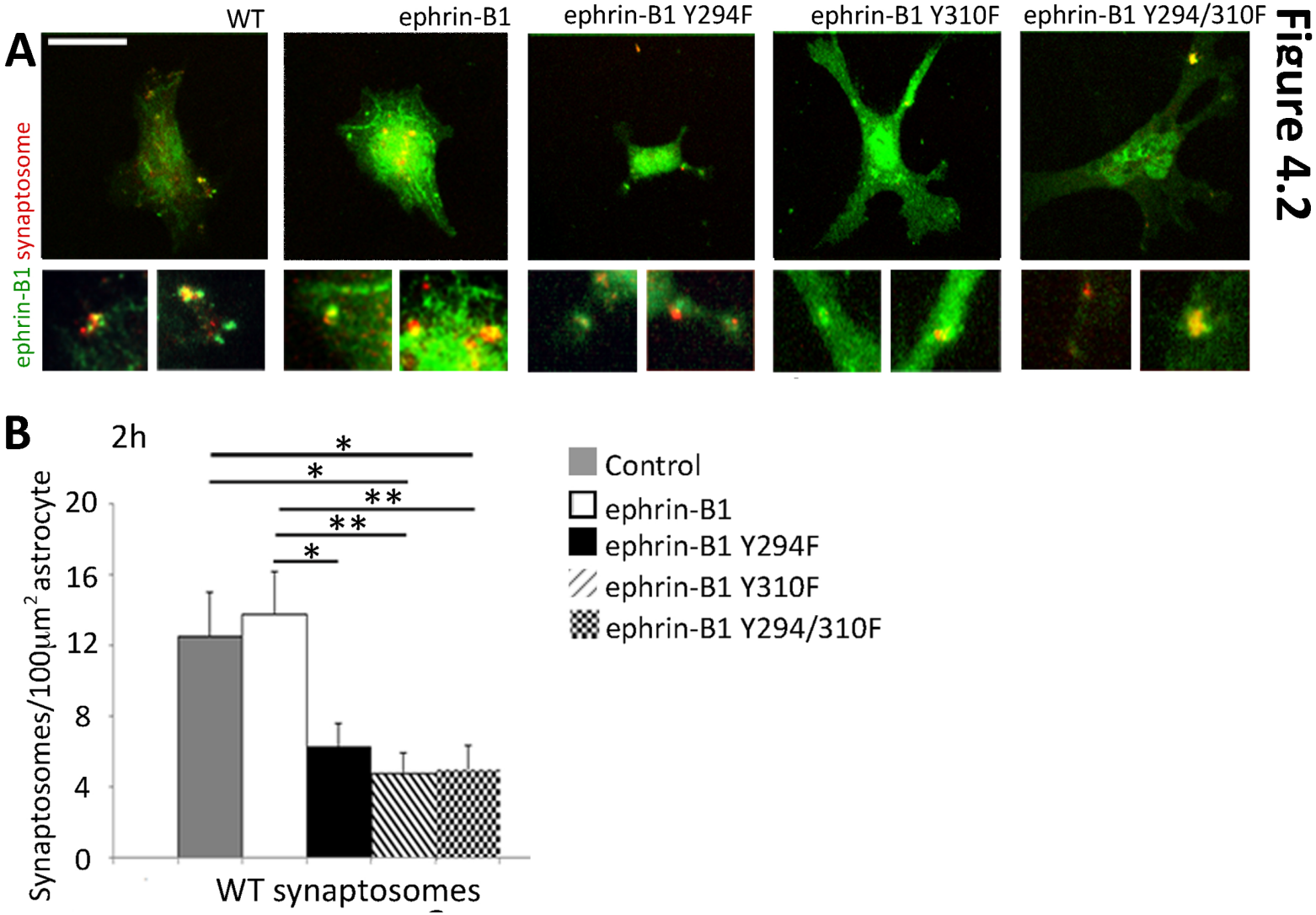
A
WT
ephrin-B1
ephrin-B1 Y294F
ephrin-B1 Y310F
ephrin-B1 Y294/310F
ephrin-B1 synaptosome
B
2h
Synaptosomes/100μm² astrocyte
20
16
12
8
4
0
WT synaptosomes
*
*
**
**
*
Control
ephrin-B1
ephrin-B1 Y294F
ephrin-B1 Y310F
ephrin-B1 Y294/310F

Figure 4.2

Figure 4.2. Ephrin-B1 reverse signaling is necessary for astrocyte mediated synaptosome engulfment.

(A) Confocal images of primary astrocytes expressing ephrin-B1, ephrinB1-Y294F, ephrinB1-Y310F, or ephrinB1-Y294/310F stained for ephrin-B1 (green) that were co-cultured with DiI-labeled synaptosomes (red) isolated from adult mouse hippocampi for 2h. (B). Graph shows the integrated density of DiI-labeled synaptosomes in astrocytes treated for 2 h with WT synaptosome Astrocytes expressing ephrin-B1Y294Y/Y310F mutant had significantly decreased synaptosome engulfment compared with astrocytes expressing ephrin-B1 (ephrin-B1Y294F/Y310F mutant astrocytes: 4.533 ± 1.05 vs ephrin-B1-expressing astrocytes: 12.406 ± 3.842, $F_{(9,248)} = 10.04$, $p = 0.009$, ANOVA). Graphs show mean values and error bars represent SEM.

Figure 4.3

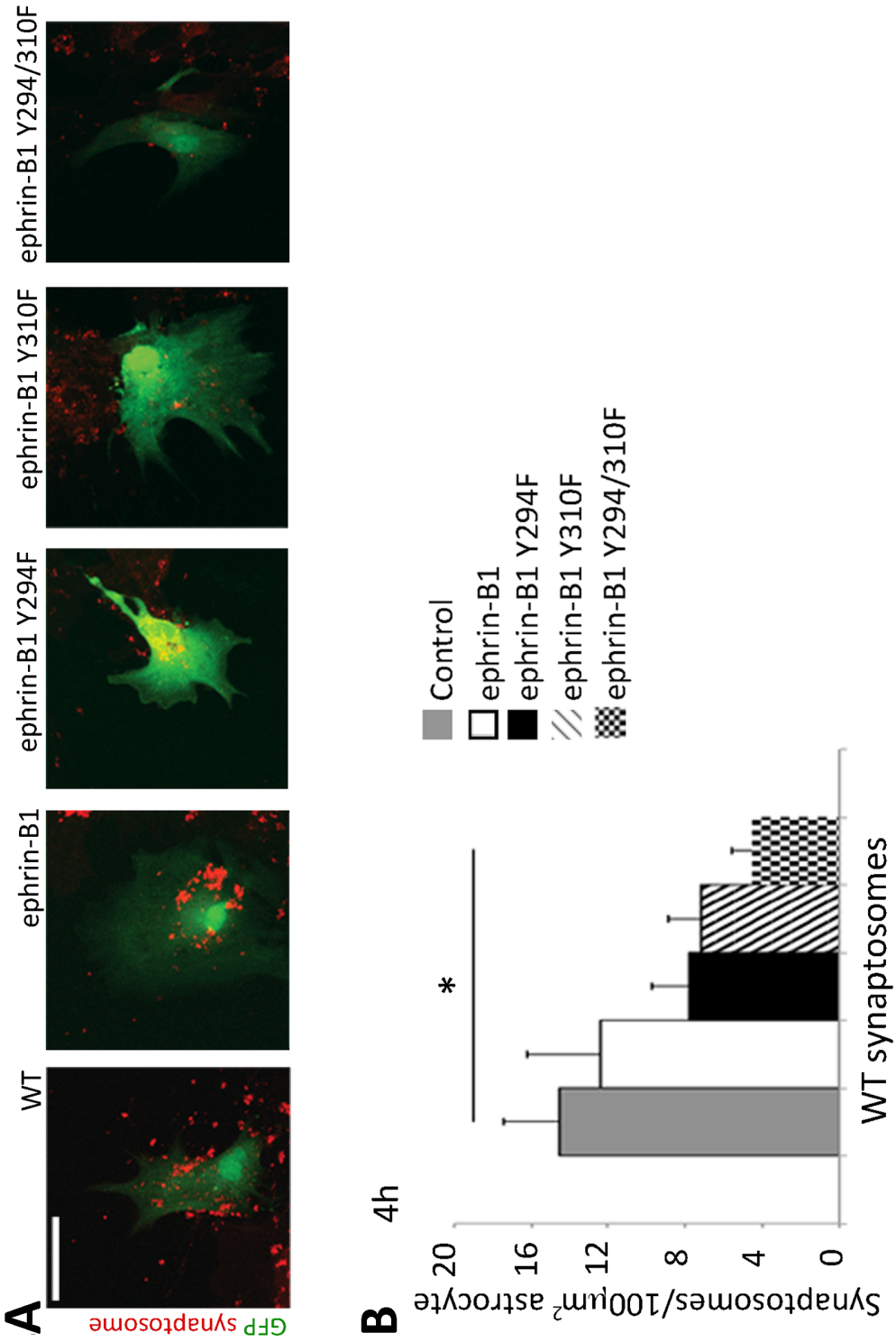
A
WT
ephrin-B1
ephrin-B1 Y294F
ephrin-B1 Y310F
ephrin-B1 Y294/310F
GFP synaptosome
B
4h
Synaptosomes/100μm² astrocyte
0
4
8
12
16
20
*
Control
ephrin-B1
ephrin-B1 Y294F
ephrin-B1 Y310F
ephrin-B1 Y294/310F
WT synaptosomes

Figure 4.3. Astrocyte engulfment of synaptosomes is reduced after 2h incubation.

(A) Confocal images of primary astrocytes expressing ephrin-B1, ephrinB1-Y294F, ephrinB1-Y310F, or ephrinB1-Y294/310F with GFP that were co-cultured with DiI-labeled synaptosomes (red) isolated from adult mouse hippocampi for 4h. (B). Graph shows the integrated density of DiI-labeled synaptosomes in astrocytes treated for 4h with WT synaptosome Astrocytes expressing ephrin-B1Y294Y/Y310F mutant had significantly decreased synaptosome engulfment compared with astrocytes expressing ephrin-B1 ephrin-B1Y294F/Y310F mutant astrocytes: 5.04 ± 1.27 vs ephrin-B1-expressing astrocytes: 12.99 ± 2.40, $F_{(5,199)} = 5.55$, $p < 0.001$, ANOVA). Graphs show mean values and error bars represent SEM.

Figure 4.3

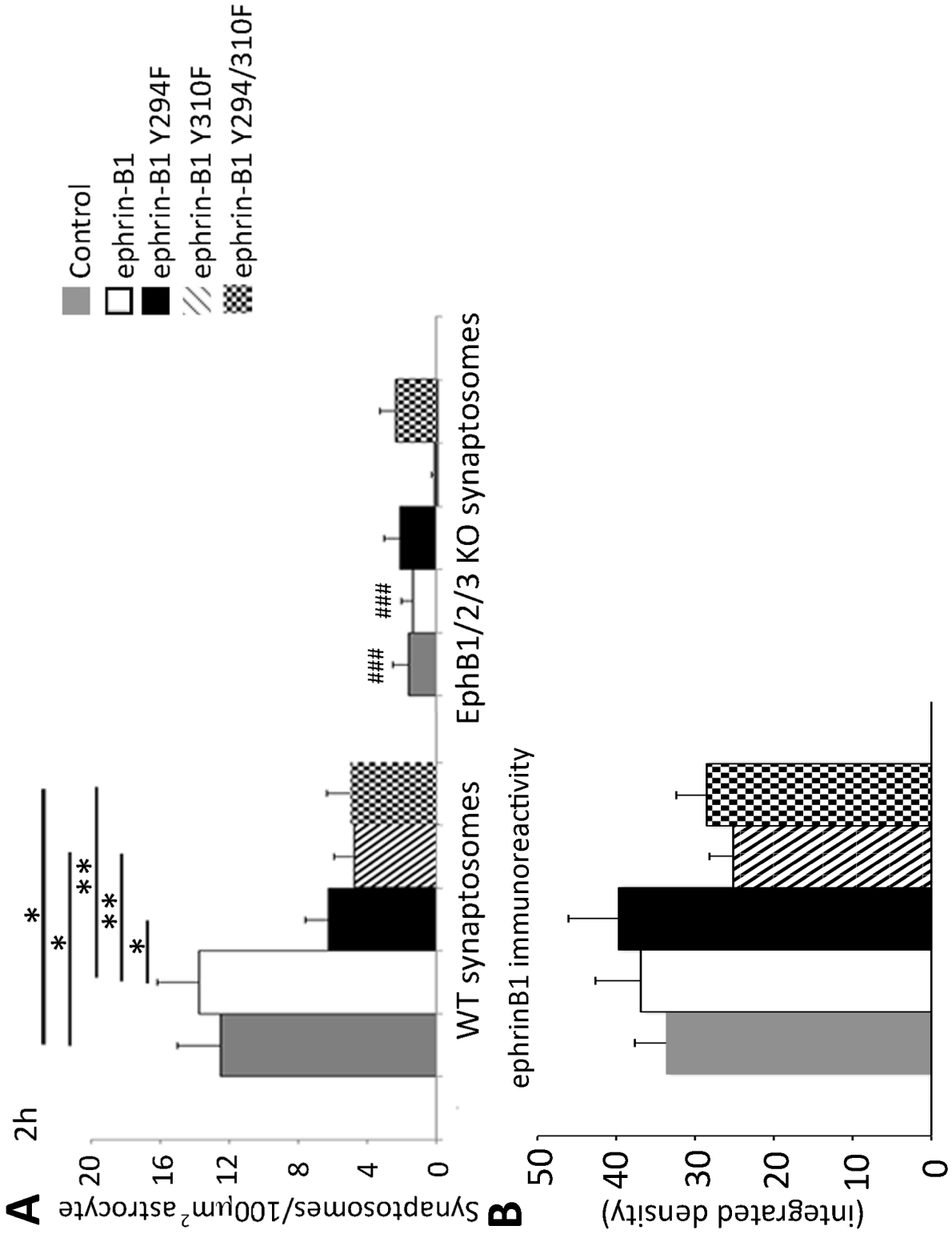
A
2h
Synaptosomes/100μm² astrocyte
0
4
8
12
16
20
Control
ephrin-B1
ephrin-B1 Y294F
ephrin-B1 Y310F
ephrin-B1 Y294/310F
*
*
**
**
*
###
###
WT synaptosomes
EphB1/2/3 KO synaptosomes
B
ephrinB1 immunoreactivity
(integrated density)
0
10
20
30
40
50

Figure 4.4. Synaptic EphB receptors are necessary for astrocytic synaptosome uptake.

(A) Graph shows the integrated density of DiI-labeled synaptosomes in astrocytes treated for 2h with WT and EphB1,2,3 KO synaptosome. (A) Astrocytes expressing ephrin-B1 contained significantly more WT synaptosomes than synaptosomes lacking EphB1/2/3 receptors 2h after addition of synaptosomes (n = 28 –30 cells; WT: 12.99 ± 2.40 vs EphB1/2/3 KO: 2.11 ± 0.71, $F_{(9,248)} = 10.04$, $p = 0.000154$, one-way ANOVA, Tukey's *post hoc* test; *$p = 0.05$, **$p = 0.01$, ***$p = 0.001$). (B) Graph shows ephrin-B1 immunoreactivity per 100 μm^2 primary hippocampal astrocytes treated with synaptosomes isolated EphB1,2,3 KO mice. Graphs show that there are no significant differences in ephrin-B1 levels in primary astrocytes transfected with *pcDNA3ephrin-B1*, *pcDNA3ephrinB1Y294F*, *pcDNA3ephrinB1Y310F*, or *pcDNA3ephrinB1Y294/310F*. Graphs show mean values and error bars represent SEM (n = 28 –30 astrocytes, one-way ANOVA followed by Tukey's *post hoc* test).

Chapter 5- Conclusion

Persistent synapse pruning and restructuring play an important role in maintaining synaptic homeostasis in the adult hippocampus (Maletic-Savatic et al., 1999; Paolicelli et al., 2011; Spacek, 2004a; Stevens et al., 2007) and contributes to life long-long learning and memory formation. In these studies I demonstrate a new role for astrocytic ephrin-B1 as a negative regulator of immature synapse formation in the adult CA1 hippocampus during memory formation. While synaptic EphB/ephrinB interactions promote the stabilization and maturation of synapses (Matthew B. Dalva et al., 2000; Henkemeyer, Itkis, Ngo, Hickmott, & Ethell, 2003; Kayser, McClelland, Hughes, & Dalva, 2006) astrocytic ephrin-B1 and neuronal EphB interactions inhibit synapse formation. Indeed, ablation of astrocytic ephrin-B1 in the adult mouse resulted in increased glutamatergic excitatory synapses in the SR region but not the SLM of the CA1 hippocampus. Decreased glutamatergic synapses are also observed specific to the SR in mice OE astrocytic ephrin-B1. Inputs from the CA1-CA3 express high levels of EphB1 and EphB2 receptors (Chenaux & Henkemeyer, 2011; Liebl, Morris, Henkemeyer, & Parada, 2002) and connect to CA1 pyramidal neurons in the SR. It is possible a lack of EphB receptor on inputs from the entorhinal cortex to the CA1 in the SLM contribute to regional differences. In addition, postsynaptic EphB receptor expression in CA1 neurons is also implicated in synaptic development (Ethell et al., 2001; Henderson et al., 2001; Henkemeyer, Itkis, Ngo, Hickmott, & Ethell, 2003b; Liebl et al., 2002; Takasu et al., 2002) by promoting clustering and recruitment of NMDA and AMPA receptors to the synapse (M B Dalva et al., 2000; Kayser, McClelland, Hughes, & Dalva, 2006b; Nolt et

al., 2011; Takasu et al., 2002). It is possible that competitive binding of postsynaptic EphB receptors disrupts trans-synaptic EphB/ephrinB interactions decreases synaptic strength. I would suspect deletion of astrocytic ephrin-B1 would promote synaptic maturation by increased trans-synaptic interactions. I did, however, find a decrease in synaptic maturation after ephrin-B1 deletion and an increase in OE mice.

Newly formed synapses are often associated with smaller postsynaptic dendritic spines characterized by a presence of NMDAR but an absence of AMPAR, and are generally considered silent (Durand et al., 1996; Isaac et al., 1995). Deletion of ephrin-B1 led to a two-fold increase in the number of dendritic spines with smaller heads and decreased synaptic AMPA receptors. In contrast OE of ephrin-B1 resulted in a 28% increase in spine volume and increased levels of synaptic AMPAR subunit GluA1. Astrocytic ephrin-B1 appears to negatively regulate immature synapses in the CA1 hippocampus possibly through the removal of excess synapses (Fig. 5.1A).

Astrocytes are implicated in synaptic pruning of synapses by trans-phagocytosis (Chung et al., 2013; Spacek, 2004). Ephrin-B1 activation may be a trigger for synaptic pruning by astrocytes. Ephrin-B1 is shown to regulate Tiam1 and Tiam2 activity and stimulate actin cytoskeleton restructuring (Gaitanos et al.,2016). Inhibition of ephrin-B1 reverse signaling resulted in a 69% decrease in synaptosome engulfment by primary hippocampal astrocytes *in vitro*, while WT ephrin-B1 expressing astrocytes readily engulfed synaptosomes after 2h of incubation. Surprisingly, engulfment rate diminished by 4h incubation possibly due to reduced surface ephrin-B1 receptors on astrocytes after initial engulfment. Deficits in WT ephrin-B1 astrocyte engulfment of EphB1,2,3 KO

synaptosomes suggest neuronal EphB receptors are an “eat me” signal for hippocampal astrocytes.

The hippocampus plays a significant role in memory formation (Milner, Squire, & Kandel, 1998; Neves, Cooke, & Bliss, 2008). More specifically activation of CA1 pyramidal neurons (Strekalova et al., 2003) raises the possibility that astrocytic ephrin-B1 regulates hippocampal synapses during memory formation. Indeed, ephrin-B1 KO mice showed a 30% increase in contextual recall and a 78% increase in contextual renewal. Increased co-localization of pre-synaptic vGlut1 and post-synaptic PDS95 suggests maturation of excess synapses in naïve mice contributed to enhanced recall.

KO mice showed an increase in the number of mature dendritic spines on activated pyramidal neurons and the recruitment of synaptic AMPAR after fear conditioning. In contrast OE mice had a 33% decrease in contextual recall and a reduction in pre- and postsynaptic co-localization after fear conditioning. Activity dependent dendritic spine formation was also inhibited in OE mice possibly due to increased synaptic pruning of newly formed immature dendritic spines on activated CA1 pyramidal neurons. Recruitment of synaptic AMPAR in WT mice after fear conditioning was not seen in OE mice, possibly due to a lack of immature synapses prior to fear conditioning that are available for new memory formation and synaptic maturation. Taken together our results suggest astrocytic ephrin-B1 mediated elimination of immature synapses is activity dependent and eliminates immature, possibly newly formed, synapses and in turn inhibit memory formation.

Hippocampal dependent memory formation requires a balance of both excitatory and inhibitory inputs. High PV expressing interneurons have a greater ratio of excitatory to inhibitory inputs compared to low PV cells (Donato et al. 2015). In addition glutamatergic innervation of PV interneurons correlates with increased PV expression after fear conditioning (Donato et al. 2013; Donato et al. 2015). This raises the possibility that astrocytic ephrin-B1 may regulate excitatory input onto PV expressing inhibitory cells. However, no difference was seen in glutamatergic inputs on CA1 PV interneurons in KO mice before or after fear conditioning. Hippocampal dependent memory formation can also be inhibited by increased inhibitory signaling to excitatory neurons (Collinson et al., 2002; Crestani et al., 2002; Yee et al., 2004). While I saw no differences in GAD65 puncta suggesting astrocytic ephrin-B1 synapse regulation is specific to excitatory synapses further studies looking at inhibitory inputs onto pryramidal neurons may show interesting results.

Our research implicates astrocytic ephrin-B1 in regulating excitatory synapse elimination in the SR region of the CA1 hippocampus by trans-phagocytosis of immature synapses diminishing the availability of potential sites for new memory formation (fig. 5.2).

References

Chenaux, G., & Henkemeyer, M. (2011). Forward signaling by EphB1/EphB2 interacting with ephrin-B ligands at the optic chiasm is required to form the ipsilateral projection. *European Journal of Neuroscience*. https://doi.org/10.1111/j.1460-9568.2011.07845.x

Chung, W. S., Clarke, L. E., Wang, G. X., Stafford, B. K., Sher, A., Chakraborty, C., … Barres, B. A. (2013). Astrocytes mediate synapse elimination through MEGF10 and MERTK pathways. *Nature*. https://doi.org/10.1038/nature12776

Collinson, N., Kuenzi, F. M., Jarolimek, W., Maubach, K. A., Cothliff, R., Sur, C., … Rosahl, T. W. (2002). *Enhanced Learning and Memory and Altered GABAergic Synaptic Transmission in Mice Lacking the 5 Subunit of the GABA A Receptor*.

Crestani, F., Keist, R., Fritschy, J.-M., Benke, D., Vogt, K., Prut, L., … Rudolph, U. (2002). Trace fear conditioning involves hippocampal 5 GABAA receptors. *Proceedings of the National Academy of Sciences*. https://doi.org/10.1073/pnas.142288699

Dalva, M. B., Takasu, M. A., Lin, M. Z., Shamah, S. M., Hu, L., Gale, N. W., & Greenberg, M. E. (2000). EphB receptors interact with NMDA receptors and regulate excitatory synapse formation. *Cell*. https://doi.org/10.1016/S0092-8674(00)00197-5

Donato, F., Chowdhury, A., Lahr, M., & Caroni, P. (2015). Early- and Late-Born Parvalbumin Basket Cell Subpopulations Exhibiting Distinct Regulation and Roles in Learning. *Neuron*. https://doi.org/10.1016/j.neuron.2015.01.011

Durand, G. M., Kovalchuk, Y., & Konnerth, A. (1996). Long-term potentiation and functional synapse induction in developing hippocampus. *Nature*, *381*(6577), 71.

Ethell, I. M., Irie, F., Kalo, M. S., Couchman, J. R., Pasquale, E. B., & Yamaguchi, Y. (2001). EphB/syndecan-2 signaling in dendritic spine morphogenesis. *Neuron*, *31*(6), 1001–1013. https://doi.org/10.1016/S0896-6273(01)00440-8

Gaitanos, T. N., Koerner, J., & Klein, R. (2016). Tiam–Rac signaling mediates trans-endocytosis of ephrin receptor EphB2 and is important for cell repulsion. *J Cell Biol*, jcb-201512010.

Henderson, J. T., Georgiou, J., Jia, Z., Robertson, J., Elowe, S., Roder, J. C., & Pawson, T. (2001). The receptor tyrosine kinase EphB2 regulates NMDA-dependent synaptic function. *Neuron*, *32*(6), 1041–1056. https://doi.org/10.1016/S0896-6273(01)00553-0

Henkemeyer, M., Itkis, O. S., Ngo, M., Hickmott, P. W., & Ethell, I. M. (2003a). Multiple EphB receptor tyrosine kinases shape dendritic spines in the hippocampus. *Journal of Cell Biology*. https://doi.org/10.1083/jcb.200306033

Henkemeyer, M., Itkis, O. S., Ngo, M., Hickmott, P. W., & Ethell, I. M. (2003b). Multiple EphB receptor tyrosine kinases shape dendritic spines in the hippocampus. *Journal of Cell Biology*, *163*(6), 1313–1326. https://doi.org/10.1083/jcb.200306033

Isaac, J. T. R., Nicoll, R. A., & Malenka, R. C. (1995). Evidence for silent synapses: Implications for the expression of LTP. *Neuron*, *15*(2), 427–434. https://doi.org/10.1016/0896-6273(95)90046-2

Kayser, M. S., McClelland, A. C., Hughes, E. G., & Dalva, M. B. (2006a). Intracellular and Trans-Synaptic Regulation of Glutamatergic Synaptogenesis by EphB Receptors. *Journal of Neuroscience*. https://doi.org/10.1523/JNEUROSCI.3072-06.2006

Liebl, D. J., Morris, C. J., Henkemeyer, M., & Parada, L. F. (2002). *mRNA Expression of Ephrins and Eph Receptor Tyrosine Kinases in the Neonatal and Adult Mouse Central Nervous System*.

Maletic-Savatic, M., Malinow, R., Svoboda, K., Zaman, S. H., Wenthold, R. J., Svoboda, K., & Malinow, R. (1999). Rapid Dendritic Morphogenesis in CA1 Hippocampal Dendrites Induced by Synaptic Activity. *Science*, *283*(5409), 1923–1927. https://doi.org/10.1126/science.283.5409.1923

Milner, B., Squire, L., & Kandel, E. (1998). Cognitive Neuroscience and the Study of Memory. *Neuron*, *20*, 445–468. https://doi.org/10.1016/S0896-6273(00)80987-3

Neves, G., Cooke, S. F., & Bliss, T. V. P. (2008). Synaptic plasticity, memory and the hippocampus - a neural network aproach to causality. *Nature Reviews Neuroscience*, *9*(January 2008), 65–75. https://doi.org/nrn2303 [pii] 10.1038/nrn2303

Nolt, M. J., Lin, Y., Hruska, M., Murphy, J., Sheffler-Colins, S. I., Kayser, M. S., … Dalva, M. B. (2011). EphB Controls NMDA Receptor Function and Synaptic Targeting in a Subunit-Specific Manner. *Journal of Neuroscience*, *31*(14), 5353–5364. https://doi.org/10.1523/JNEUROSCI.0282-11.2011

Paolicelli, R. C., Bolasco, G., Pagani, F., Maggi, L., Scianni, M., Panzanelli, P., … Gross, C. T. (2011). Synaptic Pruning by Microglia Is Necessary for Normal Brain Synaptic Pruning by Microglia Is Necessary for Normal Brain Development. *Science*, *333*(September), 1456–1459. https://doi.org/10.1126/science.1202529

Spacek, J. (2004). Trans-Endocytosis via Spinules in Adult Rat Hippocampus. *Journal of Neuroscience*. https://doi.org/10.1523/JNEUROSCI.0287-04.2004

Stevens, B., Allen, N. J., Vazquez, L. E., Howell, G. R., Christopherson, K. S., Nouri, N., … Barres, B. A. (2007). The Classical Complement Cascade Mediates CNS Synapse Elimination. *Cell*, *131*(6), 1164–1178. https://doi.org/10.1016/j.cell.2007.10.036

Strekalova, T., Zörner, B., Zacher, C., Sadovska, G., Herdegen, T., & Gass, P. (2003). Memory retrieval after contextual fear conditioning induces c-Fos and JunB expression in CA1 hippocampus. *Genes, Brain and Behavior*, *2*(1), 3–10. https://doi.org/10.1034/j.1601-183X.2003.00001.x

Takasu, M. A., Dalva, M. B., Zigmond, R. E., Greenberg, M. E., Katz, L. C., Shatz, C. J., … Grunwald, I. C. (2002). Modulation of NMDA receptor-dependent calcium influx and gene expression through EphB receptors. *Science*, *295*(5554), 491–495. https://doi.org/10.1126/science.1065983

Yee, B. K., Hauser, J., Dolgov, V. V., Keist, R., Möhler, H., Rudolph, U., & Feldon, J. (2004). GABAAreceptors containing the α5 subunit mediate the trace effect in aversive and appetitive conditioning and extinction of conditioned fear. *European Journal of Neuroscience*. https://doi.org/10.1111/j.1460-9568.2004.03642.x

Figure 5.1

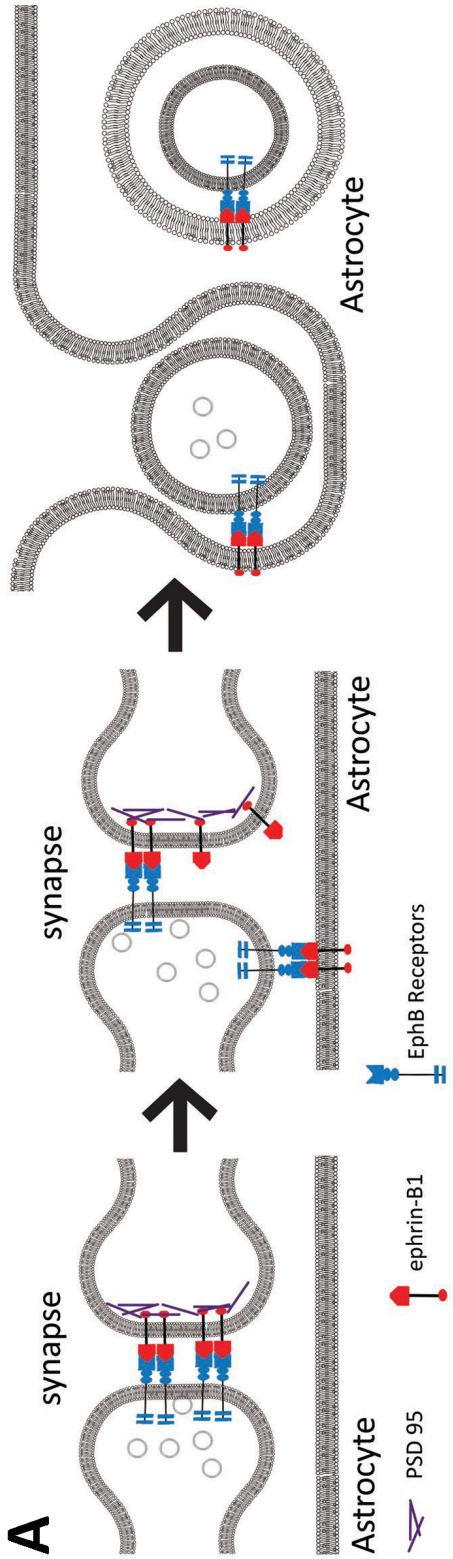
A
synapse
Astrocyte
PSD 95
ephrin-B1
synapse
Astrocyte
EphB Receptors
Astrocyte

Figure 5.1. Ephrin-B1 mediated synapse engulfment model.

(A) Astrocyte-mediated pruning of synapses is mediated through the interactions between astrocytic ephrin-B1 and synaptic EphB receptors, leading to the engulfment of synaptic sites that requires ephrin-B1 reverse signaling. Unoccupied synaptic EphB receptor may serve as an "eat me signal" to target synapses for removal.

Figure 5.2

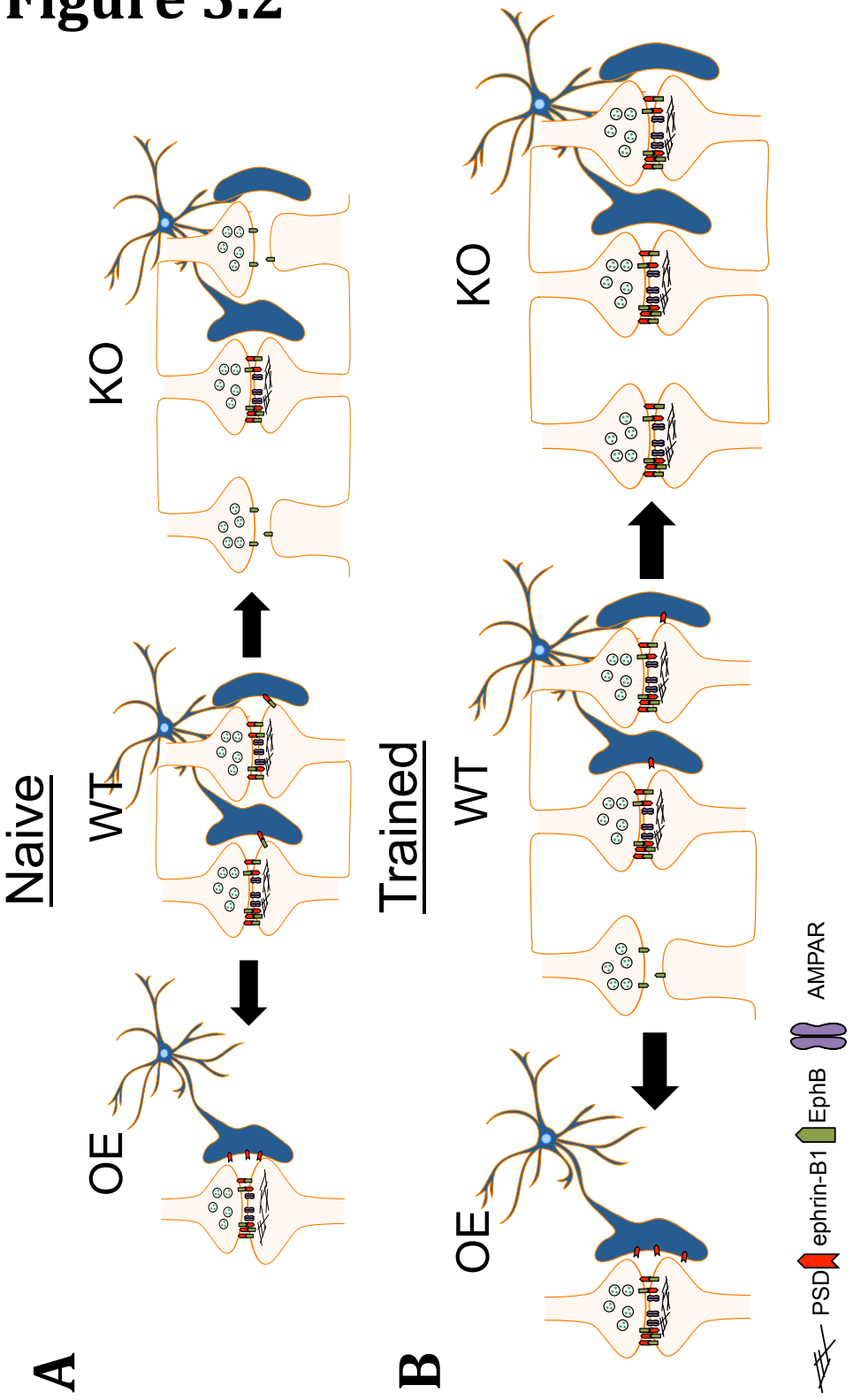

Figure 5.2. Astrocytic ephrin-B1 mediated synapse regulation before and after fear conditioning.

Illustrations show the effects of astrocytic deletion and overexpression in (A) naïve and (B) trained adult mice. Astrocytic ephrin-B1 reduces the number of immature synapses in the CA1 hippocampus, targeting activated excitatory neurons.